Structural and Functional Characterization of Human Lysyl Oxidase through Molecular Cloning, Expression and *In Silico* Studies

THESIS

Submitted in partial fulfilment
of the requirements for the degree of
DOCTOR OF PHILOSOPHY
By

R.Bhuvanasundar

Under the Supervision of
PROF. K.N.Sulochana
&
Under the co-supervision of
PROF. P.R.Deepa

BIRLA INSTITUTE OF TECHNOLOGY AND SCIENCE
PILANI (RAJASTHAN) INDIA
2015

BIRLA INSTITUTE OF TECHNOLOGY AND SCIENCE

PILANI (RAJASTHAN)

CERTIFICATE

This is to certify that the thesis entitled "**Structural and Functional Characterization of Human Lysyl Oxidase Through Molecular Cloning, Expression and *In Silico* Studies**" and submitted by Mr.R.Bhuvanasundar ID No 2010PHXF445P for award of Ph.D. Degree of the Institute embodies original work done by him under our supervision.

Signature in full of the Supervisor:

K. N. Sulochana,
Senior Professor
R. S. Metha Jain Dept. of Biochemistry and Cell Biology,
Vision Research Foundation,
Chennai – 06.

Date

Signature in full of the Co-Supervisor:

P. R. Deepa,
Associate Professor,
Department of Biological sciences,
Birla Institute of Technology and Science,
Pilani — Chennai Centre,

Date

ACKNOWLEDGEMENTS

I take this opportunity to sincerely thank, **Padmabushan Dr. S.S.Badrinath**, Chairman Emeritus, Sankara Nethralaya, Chennai, for giving me an opportunity to do this project in this esteemed institution.

I thank **Dr. Bhaskaran**, Chairman, Medical Research Foundation, **Dr.Ronnie George**, Director of Research, Vision Research Foundation, **Dr. T. S. Surendran,** Vice-Chairman, Medical Research Foundation for extending their support. I express my heartfelt thanks and gratitude to **Dr. H.N. Madhavan**, Director, Department of Microbiology and **Dr.Rama Rajaram,** Advisor, Vision Research Foundation for this wonderful opportunity to do my research. I extend my sincere thanks to **Dr. S. Meenakshi**, Director of Academics and **Mr. N. Sivakumar**, Academic officer for their support.

Beauty of this world lies in the heart of an individual. I am so blessed to be guided by a person with beautiful heart and named as, “person with beautiful eyes” (sulochana). She is source of inspiration, motivation and hard working. She taught me sense of right science. I feel proud to be her student, thank you my dear ma’am, **Dr.K.N.Sulochana**.

When I had difficulties during my master’s interview, she encouraged me and helped me clearing it. As a co-supervisor she constantly encouraged and monitored my work progress. I take this opportunity to thank **Prof. P.R. Deepa**, for her valuable time and suggestions.

I sincerely thank **Prof. B.N. Jain** Vice Chancellor and Director, BITS, Pilani for giving me the great opportunity to do my thesis under the esteemed university. I thank **Prof. S.K. Verma**, Dean, Research and Consultancy Division, BITS, Pilani, **Prof. Ashish**

Kumar Das, Past Dean, Research and Consultancy Division, BITS, Pilani, **Hemant R. Jadhav**, Ph. D. Associate Dean, Academic Research (Ph. D. Programme) Division , **Prof. Jitendra Panwar**, **Dr. Navin**, PhD Monitoring. I would also like to thank my DAC members **Dr.Shibasish Chowdhury** and **Dr.Lalita Gupta** for valuable comments and suggestions towards improving my thesis.

I would like to express my gratitude **Dr. K.Lily therese,** Department of microbiology, **Dr. A.J. Pandian**, Department of genetics, **Dr. J. Biswas,** and **Dr. S. Krishnakumar**, Department of pathology and **Dr. D. Dorren Gracious** for evaluating me throughout my lecture series. I would like to thank VRF manager **Mr.Narayan** for his support. I would like to offer my special thanks to all the staff of multimedia for their full cooperation in preparation of the posters for the presentations.

My sincere thanks to **Dr. V. Umashankar**, HoD, Department of Bioinformatics. He taught me bioinformatics and helped me a lot in organizing my work. He supported me and without him the Bioinformatics part of this thesis would not have been possible.

Thanks to **Dr. N. Angayarkanni**, HoD, Department of Biochemistry for cultivating responsibility in me and teaching me good things right from from Master's.

She taught me what research is how to do experiments. She is my well-wisher, guide and moral support and I thank you my dear **Dr. R. Selvi**.

Person who taught me the three letter word "LOX". I was amazed at her lectures and practical skills when I met her in my master's and till date I am learning those from her. Thank you, **Dr. K. Coral**.

She used to say, to get answers for your query "stay with the problem", thank you **Dr.J.Subbulakshsmi,** for guiding me in cloning work.

I learned how to maintain a disciplined work culture and many good things from her and I thank you, **Dr. A.V. Saijyothi.** She didn't even bother whether I listened to her or not, she kept pouring her ideas in me. Debatable discussions with her helped me a lot in shaping up and organizing my work and I had a good learning time whenever I discussed with her. Thank you **Dr. Iyer Gomathy Narayanan**. The enthusiastic and favorite teacher of mine, **Ms. S. Vidhya**, thank you so much for being so supportive.

He aided me a lot in the field of bioinformatics. Being a good friend supported and helped me a lot during the hard times and I thank you **Mr. S. Muthukumaran.** Mid-way through my bioinformatics work popped this man; but with his brilliant ideas, he made a significant contribution and I thank you, **Mr. Arun John.** These two people are very enthusiastic and awesome supporters of my work. For your timely help during the bioinformatics work, thank you so much **Mr. Mohammad Al Ameen** and **Ms. T. Induja.** With her linguistics, she helped me correct the tenses in my thesis. Thank you, **Ms. Rebecca Manohar**.

I would also like to thank my group of hard-working research scientists, Dr. S.Bharathi, Mr. R. Saravanan, Mr. S. Sivasankar, Mr. C. Sanket, Mr. M. Arun, Ms. M. Bharath Selvi, Ms. R. Gayathri, Ms. U. Jeyanthi and Ms. R. Punithasri.

If it is an administrative issue, my only known protocol is to seek help from **Ms. Parvathy Devi**, our Department Secretary. Thank you very much for your sustained help.

My sincere thanks to **Dr. Srujana Chitipothu** and **Ms.B.Lakshmi** for help in core lab work and there constant support.

Mr. Pradeesh kumar, Lab assistant, for helping me get the things at the right time. My heartfelt thanks to all the technical and non-technical staffs. I would also like to thank Ms. Amrithavalli, Secretary, VIBS for her support

I like to thank **IIT, Madras**, Department of Biotechnology for extending the CD spectra facility and **Bioklone**, Chennai for in-house antibody production. I would also like to express my sincere thanks to **ICMR** for their funding.

My roasted time inside the lab was made cool and easy be these people, **Mr. R.N. Naresh Kumar** (for helping me in many of the experiments and support), **Mr. K. Anand Babu** (for his support and timely help), **Ms. P. Karthikka** (for trusting me), **Ms. T. Krithiga** (for her enthusiastic nature and kind heart), **Ms. S. Suganya** (for her care and affection).

I love to be with these people and had a great time right from my MSMLT days. I thank **Ms. Fowjana Jenofar** (for her support and innovative thoughts), **Ms. M.K. Janani** (for being true hearted), **Dr. L. Dhanurekha** (for guiding and making move faster towards the goal) and **Ms. M. Vimalin Jeyalatha** (for all the help, innovative thoughts and being patient).

He is the epitome of hard work and she is splendid. These two people nurtured and are the pillars of support to me. I cannot thank them because it will be thanking me. I love you so much, my dear Appa **Mr. R. Renganathan** and Amma **Ms. R. Andal**. She is a good companion who cultivated the sense of literature in me and made me aware of worldly things. She gave her moral support and I thank you my dear sister, **Ms. R. Radha**. I extend my thanks to **Mr. S. Vijay**, my brother-in-law, for his kind nature, supportiveness and encouragement. My little angel who blows away my tiredness and bad temper with her ray of smile love you dear **S. Aahana**, my niece.

He is a silent spectator and a true witness of my happiness, anger, sorrow. He is the reason for this work who made me do all these. He prevailed everywhere and showered his blessings on me. Thank you the **Almighty**.

R.Bhuvanasundar

Table of Contents

List of figures

List of Flowcharts and Box

List of Tables

List of Abbreviations	
%	Percentage
2D	Two dimension
3D	Three dimension
Å	Angstrom
Asp	Aspartic acid
ATP	Adenosine Triphosphate
ATP7A	ATP-dependent copper transporter
bFGF	Basic Fibroblast growth factor
BMP	Bone Morphogentic proteins
cAMP	Cyclic adenosine monophosphate
CD	Circular Dichroism
CDC	Cyclic adenosine monophosphate
cDNA	Complementary Deoxyribo Nucleic Acid
CRL	Cytokine receptor like
Cu	Copper
DNA	Deoxyribo Nucleic Acid
DOCK	Dedicator of cytokinesis
E.coli	*Eschercia Coli*
EBP	Elastin binding protein
ECM	Extra cellular matrix
ELISA	Enzyme Linked Immuno Sorbent Assay
FAK	Focal Adhesion Kinase
FP	Forward Primer
g	Gram
Gly	Glycine
h	Hour
Hcys	Homocysteine
HIF	Hypoxia Inducible Factor
His	Histidine
HPLC	High Pressure Liquid Chromatography
HUVECs	Human Umbilical Vein Endothelial Cells
IFD	Induced Fit Docking
IGF	Insulin-like Growth Factor
kDa	Kilo Dalton
LDL	Low Density Lipoprotein
LOX	Lysyl Oxidase
LOXpp	Lysyl Oxidase propeptide
LPLC	Low Pressure Liquid Chromatography
LTQ	Lysyl Tyrosyl Quinone

	Lysine
M	Molar
m/z	Mass to charge ratio
MD	Molecular Dynamics
Mins	Minutes
mL	Milli Litre
mLOX	Mature Lysyl Oxidase
mM	Milli Molar
MMGBSA	Molecular Mechanics Generalized Born Surface Area
mRNA	Messenger Ribo Nucleic Acid
MS	Mass Spectroscopy
mTLD	Mammalian Tolloid
nmoles	Nano Moles
NMR	Nuclear Magnetic Resonance
Nos	Numbers
^{o}C	Degree Celsius
OHS	Occipital Horn Syndrome
PAGE	Poly Acrylamide Gel Electrophoresis
PB	Lys
PBS	Phosphate Buffered Saline
PCR	Polymerase Chain Reaction
PDB	Protein Data Bank
PDR	Proliferative Diabetic Retinopathy
PLGS	Protein Lynx Global Server
PSI-BLAST	Position Specific Iterated- Basic Local Alignment Search Tool
PXE	Pseudo Exfoliative
RBS	Ribosomal Binding Site
RFU	Relative Fluorescence Unit
RMSD	
RP	Reverse Primer
rpm	Revolutions Per Minute
RRD	Rhegmatogenous Retinal Detachment
rrg	Ras Recision gene
RT	Room Temperature
SD	Standard Deviation
SEM	Standard Error Mean
SILC	Sequence and ligation independent cloning

SNP	Single Nucleotide Polymorphism
SRCR	Scanvenger Receptor Cysteine Rich
TGF	Transforming Growth Factor
Thr	Threonine
TPQ	Topa Quinone
Tyr	Tyrosine
UV	Ultra Violet
V	Volts
Vmax	Maximal Velocity
μg	Micro Gram

CHAPTER 1 - INTRODUCTION AND REVIEW OF LITERATURE

The extracellular matrix (ECM) is a heterogeneous network made up of several structural and functional proteins. ECM chiefly contains collagen and elastin; apart from that it has micro fibrils, soluble protein and glycoprotein's [1]. Primary function of ECM is to provide mechanical support to tissues. ECM is a dynamic milieu involved in various processes like cell-cell interactions, cell migration and cell anchorage. ECM also plays an important role in the regulation of cellular functions during embryonic development, tissue repair, inflammation, tumor invasion and metastasis [2] .

Cross linked collagen and elastin matrixes give mechanical and tensile strength to the ECM. Cross linking of collagen and elastin is a post-translational modification, where covalent bond is generated between the lysine residues by the action of an enzyme called Lysyl Oxidase (LOX) [3]. By oxidative deamination process LOX converts the amino group of lysine residues into reactive aldehydes. Thus LOX plays a vital role in the ECM formation. Apart from extracellular matrix formation, LOX also has various intracellular activities, like regulation of chromatin compaction, gene transcription, cell differentiation and tissue development. It plays an important role in angiogenesis by regulating the cell migration and adhesion pathways of endothelial cells [4]. The enzyme activity is impaired in disease like atherosclerosis, aortic aneurysms, hepatic fibrosis, cutis laxa and hypertrophy scars. The increased LOX expression is considered as a marker for tumour invasiveness in breast cancer, head and neck squamous cell, prostatic and renal cell carcinomas. Apart from LOX, there are four other LOX like proteins (LOXL), which are denoted as LOXL1, LOXL2, LOXL3 and LOXL4 [5].

1.1 Lysyl oxidase (LOX)

Amine oxidases are the oxidoreductases class of enzyme, catalyst the conversion of primary amine to aldehyde group. Based on the cofactor, they are classified into flavin containing amine oxidase (Eg., monoamine oxidase-A and polyamine oxidase) and copper containing amine oxidase (Eg., diamine oxidase and lysyl oxidase) [6]. Enzymatic function of these enzymes is found inside the cell, transmembrane and extracellular region.

LOX belongs to the copper dependent amine oxidase with the Enzyme Commission number, 1.4.3.13. Pinnell and Martin in 1968, demonstrated the cross linking of elastin and collagen by the enzymatic activity of LOX [7]. LOX acts on the peptidyl lysine of collagen and elastin and converts them in to reactive aldehydes (allysine), which further reacts with the vicinal lysine or allysine and brings about the cross linking [8] [9]. This cross linking makes the final step in the maturation of collagen and elastin. Hence LOX plays a major role in the formation of the extracellular matrix.

1.2 Biosynthesis and post-translational modification of LOX

LOX belongs to the oxido reductase family of enzyme, which is secreted into the extracellular space [10] [11] [12]. The nascent mRNA translated LOX fragment is a 46 kDa polypeptide, which contains 3 segments namely, signal peptide, propeptide and mature LOX. Trackman et al demonstrated the biosynthesis of pro-LOX by immuno-precipitation using antibody developed against 32 kDa bovine LOX. By cell free translation process, mRNA of rat smooth muscle cell was translated, which resulted in 46 kDa LOX proenzyme [8] [9]. Immunoprecipitation of media and cell lysate of cultured rat smooth muscle cell resulted in bands with molecular weight of 50, 46 and 32 kDa [15]. The 46 kDa proenzyme undergoes N-glycosylation during post-translational modification and resulted in 50 kDa pro-LOX. By pulse chase, it was revealed that 50 kDa band was present in both cell lysate and media but 32 kDa was present in media only [15]. Procollagen C-proteinase acts as an endoprotease and cleaves the 50 kDa pre-LOX into 18 kDa propeptide and 32 kDa mature LOX. In mammals,

cleavage is accomplished by the action of Bone Morphogenetic Protein-1 (BMP-1) and mammalian Tolloid (mTLD) [16] [17]. LOX is transported to cell membrane through golgi apparatus in vesicles after which the vesicle buds off and fuses with the sub-cellular membrane.

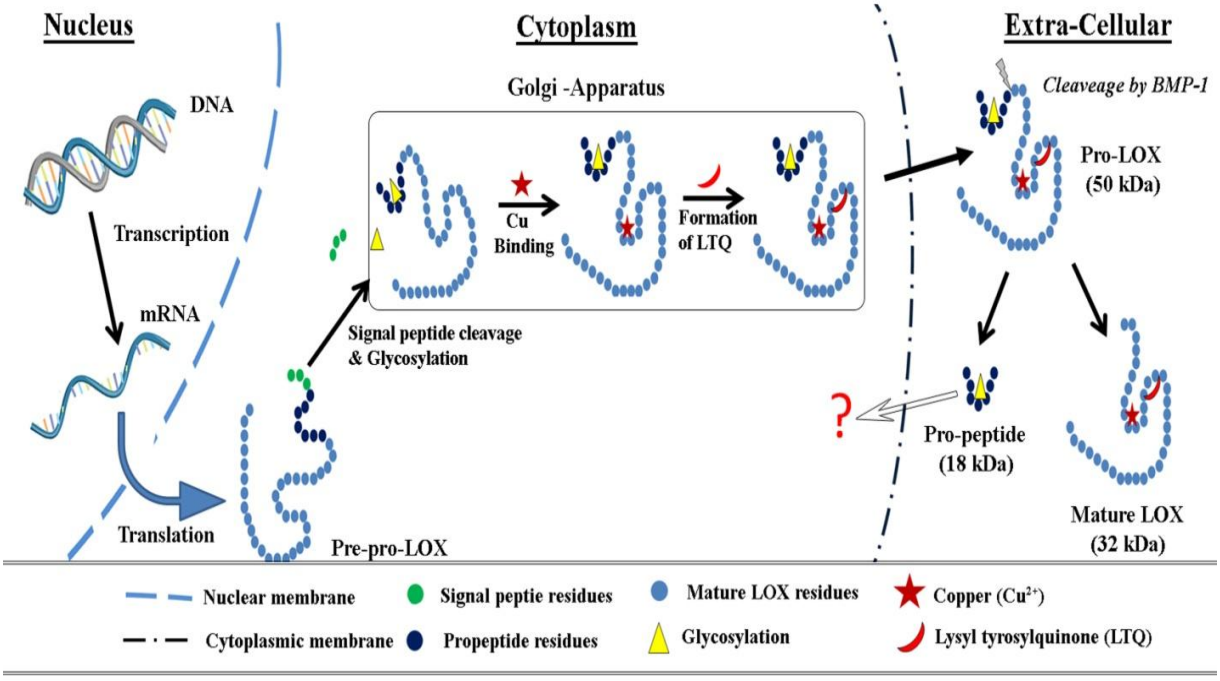

Figure 1.1: Biosynthesis of Lysyl oxidase (LOX)

The nascent translated polypeptide is called as pre-pro-LOX. It is converted into 46 kDa pro-LOX by cleavage of the signal peptide. Then pro-LOX is translocated into golgi apparatus, where post-translational modification occurs. The pro-LOX is glycosylated in pro peptide region (residues 81, 97 and 144) resulting in 50 kDa protein [15]. Then copper is incorporated at the highly conserved copper binding site (residues 286 – 296) in the C- terminal [18] and the copper induces the formation of Lysyl-Tyrosyl Quinone (LTQ) cofactor by the autocatalytic hydroxylation and oxidation of the lysine 320 and tyrosine 355 residues [19] [20]. Then it is secreted to the extracellular matrix as pro–LOX of 50 kDa. In extracellular matrix, by the action of BMP-1 cleavage occurs between

residues of glycine 168 and aspartic acid 169 which removes the N-terminal pro peptide (18 kDa) and yields the active 32 kDa LOX [21] [14]. This active 32 kDa LOX is involved in the modification of extra cellular matrix.

1.3 Co-Factors

1.3.1 Copper

Copper is an important cofactor in the LOX enzyme. It involved in the electron transfer action during the catalytic action of LOX. Presence of copper in LOX was confirmed from the purified LOX of chick aorta and bovine aorta [22][23]. The copper binding site is conserved among the LOX family members. In humans, copper binding sequence is N-terminal – 286 W*X*WH*X*CH*X*HYHS – 297 – C-terminal, this sequence was predicted to be in a random coil state but forms talon-shaped loop [24]. Copper ion is thought to harbor in the loop and has co-ordination bond in octahedral geometry tetragonally distorted [25]. The loop contains 4 histidine residues of which 292, 294 and 296 histidine residues form the co-ordinate bond with copper ion [26]. LOX belongs to type-2 copper proteins as only nitrogen group of histidine acts a ligand molecule. By atomic absorption spectroscopic method, it was established that one molecule of LOX contains one tightly bound copper ion. One tightly bound copper is present in a molecule of mature LOX which upon removal results in enzymatically inactive LOX. It is reported that apart from tightly bound Cu ion, there are 5 - 9 copper atoms loosely bound to purified LOX preparation [25].

1.3.2 Lysyl Tyrosyl quinone (LTQ)

LTQ is a carbonyl cofactor present in the LOX structure in addition to the copper cofactor. LTQ is a quinone ring structure formed by the cross linking between ε – amino group of lysine 320 and tyrosine 355 in the human LOX amino acid sequence [27]. It is formed by the auto oxidation of tyrosine residue after incorporation of copper during post-translational modification. Earlier report stated that LOX contains carbonyl cofactor

similar to bovine plasma amine oxidase based on the Raman spectra [28]. Later it was determined that bovine plasma amine oxidase contain topa quinone (TPQ) [29]. Due to huge structural difference and lack of homology in sequence between LOX and bovine plasma amine oxidase, it seems that LOX contains a different carbonyl cofactor. Later mutagenesis study confirmed the cross link between lysine and tyrosine [30].

1.4 Catalytic mechanism

Enzymatic action of LOX also follows the ping pong mechanism as other copper amine oxidases [19]. The overall enzyme reaction is to oxidatively deaminate the primary amine group to its aldehyde form. Overall reaction:

$$R\text{-}CH_2NH_3^+ + O_2 + H_2O \longrightarrow R\text{-}CHO + NH_4^+ + H_2O_2$$

The reaction takes place in two stages:

1) In first half of the reaction, the ε – amino group of peptidyl lysine binds to carbonyl cofactor LTQ and forms Schiff's base complex [31]. Through hydrogen abstraction from the substrate, rearrangement of Schiff base occurs. This action is facilitated by the active site base (aspartic acid) followed by hydrolysis, an aldehyde product and an intermediate amino quinol (reduced LTQ with amino group) product are released [32].
2) The second half of the reaction is regeneration of the enzyme using molecular oxygen. Here amino quinol will be oxidized by the bound molecular oxygen and convert it into quinoeimine. Oxygen will be reduced and released as hydrogen peroxide. Finally LTQ will be restored with the release of amino group as ammonia [33][34].

In the process of catalysis, exact role of copper ion is not elucidated clearly. Copper plays a major role in the biogenesis of LTQ formation by stabilizing the molecular oxygen binding and generation of the quinone ring [35]. When copper is replaced with other divalent metal ions, cadmium, cobalt and zinc lead to complete loss of enzymatic activity of the copper dependent amino oxidases [23].

1.5 Enzymatic action of LOX

Prime biological function of LOX is to bring about cross linking of collagen and elastin [36]. This cross linking action brings the post-translational modification in the tropo or monomeric form of elastin and collagen [37]. All the members of LOX family exhibit amine oxidase activity as the catalytic domain is conserved throughout the family members [5]. LOX catalyzes the oxidative deamination of the peptidyl lysine into δ-aminoadipic-β-semialdhyde (allysine) by the ping-pong mechanism [38]. This reactive allysine forms covalent cross link with the neighbouring amino group of lysine or peptidyl aldehyde spontaneously.

1.5.1 Collagen

Collagen is an abundant structural protein which constitutes 25 % of the total human protein mass. There are 28 types of collagen present in humans which are encoded by 45 distinct genes. Collagens are made of three polypeptide chains which are homo or heterotrimers. Collagen polypeptide contain repeating $(Glycine – X –Y)_n$ sequences and glycine makes 1 /3 rd of the total amino acid residues in collagen [39]. Predominantly X and Y positions are filled by proline and hydroxyproline residues. The precursor of collagen is called as procollagen, which undergoes various post-translational modifications and is secreted extracellularly. In the ECM, two specific proteases cleave the N- and C- termini propeptide from procollagen to yield collagen. The collagen molecules form fibrils and interact with non-collagenous and collagenous proteins. Then the fibrils are stabilized by intra and inter molecular cross-linking of lysine residues by LOX.

1.5.1.1 Cross linking of collagen

LOX acts on the lysine and hydroxylysine residues in the N and C terminal telopeptide. After the initial oxidative deamination this aldehyde residues reacts with adjacent modified or unmodified lysine and hydroxylysine residues and form the bifunctional

product such as lysinonorleucine and hydroxylysinonorleucine respectively [9]. Further reacts with histidine and lysine by aldol condensation and results in tetra functional cross link histidinohydroxymerodesmosine [40]. Bifunctional cross link product of hydroxylysine undergoes Amodori rearrangement spontaneously and results in trifunctional 2-hydroxypyridinium and lysyl pyridinium.

1.5.2 Elastin

Elastin is an important component of extra cellular matrix, which gives elasticity and resilience to the tissues like arteries, lung, elastin cartilage, skin and tendons. Elastin is encoded by a single gene localized in chromosome 7q11.2 region [41]. Human elastin gene contains 34 exons, by alternative splicing results in 11 isoforms of tropoelastin (monomeric or immature elastin) at the least [42]. After translation, tropoelastin undergoes hydroxylation of proline residues as post-translational modification and binds to 67 kDa elastin binding protein (EBP), a molecular chaperone. This EBP carries tropoelastin to the extracellular matrix [43]. There tropoelastin arranges over the microfibrillar protein like fibulin-5 and fibulin-4, through a process called as coacervation [44]. Then monomeric tropoelastin is cross linked by LOX. Most of the elastin biogenesis and maturation occur at the embryonic stage and neonatal periods. Half-life of elastin is 70 yrs [45] and least amount of elastogenesis occurs in the life time of human during wound healing process. Elastogenesis is controlled strongly by transforming growth factor (TGF) [46], tumour necrosis factor- α [47] and interleukin1β [48]. The tropoelatins protein sequence contains two domains-hydrophobic regions and hydrophilic regions. The hydrophobic region contains amino acids like glycine, valine and proline. The hydrophilic region contains lysine and alanine, involved in cross linking. The hydrophilic domain is further characterised into two domains: KA domain (rich in alanine residues) and KP domain (rich in proline residues)[49] [50]. The cross-linking of tropoelastin differs from collagen. Here only lysine residues are involved in the cross linking with the formation of lysine condensation products such as desmosines and isodesmosines.

1.5.2.1 Cross linking of elastin

Cross-linking of elastin takes place only in the lysine residues. The cross linking mechanism occurs similar to collagen, where lysine residues will be oxidatively deaminated into allysine [51] [1]. Allysine condenses with the unmodified lysine and forms lysinonorleucine and further by aldol condensation with another lysine results in trifunctional merodesmosine product. Merodesmosine reacts with allysine and forms desmosines or isodesmosines, a tetrafunctional cross link product [9]. Desmosines and isodesmosines are unique to the matured elastin and not found in matured collagen.

1.6 Substrate specificity

Immature elastin and fibrillar collagen were once thought to be the only biological substrate for LOX. Later by *in vitro* assays, it was demonstrated that the purified LOX oxidized a number of basic globular proteins with pI values > 8.0, but did not oxidize neutral or acidic globular proteins with pI value < 8.0 [52]. The electrostatic potential between LOX and its basic protein substrates was essential for productive catalysis. LOX also oxidizes non-peptidyl amine substrates such as n-butylamine and 1,5-diaminopentane leading to the development of fluorescence-based assay for LOX-dependent hydrogen peroxide production [53][54].

The sequence region within the LTQ domain between Lys 314 and Tyr 349 are rich in anionic residues. Once these two regions of LOX become covalently cross-linked to each other as the LTQ cofactor is generated, both of these regions would cooperatively provide an abundance of negatively charged sites in the microenvironment of the active site. It is likely that such an arrangement underlies the strong preference of LOX for cationic protein substrates [55]. Interestingly, the sequences surrounding the susceptible lysines in collagen are in hydrophilic sequences containing anionic residues. For example, the lysine residue within the Asp-Glu-Lys-Ser sequence which occurs at the N-terminal region of the α1(I) collagen chain within the mature type I collagen molecule is oxidized by LOX *in vivo*. However, a collagen-like synthetic peptide which contains the similar sequence was not a good substrate in assays *in vitro* and oxidation occurred if the Asp

residue was replaced with a Gly residue [56]. This observation leads to the suggestion that collagen molecules must arrange them self as microfibrils before their oxidation by LOX [38] and binding domain of LOX is located in the helical portion of collagen molecule [57]. These results led to the hypothesis that the unfavourable negative charge contributed by Asp residue can be neutralized by a specific cationic site in the neighbouring collagen molecule within the quarter-staggered microfibril, thus allowing lysine oxidation by LOX [56]. It has been reported that the propeptide regions of recombinant proenzyme of LOX mediated the binding of these enzymes to soluble precursor and fibrous form of elastin in the cultures of transfected RFL-6 fibroblasts. It leads to the conclusion that the binding of LOX proenzymes to elastin substrates was essential for the oxidation of lysine in elastin by activated LOX [58]. It has been reported that proLOX can bind to fibronectin (FN) to be proteolytically activated to the functional catalyst [37]. Histone H1 and H2 have been demonstrated to have an interaction with LOX *in vitro* [59] and incubation of Histone H1 with LOX results in the catalytic formation of hydrogen peroxide implicating that Histone H1 is a substrate of LOX [60]. Basic fibroblast growth factor was reported to be a substrate of LOX as the oxidation of lysine residues in bFGF by LOX resulted in the covalent cross-linking of bFGF monomers to form dimers and higher order oligomers and dramatically altered its biological properties [61] . Recently, LOX has been reported to be essential for hypoxia-induced metastasis because the administration of ßAPN, specific anti LOX antibody or short hair-pin RNA could inhibit the metastasis in animal model. It is still unclear whether LOX might oxidize an unknown key protein and inhibit its function in the cancer metastasis, or whether the by-product hydrogen peroxide from the oxidation plays a role in the inhibition of cancer metastasis [62].

1.7 Expression of LOX

Expression of LOX is demonstrated in normal and transformed cells like smooth muscle cells, lung fibroblast, embryonic lung fibroblast, gingival fibroblasts, perch ovary, osetoblastic and osteosarcoma cells, mesenchymal cells, corneal endothelial cells, [63], liver parenchymal cells, renal cell lines and renal tubular epithelial cells [64]. Expression

of LOX at mRNA and protein was shown in both normal and pathological conditions like wound healing, copper deficiency, inflammation, fibrosis, tumorigenesis and metastasis. Factors reported to regulate LOX include tissue specific transcriptional factors, metal ions [65], cytokines and growth factors including FGF-2, IGF-1[66] [67] and TGF-β [68], hormones such as testosterone, prostaglandins and progestin [69] and signalling molecules such as ras, cAMP [70]. Expression of LOX in humans is found to vary from developmental to later stages of life. The highest expression is found during the gestational period of 12 -14 weeks and the lowest expression is observed from 20 -24 weeks [71]; in adulthood LOX associated with elastin fiber is found to be mostly negative [72]. Localization of LOX is associated with the assembly of collagen and elastin fibers.

1.8 Cytokine receptor like (CRL) domain

Human LOX C-terminal is called as cytokine receptor like (CRL) domain. The LOX family members show a conserved sequence, C-x9-C-x-W-x26-32-C-x10-13-C (where, C is cysteine, W is tryptophan, and Xn is a defined number of any amino acid) in the C-terminal [73], which is homologous to the N-terminal extracellular domain of class I cytokine receptor super family. CRL domain in LOX exhibits cell adhesion, motility and interaction with various other proteins as that of cytokine receptor family.

1.9 Scavenger Receptor Cysteine Rich (SRCR) Domain

SRCR domain is a highly conserved domain present in the cell surface protein associated with the immune system. It is involved in the protein-protein interaction and cell mediated adhesion. The domain is classified into two types based on the number of cysteine residues-Group A containing six cysteine residues and Group B containing eight cysteine residues. LOX and LOXL1 lack the SRCR domain but the LOXL2, LOXL3 and LOXL4 contain four Group A domains, which are involved in the cell adhesion and signalling [5].

1.10 Isoforms of LOX

Enzyme different in their physical and chemical properties yet performing the same catalytic activities are called as isoenzymes or isoforms. Earlier reports on the purification of LOX from tissues extracts activity in multiple fractions lead to the hypothesis that isoforms of LOX may exist. By the 1990s, four additional LOX like genes were identified and sequences were determined and named as LOXL1, LOXL2, LOXL3 and LOXL4. These enzymes are different in their amino acid sequences and length. All these isoforms are involved in the amine oxidase action and crosslink elastin and collagen [74][75][76][77]. The expressions of these enzymes are varied in each tissue and show difference in their substrate specificity towards collagen types. The C- termini of isoforms are highly conserved and contain the copper binding region, LTQ and CRL domain [5]. LOX and LOXL 1 contain the pro-peptide region and other isoforms lack the pro-peptide region. LOXL1 contains proline rich region in the N- terminal of its mature form, but the function is not clearly elucidated. LOXL2, LOXL3 and LOXL4 contain scavenger receptor cysteine rich (SRCR) domain.

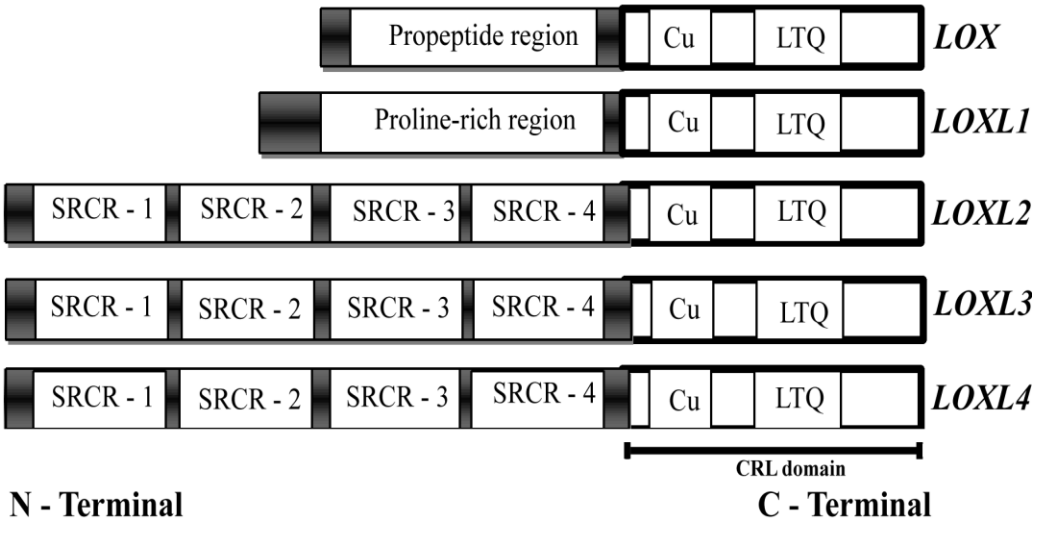

Figure 1.2: Structure of LOX family members [78]. LOX – Lysyl oxidase, LOXL - Lysyl oxidase like protein, Cu - Copper, LTQ - Lysyl Tyrosyl Quinone, SRCR - Scavenger Receptor Cysteine Rich Domain and CRL - Cytokine Receptor like Domain.

Table 1.1: Distribution of LOX and its isoforms [79]

Protein	Human chromosome	Adult tissue distribution	Amino acid residues	Similarity with LOX	SRCR domain
LOX	5	Lung, skeletal muscle, Kidney, Heart	417	100 %	Nil
LOXL1	15	Lung, heart, spleen, skeletal muscle, pancreas, Eye.	574	85 %	Nil
LOXL2	8	Lung, Thymus, Skin, Ovary, Eye.	774	58 %	4
LOXL3	2	Heart, Uterus, Testis, ovary	753	65 %	4
LOXL4	10	Skeletal muscle, Testis, Pancreas	756	62 %	4

1.11 Regulation of LOX

LOX is a secretory enzyme and its regulation takes place at three levels: at the nuclear level by transcriptional regulatory mechanism, during the post-translational modification and in the extra cellular matrix [80]. The hypoxia inducible factor – 1 α (HIF-1 α) is known to modify the LOX expression at transcriptional level [62]. It is reported that nuclear factor κB (NF- κB) binds to the LOX promoter and induces its expression at mRNA level under the influence of advanced glycation end products (AGEs) [81] [82]. In humans and rat it is shown that LOX mRNA is stabilized and the synthesis of precursor, pro-LOX is enhanced by transforming growth factor-β (TGF- β). TGF- β also acts at the maturation of LOX by regulating the protein BMP-1 and mTLD, which converts the pro-LOX into mature LOX. In the inflammatory response, connective tissue prostaglandin E2 is demonstrated to reduce LOX at transcriptional level. LOX mRNA level increases with the stimulus of the cellular reactive oxygen species (ROS) [83]. ROS plays a role in accumulation of LOX activity in the fibrotic conditions of myocardium, lung and bone marrow [80].

1.12 Lysyl oxidase in human diseases

LOX is involved in various normal physiological conditions and also its expression and activity are found to be altered in many human pathological conditions.

1.12.1 Copper deficiency and reduced LOX activity

LOX family members are copper-dependent enzymes; therefore nutritional deficiency of copper affects these copper enzymes. Change in dietary copper levels is shown to affect the functional activity of LOX enzyme. Copper deficiency leads to reduced LOX in the chick aorta [84], tendon [85], bone [86], as well as in rat skin [87] [88]. Reduced LOX activity is observed in genetic disorder like, Menkes' disease and occipital horn syndrome (OHS) [89] [90]. Here, gene encoding ATP-dependent copper transporter (ATP7A) is found to be mutated [91] [92]. During copper metabolism, after ingestion, copper is absorbed by the small intestine and stored in the liver. Copper is eliminated from the body majorly by biliary excretion and in lesser amount through urine. Due to defect in the ATP7A, copper is accumulated in the intestinal cells, kidney and vascular endothelial cells in the blood brain barrier of Menkes' and OHS patients. Bladder diveticula, hyperextensibility and laxity of skin, skeleton abnormalities, neurological degeneration and mental retardation are the disease manifestations. Patients with Menkes' syndrome show reduced LOX activity, as a result of defective copper metabolism. Fibroblast cells cultured from the patient with Menkes' and OHS showed reduced LOX activity in the medium. Due to the copper impairment biosynthesis of LOX is impaired.

1.12.2 Lathyrism

Lathyrus odoratus (sweet pea) contains β-(γ-glutamyil) aminopropionitrile, which is metabolised to β-aminopropionitrile (βAPN), a known inhibitor of the activity of LOX family members [93] [94]. Chronic ingestion of sweet pea leads to Lathyrism. Inhibition of LOX leads to the reduced cross-linking of collagens and elastin, thus leading to defective connective tissue. Khyphoscoliosis, bone deformities, weakening of skin and

cartilage, hernias, aortic aneurysms and weakening of tendons are the manifestations of lathyrism. The connective tissue defect observed in lathyrism resembles the manifestation of Menkes' syndrome and OHS [92]. These observations suggest that LOX and its family members play a central role in the connective tissue formation.

1.12.3 Lysyl oxidase in Hypercholesterolemia

Lysyl oxidase plays structural or other novel regulatory roles in extracellular matrix (ECM) assembly. The effect of high concentrations of native low density lipoprotein (LDL) on endothelial cell gene expression showed that the mRNA level of LOX was down regulated by LDL treatment in a dose- and time-dependent manner [95]. This reduction of LOX expression was associated with a decrease in LOX activity suggesting that down regulation of LOX by LDL could contribute to the endothelial dysfunction caused by hypercholesterolemia, therefore contributing to atherosclerotic plaque formation [96].

1.12.4 Lysyl oxidase in endothelial dysfunction by Homocysteine

Hyperhomocysteinemia is associated with extracellular matrix (ECM) alterations including changes on the elastic properties of the vascular wall [97]. Homocysteine (Hcys), a well-known inducer of endothelial damage, inhibits LOX activity in vascular endothelial cells through a mechanism mediated by ROS. Exposure of aortic endothelial cells to high Hcys concentrations showed a significant down-regulation of LOX mRNA levels through a reduction of LOX promoter activity. The lost ECM properties associated with LOX inhibition is related to an increase of atherosclerotic lesion vulnerability. This hypothesis was supported by a recent finding describing that LOX-deficient mice show premature death, multiple aneurysms and severe alterations in vascular wall structure that compromises normal vascular functions [98].

1.12.5 Increased LOX activity and fibrosis

Extensive accumulation of collagen fibers is called as fibrosis. Aberrant expression of LOX reported in link to the abnormal collagen deposition in various organ or tissue but often occur in the lung [99], liver [100], kidney [101] and myocardial [102]. Fibrosis leads to disfigurement, progressive disability and death. In humans, CCl_4-induced liver fibrosis showed increased mRNA levels of LOX. LOX activity increased in the medium of cultured mesenchymal cells from the cirrhotic human liver when compared to a normal liver [103]. Generally, LOX activity is negligible in normal human serum but activity is found to be increased in the serum of fibrotic liver patients, since serum LOX can be a diagnostic marker [104]. Collagen deposition and increased LOX activity are major steps leading to fibrotic diseases. Hence inhibiting the LOX activity will help in combating fibrosis and LOX can serve as the marker for detecting fibrosis.

1.12.6 Lysyl oxidase in tumorigenesis

In tumour conditions, LOX levels have been reported to be altered in both mRNA and in activity levels. Earlier it was shown that LOX possess tumour suppressor activity through inhibition ras oncogene activity, and thus LOX is known as ras recision gene (rrg) [105]. Later Chengyin et al demonstrated that tumour suppressor activity of LOX is attributed to LOX-propeptide region. Using Ewing sarcoma cell lines tumour suppressor activity of LOX propeptide (LOXpp) and oncogenic property of mature LOX (enzymatic active domain) were demonstrated. LOX actively participates in the various stages of cancer (cell migration, invasion and metastasis condition) [106].

It has been observed that LOX activity and collagen synthesis are markedly reduced in malignantly transformed human cell lines. Myofibroblast and myoepithelial cells surrounding the tumour cells showed increased expression of LOX at mRNA and protein levels.

Assessment of LOX expression at the protein and mRNA levels by immunohistochemistry and *in situ* hybridization, respectively, in breast carcinoma tissue revealed that maximal expression of LOX and its type I collagen substrate was observed

in myofibroblasts and myoepithelial cells around *in situ* tumors and in the fibrotic deposits facing the invasion front of infiltrating tumors [78].

Studies have previously demonstrated that LOX mRNA is highly up regulated in invasive breast cancer cells compared to poorly invasive cells. It is also shown that LOX activity facilitates breast cancer cell invasion. Recently, Payne et al reported that LOX regulates breast cancer cell motility/migration through changes in cell-matrix adhesion [107]. These changes are the result of a hydrogen peroxide-mediated mechanism involving the FAK/Src signalling pathway [108].

A decrease in LOX mRNA and/or protein has been reported in basal and squamous cell, bronchogenic, colon, esophageal, gastric, head and neck squamous cell, pancreatic, prostatic carcinomas and melanoma. Significant clinical correlations have been reported between LOX expression and tumor progression in breast, head and neck squamous cell, prostatic and clear cell renal cell carcinomas. The expression of high levels of LOX mRNA or protein is considered as a poor prognostic factor and is associated with poorly differentiated, high grade tumors, increased recurrence rates, and decreased overall survival [106].

Studies revealed that inhibition of LOX activity in invasive breast cancer cells leads to a corresponding increase in actin stress fiber formation as visualized using a phalloidin stain. LOX activity led to an increase in Rac and Cdc42 activity and a decrease in Rho activity. These changes correspond to a motile phenotype in the presence of LOX activity which is activated by Rac through the p130Cas/Crk/ DOCK180 signalling complex [109]. Thus LOX functions through novel intracellular signalling pathway to regulate cell motility and migration through changes in actin filament formation. Understanding the molecular mechanisms by which LOX functions to regulate breast cancer cell motility/ migration will contribute to novel anti-cancer treatment modalities [109].

1.12.7 Lysyl oxidase in ocular diseases

Until July 2007, there were no reports on the enzyme LOX in ocular tissues. The first report was from Urban who found that there was a reduced number of cross-linking

domains in elastin and decreased LOXL2 expression leading to decreased amount of mature elastin in optic nerve heads in healthy African American individuals compared with Caucasian American donors [110]. Later, a genome wide association study done on Icelandic patients identified three SNPs on chromosome 15q24.1 to be significantly associated with pseudo exfoliative (PXE) [111]. Yu et al has reported a defective elastin fiber that has been associated with increased susceptibility to laser induced choroidal neovascularization in LOXL1 knockout mouse model [112]. Yelena et al showed the polymorphisms of LOX gene in the patient with keratoconus conditions [113]. It has been proposed that in open angle glaucoma, the cross linking of ECM is increased through LOX and LOXL1 activation by TGF-β [114].

Previous report from our lab showed that LOX activity was decreased in the vitreous of proliferative diabetic retinopathy (PDR) and rhegmatogenous retinal detachment (RRD) patients along with increased MMP activity, associated with increased turnover of collagen as revealed by the increase in hydroxyproline content [115]. In addition, some epiretinal membranes from PDR showed increased LOX localization that shows a role of LOX in these membrane formation, wherein cells such as the RPE are present. The decrease in LOX activity may contribute to inadequate collagen cross-linking and with improperly cross linked collagen, there is a net vitreous degradation leading to liquefaction [115].

1.13 Literature survey on LOX purification

Reports on LOX purification date back from 1970's. Enzymatic activity of LOX was reported from crude extract of embryonic chick aorta and bone by Pinnell et al in 1968 [7]. Later they purified LOX from chick embryo cartilage using molecular sieve chromatography. They observed LOX enzymatic activity at the molecular weight of 170,000 kDa with purification yield of 23%, the purified fractions retained its enzymatic activity only for 24 hours [8]. Kagan et al in 1974 demonstrated LOX enzymatic activity from the saline insoluble fractions of chick embryo [116]. Presence of LOX in the insoluble fraction explains the low purification yield in the Pinnell et al study [8]. It was postulated that through hydrophobic interactions, LOX bound to ECM proteins and

remains in the saline insoluble fraction. Harris et al used 8 M urea to solubilise the saline insoluble fraction from bovine aorta. Urea solubilised fraction was subjected to purification using weak anion exchange chromatography and collagen affinity chromatography. With this modified purification he achieved purification yield of 63% [117]. In 1977 Jordon et al [118] purified LOX from bovine aorta as described by Harris et al [117] and identified the molecular weight of LOX as 32,000 Da using SDS-PAGE. They also showed aggregative nature of LOX in absence of urea into higher molecular weight of 60,000 and 10,0000 Da. In 1979 Kagan et al showed four variant of LOX from the bovine aorta with a total purification yield of 80%. He extracted protein from insoluble fraction using 4 M urea. Extracted protein was first fractionated based on affinity chromatography using collagen affinity column followed by weak anion exchange chromatography using DEAE-cellulose column and finally by molecular sieve chromatography using sephacryl S-200 column. Kagan et al used buffers with 6 M urea in the entire purification step [119]. Purification and isolation of LOX from various tissue Chick embryo cartilage [120], bovine lung [121], turkey aorta [122], bovine aorta [119], bovine lung [118], human placenta [123], calf aorta smooth muscle cells [124]. All these studies followed affinity chromatography, weak anion exchange chromatography and molecular sieve chromatography to purify LOX. In all the LOX purification studies, urea was used to avoid aggregation of LOX.

Using cloning technique LOX gene was expressed in *E.coli* system and purified. Ozunnie et al attempted to get solubilised LOX protein by targeting it into periplasmic space by expressing along with pelb sequence. LOX purified from periplasmic space was only 0.3 mg / L of culture whereas LOX purified from inclusions bodies was 5 mg / L [125]. Later Herwald et al [126], X.chen and F. Greenaway reported [127] cloning and purification of LOX. Both reports expressed the LOX gene using pET vector system in bacterial system and purified using His tag affinity method. As the expressed LOX protein was present in inclusion bodies both the studies performed purification using 8 M urea containing buffer [126] [127]. However, Herwald et al [126] reported that they solubilised the recombinant LOX in potassium phosphate buffer without urea. They followed stepwise dialysis to remove urea from the purified recombinant LOX. But no reports came up in regards to

LOX structural details using this buffer. Thus studies on LOX purification both conventional method and recombinant technology used urea to solubilise LOX. Presence of urea however, creates a major obstacle in elucidating the structural and functional properties of LOX.

1.14 Research Gap

For developing an efficient drug to modulate the activity of a molecule, the primary need is to have good understanding about the molecule. In case of targeting a protein as a drug target, knowledge about its structure, active cavity and its binding nature towards its substrate or downstream molecule are required. LOX has been researched since 1970's as an enzyme involved in building up of extra cellular matrix. Later isoforms of LOX have been discovered and now there are 5 members in the LOX enzyme family. Importance of LOX and its family members as an enzyme or by its signalling action or aberrant expression (either decreased or increased) in various pathological environment are being investigated. LOX and its family members are reported as a marker for various pathological conditions like fibrosis [148], tumour metastasis and angiogenesis [149] and identified as an biomarker for ovarian cancer [150].

Though various studies explain the importance of LOX in pathological conditions, studies addressing structure of LOX are few in number. LOX aggregates in the aqueous solution devoid of urea; this is the major obstacle in elucidating its structure and binding nature towards substrate and other molecule. Knowledge about the nature of activity, structure and interacting partner will intensify the research about developing specified drug towards LOX. This thesis investigated the outlined in the following chapter.

CHAPTER 2 - AIM AND OBJECTIVES

2.1 Aim

LOX is a copper dependent enzyme and involved in the cross linking of elastin and collagen. LOX importance has been demonstrated in various connective tissue disorders, hypoxia induced tumour and fibrotic diseases. Structural and functional details about LOX are not available in literature. This thesis work aimed to decipher the structure and physio chemical properties of LOX through *in vitro* and *in silico* methods.

2.2 Outline of the work

2.2.1 *In vitro* approach

Conventional anion exchange purification method was implemented to purify LOX from the bovine aorta, due to the poor yield, low activity and also tedious process alternative cloning method was used to purify LOX. Infusion cloning method was followed to construct the vector and Ni-NTA affinity column was used purify the over expressed LOX. Purity was confirmed by western blot and mass spectroscopy. Enzyme kinetic value K_m and V_{max} was determined for the recombinant LOX under optimized temperature and pH using Amplex red assay. Intrinsic and extrinsic protein fluorescence was used to understand the folding of LOX. With the recombinant LOX, in-house anti body was developed using this antibody co-immuno precipitation was performed and interacting partners for LOX was identified using mass spectroscopy.

2.2.2 *In silico* approach

By *ab intio* modelling, LOX structure was predicted and generated copper co-ordinate bonds with specific histidine residues in allowed bond length. Molecular Dynamic studies showed that predicted structure was stable and stereo chemical properties are checked using Ramachandran plot. With the validated structure, induced fit docking studies were

done against substrate and known inhibitor of LOX. Homocysteine was found to be binds with LOX at higher affinity followed by beta- Aminoproinonitrile and homocysteine thio lactone. The docking results were correlated with the in vitro Amplex red assay against recombinant LOX. From conserved sequence of LOX 5 peptides were designed. Peptide properties were assessed by CD spectra, mass spectroscopy analysis and inhibitor effect of these peptide against LOX was studied using Amplex red assay. Reported inhibitors of LOX works at micro molar concentration whereas designed peptides showed inhibition at nano molar concentration, thus this can be potent inhibitor of LOX.

2.3 Objectives

1. To isolate, purify and characterise human LOX enzyme.
2. To predict the structure of LOX by *in silico* approach and to validate the structure.
3. To design LOX inhibitors and to study its effect on LOX activity.

CHAPTER 3 - MATERIALS AND METHODS

3.1 Materials

The important chemicals, reagents, assay kits, instruments and other consumables used in the present study, have been tabulated below with their Company source and catalogue information.

Table 3.1.1 Chemicals and reagents

Chemical / Reagent	Catalogue number, Suppliers
(2,2'-Azino-di-3-ethyl benzthiazoline sulfonate) di ammonium salt (ABTS)	11204521001, Roche
1.5,Diaminopentane	C8561, Aldrich
2-mercaptoethanol	194705, MP Biomedicals
8-Anilino-1-naphthalenesulfonic acid (ANSA)	A1028, Sigma
Acetic acid	ACBA630139, Merck
Acetonitrile	34967, Fluka
Acrylamide	A3553, Sigma
Agar	014011, SRL
Agarose	50004, Lonza
Ammonium bicarbonate	A6141, Sigma
Ammonium persulphate	0148134, SRL
Ammonium sulfate	QD1Q610103, Merck
Ampicillin	A0166, Sigma
Amplex red	A12222, Invitrogen
Beta amino propoino nitrile (β-APN)	A3134, Sigma
Bis Acyrlamide	161-0201, Bio-Rad
Blue Dextran	D5751, Sigma
Borax	27965, Fisher scientific
Boric acid	Q12Q622480, Merck
Bovine serum albumin (BSA)	MB083, Himedia
Brilliant Blue G	B0770, Sigma
Bromopheno blue	AA1A601068, Merck
Calcium chloride	ME7M570903, Merck
Citric acid	ME8M581042, Merck
Cobaltous chloride	27790, BDH
Collagen	C3511, Sigma

Copper (II)chloride	C3279, Sigma
Copper chloride	C3279, Sigma
Diethylaminoethoanol (DEAE)	D0909, Sigma
Disodium hydrogen phosphate	QJIQ611768, Merck
Dispotassium hydrogen phosphate	MG9M591711, Merck
Dithiothreitol (DTT)	161-0611, Bio-Rad
Soluble elastin	E6527, Sigma
Formic acid	56302, Fluka (Sigma)
Glycerol	DC4P640148, Merck
Glycine	G8790, Sigma
Guanidine hydrochloride	074843, SRL
HEPES	Sigma
Hydrochloric acid	CE4C6404448, Merck
Hydrogen peroxidase, type IV	P8375, Sigma
Hydrogen peroxide	18755, Fisher scientific
Imidazole	RM 559, Himedia
Iodo acetamide (IAA)	163-2109, Bio-Rad
Isopropyl β-D-1-thiogalactopyranoside (IPTG)	I6758, Sigma
Kanamycin disulfate salt	K1876, Sigma
L-Homocysteine (Hcys)	H4628, Sigma
L-Homocysteine thio lactone (HCTL)	H6503, Sigma
Methanol	65524, SRL
Paraformaldehyde	MA0M60057,Merck
Potassium chloride	MC4M540102, Merck
Potassium dihydrogen phosphate	MH0M602423, Merck
Potassium iodide	MLM8M583734, Merck
Silver nitrate	Sigma
Sodium Dodecyl sulphate	L3771, Sigma
Sodium Azide	1687, Loba chemie
Sodium carbonate	QB4Q649519, Merck
Sodium chloride	QB4Q640044, Merck
Sodium dihydrogen phosphate	17845, Merck
Sodium hydroxide	QE2Q620871, Merck
Sodium iodide	RM706, Himedia
Sodium thiosulfate	17536, Merck
TEMED	194019, MP Biomedicals
Trifluro acetic acid	AJ0A600708, Merck
Triton-X-100	10655, Fisher scientific
Trizma Base	T6066, Sigma
Trypsin	TC245, cell culture grade ,Himedia
Trypsin , proteomics grade	T6567, Sigma
Tween 20	SJ3S630526, Merck
Urea	194857, MP Biomedicals

Table 3.1.2 Plasmid vectors

Plasmid name	Feature	Supplier
pQE 30-Xa	T5 Promoter, double Lac operan, 6X His tag, Factor Xa recognition site & Multiple cloning site	Qiagen, Hilden, Germany

Table 3.1.3 Peptides

All peptides were procured from USV custom peptides, Mumbai

Name	Number of residues	Sequence
C1	13	VAEGHKASFCLED
C2	12	ESDYTNNVVRCD
C3	12	DIDCQWIDITDV
M1	11	WEWHSCHQHYH
M2	8	HSCHQHYH
Scramble	9	KAYNDADPP

Table 3.1.4 Bacterial Strains

Name	Source
M15 (pREP4)	Qiagen, Hilden, Germany

Table 3.1.5 Oligonucleotides

Oligonucleotides were procured from Shrimpex, Chennai**.**

Name	RE site	Sequence (5' - 3')
Infusion LOX forward primer	Stu I	GGTATCGAGGGAAGGCCT GACGACCCTTACAACCCC
Infusion LOX reverse primer	Hind III	TCAGCTAATTAAGCTTCTA ATACGGTGAAATTGT

Table 3.1.6 Media

Media	Supplier
Dulbecco's modified eagle medium (DMEM)-F12 media	D8900-1, Himedia
Endothelial Basal media (EBM)	CC-3156, Lonza
Endothelial Growth media (EGM) -2 single Quote	CC-4176, Lonza
Luria-Bertani (LB) broth	M1245, Himedia

Table 3.1.7 Molecular weight standards

Name	Supplier
Broad range protein marker	0231104700A, Genei
DNA 100 – 1000 base pair	GM343, Gene technologies
DNA 500 – 10 kilo base pair	M103O-1, Bio Basic Canada
Unstained protein MW marker	26610,Thermo scientific

Table 3.1.8 Antibodies

Name	Supplier
Collagen	PA1-36058, Pierce
Goat anti rabbit IgG – HRP	SC-2004, Santa cruz
Rabbit anti goat IgG – HRP	SC-2768, Santa cruz
LOX	SC-32409, Santa cruz biotechnology
LOX (from in house)	Bioklone, Chennai

Table 3.1.9 Kits

Name	Contents
Coomassie Plus (Bradford) Assay Kit	23236, Pierce, Thermo scientific
ECL prime Western Blotting detection reagent	RPN2232, Amersham
Factor Xa Protease	33223, Qiagen, Hilden, Germany
Factor Xa removal resin	33213, Qiagen, Hilden, Germany
Infusion cloning kit	638909, Takara Clontech
iScript cDNA synthesis kit	170-8891, Biorad
MinElute Gel extraction kit	28604, Qiagen, Hilden, Germany
Pierce Co-immuno precipitation kit	26149, Thermo Scientifics
Qiagen plasmid min kit	12123, Qiagen, Hilden, Germany
Qiaprep Spin Miniprep	27104, Qiagen, Hilden, Germany

Table 3.1.10 Miscellaneous materials

Materials	Supplier
0.22 μm Cellulose acetate	8160, Corning
Cell culture T25 Non vented & vented flask	430168 & 430720, Corning
Cell culture T75 Non vented & vented flask	430639 & 430641, Corning
Micro titre plate, 96 well, clear bottom	655101, Geriner bio one
Micro titre plate, 96 well, opaque bottom	655076, Geriner bio one
OasisHLB	WAT094225, Waters Corporation, USA
PVDF	10600023, Amersham
HPLC Jupiter column	Phenomenex, 00G-4053-E0

Table 3.1.11 Instruments

Name	Company
AAnalyst 7000, Atomic absorption spectrophotometer	Perkin Elmer, USA
Agilent Series 1100 HPLC	Hewlett Packard, USA
Biologic Duo flow (Low pressure Liuid)	Bio-Rad, USA
DU 800 Spectrophotometer	Beckman Coulter,
Fluorchem FC3	Protein simple, USA
GeneAmp PCR system 9700	Applied Biosystem, USA
Spectramax M2^{e}	Molecular Devices, USA
Xevo G2-S Qtof ESI MS	Waters, USA

3.2 Methods

3.2.1 Indirect fluorescent Amplex red assay – LOX enzymatic assay

Indirect Amplex red fluorescence method was used to assess the enzymatic activity of LOX [54] with modification. This is an enzyme coupled reaction. The first step of this enzyme coupled reaction is catalyzed by LOX where LOX enzyme acts on the pseudo substrate, Diamino pentane (DAP) and converts it to its aldehyde form and releases hydrogen peroxide (H_2O_2). The released hydrogen peroxide reacts with Amplex red in the ratio of 1:1. The second reaction is catalyzed by horseradish peroxidase (HRP), it oxidise Amplex red **(**N-Acetyl-3, 7-dihydroxyphenoxazine) using hydrogen peroxide, which produces fluorescent resorufin. Resorufin was measured with an excitation maximum at 563 nm and with an emission maximum at 587 nm. The fluorescent intensity of resorufin is propositional to the amount of hydrogen peroxide released by the enzymatic activity of LOX.

Reagents

I. 1,5- Diamino pentane (DAP), 2 M
II. Hydrogen peroxide, 3%
III. Hydrogen peroxidase (HRP), 200 Units / mL
IV. Amplex red, 20 mM
V. Assay buffer (0.1 M boric acid, 0.15 M sodium chloride, pH 8.2)
VI. Milli-Q water

Table 3.2: Preparation of reaction mixture for Amplex red assay

S.No.	Constituents	Volume µL	Final conc. in 200 µL
1	Assay buffer	500	
2	Milli-Q water	486.5	
3	DAP	10	10 mM
4	HRP	1	0.1 Units / mL
5	Amplex red	2.5	50 µM

Protocol

Prior to the experiments, all the reagents were brought to RT. The assay was performed in micro titre 96-well black plate. The reaction mixture 100 µL and sample 100 µL were added to the wells and mixed. Readings were then taken in Spectramax M2^{e} for 90 mins at an interval of 5 min. The system temperature was maintained at 37 °C throughout the experiment.

3.2.1.1 Standard curve

Reaction rate of LOX was measured based on amount of hydrogen peroxide released. Thus using known concentration of hydrogen peroxide, standard curve was plotted for Amplex red assay. Standard curve was plotted from 0 – 2000 nanomoles of Hydrogen peroxide. The strength of the stock hydrogen peroxide was determined by titrating against standardized potassium permanganate. The standard curve was used to calculate the amount of hydrogen peroxide released by LOX present in the test samples.

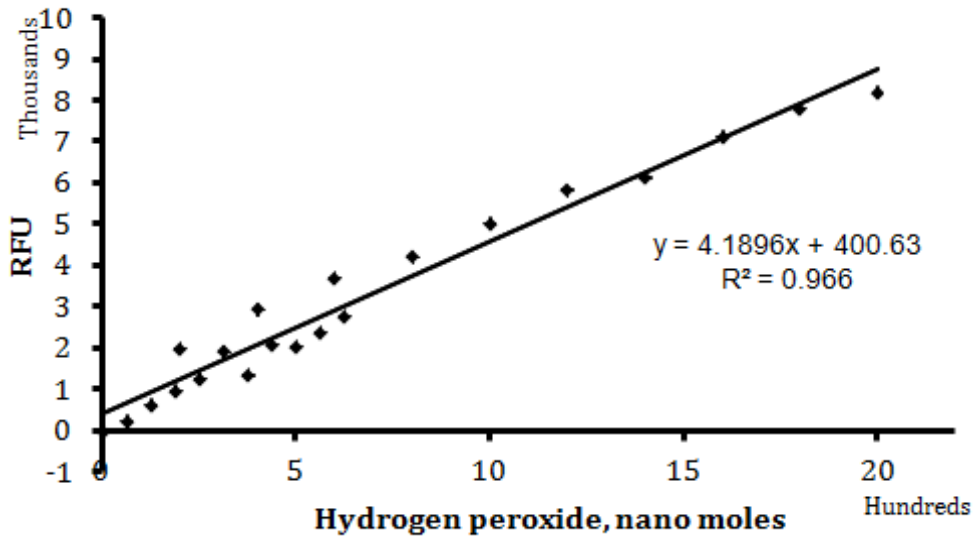

Figure 3.1: Amplex red standard curve. Standard curve was prepared by using stock hydrogen peroxide. Data shown represent mean ± SD from three independent experiments. (RFU – Relative Fluorescence Unit)

3.2.2 Protein estimation- Bradford assay

Bradford assay is a colorimetric protein quantification method where Coomassie G-250 dye acts as the chormogen. In acidic pH, protein binds to the reddish/brown dye (465 nm) and forms a bluish colored protein-dye complex (610 nm). This complex is measured at 595 nm.

Reagent- Bradford assay kit
Standard – Bovine Serum Albumin (BSA), 1 mg/ 1 mL.

Table 3.3: Bradford assay protocol

PARTICULARS	BLANK	STANDARD	TEST
Normal saline (µL)	100	100	100
Reagent (µL)	100	100	100
Standard (µL)	-	1	-
Test (µL)	-	-	1
Incubated for 10 mins at RT and measured at 595 nm			

3.2.3 Sodium Dodecyl sulphate – Poly Acrylamide Gel Electrophoresis (SDS-PAGE)

SDS-PAGE was used to assess the protein expression and purification process. For all experiments, 10 % SDS-PAGE gels were used.

Materials required

- Acyrlamide (30%): Acrylamide - 29.2 g, Bisacrylamide - 0.8 g, Milli-Q water - 100 mL
- Tris-HCl 1.5 mM, pH 8.8
- Tris-HCl 0.5 mM, pH 6.8
- Running buffer: 0.025 M Tris, 0.192 M glycine and 0.1 % of SDS, pH 8.6.
- Laemmli buffer (2X): 4 % SDS, 20 % glycerol, 10 % 2-mercaptoethanol, 0.125 M Tris pH 6.8, 0.004 % bromophenol blue.

- 10 % Ammonium per sulphate (APS)
- 10 % Sodium Dodecyl sulphate (SDS)
- Tetra methyl ethylene diamine (TEMED)

Table 3.4: Preparation of SDS – PAGE gel

S. No.	Reagents	Stacking gel (4 %)	Separating gel (10 %)
1.	Acrylamide 30 % (mL)	1.33	2.5
2.	Tris HCl (mL)	2.5 (pH 6.8)	3.33 (pH 8.8)
3.	Milli-Q water (mL)	6.1	4.17
4.	10 % APS (µL)	50	50
5.	10 % SDS (µL)	100	100
6.	TEMED (µL)	5	10

.

Samples were mixed with equal volume of 2 X Laemmli buffer and boiled for 10 mins. Then the samples were loaded on to the gel and electrophoresis was performed at 90 V current. After separation, bands were visualized by silvers staining method.

3.2.3.1 Silver staining

Materials Required:

- Sodium thiosulphate -120 mg/ 100 mL of Milli-Q water
- Stain - Silver nitrate -250 mg/ 125 mL of Milli-Q water with 50 µL of formalin
- Developer -Sodium carbonate - 2% of sodium carbonate with 50 µL of formalin
- Stopping solution- 7% acetic acid

Procedure:

1. Sodium thiosulphate was added to the gel and rocked for 1 min.
2. Silver nitrate was added, and incubated for 20 min.
3. Three washes of Milli-Q water were done
4. Sodium carbonate was added cold to the gel was used for developing the gel.
5. The reaction was stopped using acetic acid and gel was kept in Milli-Q water and gel was documented

3.2.3.2 Western Blot

Western blot is an analytical method used to detect protein of interest in the sample. Initial sample was separated by SDS-PAGE and then electro transferred onto nitrocellulose membrane. Transfer was facilitated by application of 100 V of current and the system was maintained by transfer buffer (25 mM Tris, 190 mM glycine, 20% methanol and 0.1% SDS). After transfer, the membrane was blocked with 5 % skimmed milk to prevent non – specific binding of the primary antibody. The membrane was then incubated with primary antibody of protein of interest overnight at 4^{o}C. The membrane was washed with PBST thrice and was incubated with specific secondary antibody conjugated with enzyme (HRP / AP) for 2 h at room temperature. The membrane was washed thrice with PBST and finally once with PBS. Then the membrane was developed with ECL kit and was visualized using FC3 fluorchem instrument.

3.2.4 Purification of Lysyl oxidase from aorta

3.2.4.1 Homogenization

Bovine aorta was procured from slaughter house and washed with 16 mM potassium phosphate buffer, pH 7.0 and stored in -80^{o}C till it was processed. Cleaned aorta was cut into small pieces and then homogenized using mechanical blender with 2.5 mL of 16 mM potassium phosphate buffer, pH 7.0 containing 5 M urea for 1 gram of the tissue. The homogenate was centrifuged at 10,000 rpm for 30 min at 4^{o}C and the supernatant was collected, this procedure was performed twice and collected supernatant was pooled.

Salting out was performed to concentrate the protein by saturating with 70% ammonium sulfate and then centrifuged at 10,000 rpm for 30 mins and the pellet was collected. The pellet was dialyzed against 16 mM potassium phosphate buffer with 5 M urea to remove the ammonium sulfate salt. Dialysis was performed at 4^{o}C for 48 h using dialysis membrane with a pore size of 3kDa. The dialyzed solution was clarified by centrifugation at 10,000 rpm for 30 min and applied to a weak anion exchange column.

3.2.4.2 Isolation of LOX by weak anion exchange chromatography

Weak anion exchange chromatography was performed to purify LOX from the dialysate supernatant. Here, Diethylaminoethanol (DEAE) acts as the weak anion exchanger and it binds to the negatively charged proteins. Elution is generally performed by increase in the ionic strength or pH using gradient buffer system. DEAE-cellulose beads were activated and packed into the column without any air bubble. Column volume was calculated using blue dextran and Low pressure liquid chromatography (LPLC) was performed.

Run program

Buffer A: 16 mM potassium phosphate with 5 M urea, pH 7.0.
Buffer B: 0.4 M sodium chloride in buffer A.
Elution method: Linear gradient.
Detection: UV absorbance at 280 nm using 0.1 mm flow cell.

Table 3.5: LC parameters for ion exchange chromatography

S.No.	Buffer B, %	Time, mins	Flow rate, mL / min
1	0	0	0.2
2	0	30	0.2
3	100	270	0.2
4	100	300	0.2
5	0	315	0.2
6	0	345	0.2

The fractions were collected in an automated fraction collector. Each fraction tube collects elutes for 15 min. The protein concentration was assessed by Bradford method and LOX activity of all the fraction was estimated by indirect fluorescent Amplex red assay.

3.2.5 Cloning of mLOX gene

3.2.5.1 Construction of pQE-30-Xa +mLOX vector

DNA cloning or molecular cloning refers to the procedure of isolating a defined DNA sequence and obtaining multiple copies of it *in vitro*. Cloning is frequently employed to amplify DNA fragments containing genes, but it can be used to amplify any DNA sequence such as promoters, non-coding sequences, chemically synthesized oligonucleotides and randomly fragmented DNA. Cloning is used in a wide array of biological experiments and technological applications such as large scale protein production.

Human mLOX was cloned in the bacterial expression pQE30-Xa vector by infusion cloning method. Infusion cloning is based on the principle of sequence and ligation independent cloning (SILC) [151]. Here, target DNA will contain single stranded nucleotide (15 – 22 nos) over hangs on both ends. These over hangs will be complementary to the selected vector restriction site and allow annealing of insert DNA to vector during the infusion reaction.

3.2.5.2 Features of pQE 30-Xa vector

It is a bacterial expression vector that works based on the T5 promoter transcription-translation system. This T5 promoter is controlled by two lac operon operator sequence. The high translation rate of gene of interest is ensured by the presence of Ribosomal Binding Site (RBS II). The gene of interest will be inserted into plasmid with the help of restriction enzyme sites in the multiple cloning sites. The expressed protein will contain 6X His tag at N-terminal, which help in single step affinity purification of over expressed protein. Factor Xa recognition site is encoded between His tag and protein sequence, enabling removal of his tag from the target protein after purification using the enzyme Factor Xa. The vector contains β-lactamase gene (bla), hence the bacterial strain transformed exhibit resistance to ampicillin antibiotic.

3.2.5.3 Sequence retrieval of mLOX

In humans, LOX gene was mapped to 5q23 chromosome. Complete gene sequence of human LOX with the NCBI Accession ID NM_002317 and with the version ID of NM_002317.5 is available in the NCBI database. Coding sequence of LOX gene lies from 376 to 1629 bp of the total 5177 bp. Of the coding sequence, 376 to 438, 439 to 879 and 880 to 1626 encode signal peptide, a propeptide and mature LOX, respectively. In order to clone the mLOX, a primer was designed to amplify the nucleotide sequence from 880 to 1629 (totally 750 bp) of the LOX CDS region.

Box 3.1: Amino acid and coding sequences of mature LOX

249 Amino acid residues

N-Terminal(169)-
DDPYNPYKYSDDNPYYNYYDTYERPRPGGRYRPGYGTGYFQYGLPDLVADPYYIQASTYVQKMSM
YNLRCAAEENCLASTAYRADVRDYDHRVLLRFPQRVKNQGTSDFLPSRPRYSWEWHSCHQHYHSM
DEFSHYDLLDANTQRRVAEGHKASFCLEDTSCDYGYHRRFACTAHTQGLSPGCYDTYGADIDCQW
IDITDVKPGNYILKVSVNPSYLVPESDYTNNVVRCDIRYTGHHAYASGCTISPY(417)-**C Terminal**

750 base pair Gene coding sequence

5′GACGACCCTTACAACCCCTACAAGTACTCTGACGACAACCCTTATTACAACTACTACGATACT
TATGAAAGGCCCAGACCTGGGGGCAGGTACCGGCCCGGATACGGCACTGGCTACTTCCAGTACGG
TCTCCCAGACCTGGTGGCCGACCCCTACTACATCCAGGCGTCCACGTACGTGCAGAAGATGTCCA
TGTACAACCTGAGATGCGCGGCGGAGGAAAACTGTCTGGCCAGTACAGCATACAGGGCAGATGTC
AGAGATTATGATCACAGGGTGCTGCTCAGATTTCCCCAAAGAGTGAAAAACCAAGGGACATCAGA
TTTCTTACCCAGCCGACCAAGATATTCCTGGGAATGGCACAGTTGTCATCAACATTACCACAGTA
TGGATGAGTTTAGCCACTATGACCTGCTTGATGCCAACACCCAGAGGAGAGTGGCTGAAGGCCAC
AAAGCAAGTTTCTGTCTTGAAGACACATCCTGTGACTATGGCTACCACAGGCGATTTGCATGTAC
TGCACACACACAGGGATTGAGTCCTGGCTGTTATGATACCTATGGTGCAGACATAGACTGCCAGT
GGATTGATATTACAGATGTAAAACCTGGAAACTATATCCTAAAGGTCAGTGTAAACCCCAGCTAC
CTGGTTCCTGAATCTGACTATACCAACAATGTTGTGCGCTGTGACATTCGCTACACAGGACATCA
TGCGTATGCCTCAGGCTGCACAATTTCACCGTATTAG-3′

3.2.5.4 Designing of infusion specific primers

Nucleotide sequence of mLOX was retrieved from the NCBI database as described below. Infusion cloning primers were designed with the manufacturer's online tool with selected vector (pQE30-Xa vector), mLOX sequence and restriction enzymes (*Stu*I and *Hin*dIII).

Forward primer**:** (has the restriction site of *Stu*I)

GGTATCGAGGGAAGGCCTATGCGCTTCGCCTGGACC

Reverse primer: (has the restriction site of *Hin*dIII)

TCAGCTAATTAAGCTTCTAATACGGTGAAATTGT

3.2.5.5 PCR amplification of mLOX gene for infusion cloning

Human Umbilical Vein Endothelial Cells (HUVECs) express the LOX protein. The cDNA of HUVECs was used for preparation of mLOX gene insert for cloning. HUVECs total RNA was isolated by TRIZOL method and template cDNA was synthesized using iScript cDNA synthesis kit method. PCR was set using prepared HUVECs cDNA as template with the designed infusion primer as below.

Table 3.6: PCR protocol for LOX DNA inserts amplification

Contents	Volume, µL
DNTPs	4 µL
Buffer (10 X)	2.5 µL
FP (10 pmols)	1.5 µL
RP (10 pmols)	1.5 µL
Taq Polymerase	0.3 µL
Milli-Q water	13.2 µL
cDNA	2.0 µL
Total volume	25 µL

A negative control was also set. (The above reaction mix was prepared where instead of cDNA, Milli-Q water was added)

Touchdown PCR profile

Step 1: 95°C, 2 min.
Step 2: 95°C, 30 sec.
Step 3: 53.1°C decrease 0.5°C per cycle, 30 sec.
Step 4: 72°C, 80.0 sec.
Step 5: Steps 2 – 4 repeated 14 times
Step 6: 95°C, 30 sec.
Step 7: 46.1°C, 30 sec.
Step 8: 72°C, 80.0 sec.
Step 9: Steps 6 – 9 repeated 19 times
Step 10: 72°C, 5 min.
Step 11: 4°C, hold.

The PCR product was run in 2% agarose gel and was visualized using ethidium bromide under UV light. The PCR-amplified mLOX DNA was eluted by gel extraction method.

3.2.5.6 Linearization of pQE-30Xa vector

Vector was linearized using the selected S*tu*I and H*ind*III restriction enzymes. Reaction mixture was prepared as mentioned in the below table. The reaction mixture was incubated at 37 °C for 16 hours. The digested product was run in 1 % agarose gel along with molecular weight marker. After electrophoresis, gel elution was carried out to purify the digested product by gel extraction method.

Table 3.7: Reaction protocol for vector digestion

Reagents	Volume	Final Concentration
10X Buffer	2 µL	1 X
DNA	5 µL	2 µg
*Stu*I	0.5 µL	2 U
*Hind*III	0.5 µL	2 U
Milli-Q water	2 µL	
Total volume	10 µL	

3.2.5.7 Infusion reaction and Transfection

The infusion reaction was performed as per the manufacture's instruction. Infusion reaction mixture contained linearized vector and DNA insert in the molar ratio 2:1 with infusion enzyme.

Table 3.8: Reaction protocol for infusion reaction

Reagents	Volume,
5X In-Fusion HD Enzyme Premix	2.0 µL
Linearized Vector (100 ng)	4.0 µL
PCR DNA insert (45 ng)	2.6 µL
Milli-Q water	1.4 µL
Total volume	10.0 µL

The total reaction volume was made up to 10 µL using sterile Milli-Q water. The Reaction mixture was incubated at 50°C for 15 min, and then was placed on ice. Then the infused vector DNA product was transfected into the competent cells and inoculated on to the selective LB plate.

3.2.5.8 Transformation of pQE-30-Xa + mLOX vector into competent M15 *E.coli* strain

Transformation is an important step in the cloning process. In transformation, foreign DNA will be taken up by bacteria under laboratory conditions. There are two types of transformation methods: chemical method and electroporation method. The method here followed is chemical transformation method using calcium chloride.

Chemical method follows two steps: 1) Bacterial cells will be converted into competent cells to take up the plasmid DNA by treating with polyvalent cations ($CaCl_2$ / $MgCl_2$). At a low temperature when the bacterial cells are exposed to cations, their membrane channels will be opened transiently. 2) Second phase is heat shock. Here competent bacterial cells were mixed with plasmid DNA and were exposed to 42°C for 60 – 120

sec. then the cells will be recovered in complete LB media and inoculated on to the selective LB agar plate. The competent cells which are successfully transformed and expressing the plasmid will grow on the selective LB agar plate.

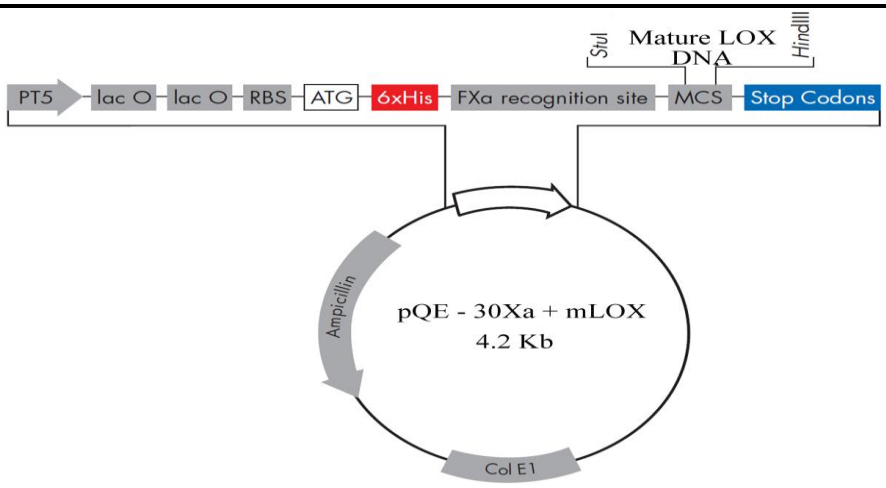

Figure 3.2: pQE-30-Xa + mLOX vector map. Adapted from Qiagen manual.

Recovery phase is where the heat shock competent cells were suspended in the sterile LB media and was incubated at 37 °C for 1 h. then the cells were inoculated on to the selective LB plate. The competent cells which are successfully transformed and expressing the plasmid will grow on the selective LB agar plate.

Reagents required:

1. Luria-Bertani (LB) media (autoclaved)
2. 1 M $CaCl_2$ (filter sterilized)
3. 0.1 M $CaCl_2$ (filter sterilized)
4. 50 % Glycerol (sterilized by steaming)
5. 1 M $CaCl_2$ + 15 % glycerol (sterilized by steaming)
6. Sterile LB media, non-selective (Sterilized by autoclaving)
7. Sterile LB agar plate (ampicillin 100 µg / mL and kanamycin 25 µg / mL)

Competent cell preparation

1. Overnight culture of *E.coli* strain was suspended in the sterile LB media to a final concentration of 1 % and was incubated at 37 °C.

2. Cells were pelleted down when culture is in growth phase i.e. optical density (OD) of the culture was between 0.4 and 0.6 at 600 nm wavelength.
3. Then cells were re-suspended in 0.1 M $CaCl_2$ and were incubated at 4 °C for 30 min.
4. The cells were centrifuged at 15,000 rpm for 10 min at 4 °C.
5. Then the pellet was re-suspended in 1 M $CaCl_2$ with 15 % glycerol. Thus the bacterial cells were converted to the competent bacterial cells, which can take up the exogenous plasmid DNA. The cells will be competent for 6 months at -80 °C.

Transformation procedure

1. Competent cells were mixed with plasmid DNA and were incubated at 4^oC for 30 minutes. Generally, 25 ng of plasmid DNA was added for 50 µL of competent cells.
2. The cells were exposed to 42 °C for 90 seconds and immediately transferred to 4^oC, providing heat shock to the cells.
3. After heat shock, the cells were incubated with 750 µL of LB media at 37 °C for 1 h with gentle shaking.
4. The cells were centrifuged at 10,000 rpm for 3 min, pellet was re-suspended with 300 µL of LB media. The 300 µL inoculums was inoculated on to selective LB agar plate (kanamycin 30 µg / mL and ampicillin 100 µg / mL) by spread plate method and was incubated at 37 °C for 24 h.
5. Transformed competent cells which expressed plasmid containing antibiotic resistant gene were grown on the selective plate.
6. To confirm the transformation, plasmid was isolated from the clones on selective LB agar plate. The isolated plasmid was subjected to restriction digestion with Stu I and HIND III and the restriction product was subjected to 2 % agarose gel electrophoresis.

3.2.5.9 DNA Sequencing

To confirm that there was no mutation in the insert DNA, the isolated vector constructs were subjected to DNA sequencing. The sequencing was performed based on the Sanger's dideoxy method in ABI 3100 - Avant Genetic Analyzer. With the infusion primers the LOX insert DNA was amplified from the isolated plasmid DNA and was sequenced. The resulting sequence was analyzed by Bio-edit software.

3.2.6 Expression of recombinant mLOX in M15 (pREP4) *E.coli*

3.2.6.1 Optimization of recombinant mLOX expression

Expression of insert DNA in the pQE-30Xa vector is control by double lac promoter and T5 operator system. Isopropyl β-D-1-thiogalactopyranoside (IPTG) is an analog of allolactose, a lactose metabolite. IPTG was used as a molecular mimic of allolactose that triggers transcription of the lac operon. IPTG binds to the lac operon and releases the tetrameric repressor from the lac operator and allows the binding of DNA polymerase to the T5 operator system and leads to the transcription of the gene. IPTG is not metabolized by *E.coli* thus maintaining the concentration constant throughout the induction. Expression of mLOX from *E.coli* M15 (pREP4) was standardized for concentration and time of IPTG induction (0.2 – 1 mM) and time for induction (2, 4, 6 and 16 h) at 30^{o}C. The conditions were examined and the optimal concentration and time were standardized and used further. After inducing with the respective conditions, 20 µL of broth was boiled with 5 µL 5X Laemmli bbuffer and subjected to 10% SDS –PAGE and visualized by Coomassie staining.

3.2.6.2 Purification of recombinant mLOX

Purification was based on one step affinity purification using Ni-NTA (Nickel – Nitrilotriacetic acid) agarose beads.

Materials required

1. Ni-NTA (Nickel – Nitrilotriacetic acid) agarose beads
2. Protease inhibitor cocktail (PIC)
3. Lysis buffer: 50 mM sodium dihydrogen phosphate, 300 mM sodium chloride and 8 M urea with PIC, pH 8.0.
4. Wash buffer: 30 mM of imidazole in lysis buffer.
5. Elution buffer: 250 mM of imidazole in lysis buffer.

Consecutive 6 histidine residues form the 6X His tag; this exhibits higher affinity towards Ni-NTA. The recombinant mLOX contains 6X His tag at its N-terminal. Thus mLOX will binds to Ni-NTA with higher affinity than other *E.coli* proteins. The bound mLOX was eluted by affinity displacement. After treating with *E.coli* lysate Ni-NTA agarose beads were washed with 25 mM imidazole buffer to remove non-specifically bound proteins. Then mLOX was eluted with 250 mM imidazole buffer.

Preparation of M15 (pREP4) cell lysate:

After IPTG induction the cells were pelleted down by centrifugation at 7,500 rpm for 20 min. Then the pellet was suspended in lysis buffer. The cell suspension was sonicated for 30 seconds for 3 cycles. After sonication, cell debris was removed by centrifugation at 10,000 rpm for 30 min. The supernatant was further purified.

Ni-NTA agarose beads were packed into a column. The column was then equilibrated with lysis buffer. The supernatant was passed through the equilibrated Ni-NTA column. To remove any non-specific proteins, the column was washed with 10 mL of wash buffer. Then bound the 6X His tag mature LOX was eluted from the column by treating the column with 10 mL elution buffer. Throughout the process 0.20 mL / minute flow rate was maintained. Then the fractions were examined by performing electrophoresis on a 10% SDS-PAGE gel to determine the fraction containing mLOX.

3.2.7 Confirmation and Purity of recombinant mLOX

The recombinant mLOX protein purity was assessed by SDS-PAGE and Western blot as described in the section 3.2.3.

3.2.7.1 Confirmation of recombinant mLOX by Mass spectroscopy

Mass spectroscopy (MS) has become the method of choice for all proteomic approaches available so far. As the name indicates, "mass spectrometry" determines the molecular mass of a charged particle by measuring its mass-to-charge (*m/z*) ratio. Basically, a mass spectrum is a plot of ion abundance versus *m/z.* MS consists of an ion source that converts molecules to ionized analytes, a mass analyser that resolves ions according to *m*/*z ratio,* and a detector that registers the number of ions at respective *m*/*z* value. Three key factors determine mass analyser viz: sensitivity, resolution, and mass accuracy. The sensitivity, resolution, and accuracy of advanced mass spectrometers help in detecting femto gram levels of individual proteins in complex mixtures. MS is a powerful analytical technique used to quantify known materials, to identify unknown compounds within a sample, and to elucidate the structure and chemical properties of different molecules.

Tryptic digestion of mLOX

For MS analysis, mLOX were reduced with DTT, alkylated with IAA and subjected to tryptic digestion. Trypsin cleaves the polypeptide at the carboxy terminal of lysine and arginine residues. Thus the mLOX is converted into peptide fragment. These peptide fragments were analyzed in Xevo G2S QTOF MS. The resulting MS spectrum was analyzed by the PLGS (Protein Lynx Global Server) software 2.5.3 using Uniprot protein database as protein library.

Reagents:

1. Ammonium bicarbonate 50 mM, pH 9.5
2. Dithiothreitol (DTT) 100 mM
3. Iodo acetic acid (IAA) 20 mM
4. Sequencing grade Trypsin

Flow chart 3.1: Mass spectroscopy sample preparation

1µg of protein (mLOX)

↓

Added 50 µL of 50 mM ammonium bicarbonate [$(NH_4)_2CO_3$].

↓

Added 1 µL of 100 mM DTT and incubated at 60 °C for 15 min.

↓

After that added 1 µL of 20 mM IAA added and incubated at RT for 30 min.

↓

Added 1:20 ratio of Trypsin to protein and incubated at 37^0C overnight.

↓

Reaction was stopped by addition of 2 µL of formic acid and kept at RT for 20 minutes.

↓

Centrifuged at 10,000 rpm for 5 minutes and supernatant was vacuum dried

↓

Reconstituted with 25 µL of 2% acetonitrile + 0.1 % TFA

↓

Pass through 0.22 µ cellulose acetate column by centrifugation at 12,000 rpm for 15 min.

↓

Analyzed by nano UPLC ESI MS

3.2.8 Refolding of recombinant mLOX

3.2.8.1 Screening for various buffers

Recombinant mLOX was purified under denaturing condition (8 M urea). In order to refold and to prevent aggregation of purified mLOX protein in solution devoid of urea, it

was screened with various buffers of pH ranging from 7 to 9. For screening, 50 µg of recombinant mLOX was suspended in 50 µL of buffer and allowed to stand for 15 min in RT. Screening was performed as follows

1. After incubation, solution was checked for visible aggregation.
2. Centrifuged at 10,000 rpm for 10 min and checked for pellet.
3. Protein in the supernatant was estimated and compared with the initial protein concentration.

Table 3.9: Screening of various buffers for recombinant mLOX solubility

Buffer	Visible aggregation check	Centrifugation at 10,000 rpm for 10 mins	Protein conc. compared to the original conc.
HEPES buffer	Aggregated	Pelleted	Less than 10 %
Tris Buffer	Aggregated	Pelleted	Less than 1 %
Potassium phosphate buffer	Aggregated	Pelleted	Less than 20 %
Borate buffer	No aggregation	Small pellet	50 %
Arginine buffer	Aggregated	Pelleted	Less than 10 %
Glycine – NaOH buffer	No aggregation	No pellet	More than 95 %

By this screening procedure, it was identified that in 200 mM glycine-NaOH buffer with 10 % glycerol at pH 8.0 purified mLOX will be in solution form without any aggregation.

3.2.8.2 Dialysis - Removal of urea from recombinant mLOX

Dialysis is the movement of molecules by diffusion from high concentration to low concentration through a semi-permeable membrane. Only those molecules that are small enough to pass through the membrane pores are able move through the membrane and reach equilibrium with the entire volume of solution in the system. Once equilibrium is reached, there is no further net movement of the substance because molecules will be

moving through the pores in and out of the dialysis unit at the same rate. By contrast, large molecules that cannot pass through the membrane pores will remain on the same side of the membrane as they were since the dialysis was initiated. To remove unwanted substance, it is necessary to replace the dialysis buffer so that a new concentration gradient can be established. Once the buffer is changed, movement of particles from high (inside the membrane) to low (outside the membrane) concentration will resume until equilibrium is once again reached. With each change of dialysis buffer, substances inside the membrane are further purified by a factor equal to the volume difference of the two compartments.

The purified protein in the urea solution was dialysed using the 3 kDa membrane against 200 mM glycine-NaOH buffer, pH 8.0 along with 10% glycerol (glycerol act as co-solvent) for 8 hrs with stepwise reduction in the urea concentration from 8 M to 0 M urea. Checked for aggregation by visually and centrifugation at high speed at each step.

3.2.8.3 His tag removal from recombinant mLOX

His tag from the N-terminal of the purified mature LOX was cleaved using the Factor Xa enzyme following the manufacturer's instruction (Qiagen) with modification. Mature LOX was suspended in 200 mM glycine-NaOH buffer with 10% glycerol and 2 mM calcium chloride and incubated overnight at 37 °C. Two units of factor Xa enzyme was used to cleave 25 µg of purified protein. Then reaction was stopped using the factor Xa removal resin and the His tag uncleaved protein was removed using Ni-NTA. His tag cleaved protein was subjected to western blotting along with the uncleaved protein and was probed separately with His tag antibody and LOX antibody.

3.2.8.4 Estimation of copper in recombinant mLOX

Copper bound in the recombinant mLOX was estimated by atomic absorption spectroscopy (AAS) (Perkin Elmer AA700). Every element emits excess of energy in

unique wavelength to achieve stable ground state level from the high energy level. Based on this principle metals will be identified in AAS. The concentration of each element will be determined by absorption spectrometry, which work based on Beer- Lambert law.

Materials required:

- Vials
- Nitric acid - 0.2 % HNO_3 prepared in Milli-Q water.
- Purified mLOX.

Purified mLOX (100 μg / 100 μL) was reconstituted to 1 mL using 0.2 % nitric acid and Cu was estimated using hallow cathode lamp Cu was estimated using a hallow cathode lamp. Cu was atomized at the 23000°C detected using graphite furnace system.

3.2.9 Characterization of recombinant mLOX

The pH dependence, temperature dependence, substrate specificity, secondary structure measurement by Far-UV spectrum, and kinetic values were determined for the purified mLOX. Activity was assessed by Amplex red assay as explained in the section 3.2.1.

3.2.9.1 Secondary structure analysis and thermal stability measurement of recombinant mLOX

Far UV - Circular Dichroism (CD) spectroscopy was employed to analyze secondary structure and thermal denaturation of mLOX. The sample was analyzed with JASCO J815 CD spectrometer (Biotechnology department, IIT, Madras) using quartz cell of 1 mm path length. The CD spectrum was collected between 200 and 240 nm with mLOX concentration of 1 mg / mL. The percentage of secondary structure was analyzed by K2D2 online software with the resultant spectrum. To determine thermal stability, the system temperature was steady increased from 20 °C to 80 °C with mLOX in the cuvette. After the system reaches 80 °C, CD spectrum was collected again. The structural stability can be assessed by difference in the spectrum between 20 °C and 80 °C. For all samples, three spectra were collected and accumulated average was taken for final analysis.

3.2.9.2 Intrinsic fluorescence of recombinant mLOX

Intrinsic fluorescence of a protein arises from the aromatic amino acids (Tryptophan, Tyrosine and Phenylalanine) present in it. Among the three amino acids, tryptophan is used to probe the folding of the protein. Besides, emission spectrum of tryptophan alone can be collected by exciting specifically at 295 nm and quantum yield is comparatively higher than other two amino acids [152]. Tryptophan emission spectrum is based on the position and environment where it localizes in a protein. Tryptophan present in the surface will give emission maxima above 340 nm and based on the degree of buried nature and environment the emission can be quenched.

Protocol:

Tryptophan fluorescence of mLOX was measured using SpectramaxM2^{e} instrument. Fluorescence emission spectra were taken by excitation at 295 nm and recorded over the range of 300 – 400 nm. The mLOX (3 μM) was suspended in 200 μL in 200 mM of glycine-NaOH buffer, pH 8.0 with 10% glycerol.

3.2.9.3 Extrinsic Fluorescence of recombinant mLOX

In several proteins, the natural fluorescence property of macromolecules is not adequate for the desired experiment. In this case the fluorophore foreign to the system under study but displaying improved spectral properties are chosen. They can be either covalently or non-covalently bound to the protein. The fluorescence signal reflects polarity of the molecules surrounding the polarity-sensitive probe. If the dye has a specific binding site on a macromolecule, it is possible to assess the polarity of the site. The dye is thus a useful probe of the degree of exposure of hydrophobic sites as the structure of a protein is perturbed [16]. The selection of the dye generally depends on application. In cases where, sensitivity is critical, such as ligand binding, the visible-absorbing fluorescein dyes with high molar absorptivity and quantum yields are frequently used. Dansyl chloride is widely used to label proteins where polarization measurements are anticipated. l-Anilino-8-napthalene sulfonic acid (1,8-ANS or ANS), 2-p-11 toluidinylnapthalene-6-sulfonic

acid (2,6-TNS or TNS), and similar derivatives are frequently used as non-covalent labels for proteins and membranes. ANS is essentially non fluorescent in water, but are highly fluorescent when dissolved in non-polar solvents or when bound to macromolecules [17]. It binds only to small hydrophobic pockets on a protein's surface and, hence, generally does not bind to native proteins. This therefore provides a useful method to track protein folding.

Protocol:

Extrinsic Fluorescence of mLOX was measure by ANSA binding using SpectramaxM2^{e} instrument. Fluorescence emission spectra were taken by excitation at 370 nm and recorded over the range of 400 – 500 nm. The mLOX (3 μM) was suspended in 200 μL in 200 mM of glycine-NaOH buffer, pH 8.0 with 10% glycerol and ANSA was added in 1:100 ratios to mLOX.

3.2.9.4 Immuno fluorescence staining of Collagen

Collagen is one of the endogenous substrates for LOX. So mature LOX will augment the cross linking of collagen cross. ARPE-19 cells were grown to 70 - 80% confluence and serum starved overnight. Then treated with various concentrations of recombinant mLOX for 72 h and stained for collagen by immuno fluorescence method. TGF-β was used as the positive control for this experiment.

Immuno fluorescence principle**:**

Immuno fluorescence staining is a fluorescent microscopy based visualization of the interaction between an antigen and the specific fluorescent labelled antibody. After fixing and permeabilizing, cells will be treated with the primary antibody for the target protein and incubated with fluorescent labelled antibody, which serve as the reporter. Then the cells will be visualized with fluorescent microscope under specific excitation and emission filters respective to the fluorescent tag.

Reagents

a. Para formaldehyde, 4 % in PBS (pH 7.0)
b. Triton X 100, 0.2 % in PBS.
c. BSA, 2.5 % in PBS
d. Primary antibody in 2.5 % BSA in PBS.
e. FITC conjugated secondary antibody in 1:700 dilution.
f. DAPI (4,6 Diamino 2 phenylindol, Sigma).
g. Stock: 5 mg/mL in PBS (pH7.0); Working: 1:50000 dilutions in PBS

Flow chart: 3.2: Immuno fluorescence staining protocol

Cells were plated in 24 wells plate with 22 mm cover slip

↓

At 70 - 80 % confluence, serum starved overnight and exposed to conditions

↓

Washed thrice with ice-cold PBS

↓

Fixed with 4 % para formaldehyde for 20 min at RT

↓

Permeabilized with 0.2 % triton for 10 min at RT

↓

Blocked by 2.5 % BSA in PBS for 10 min at RT

↓

Primary antibody for overnight at $4^{o}C$

↓

Washed thrice with PBS

↓

FITC conjugated secondary antibody for 1 h at RT in dark

↓

Washed thrice with PBS

↓

Counter stained with DAPI (1:50,000) for 2 min at RT in dark

↓

Washed in PBST thrice and finally one wash in PBS

↓

Mounted with 50 % glycerol and viewed under fluorescent microscope.

3.2.10 In-House LOX antibody production

3.2.10.1 Production and purification of polyclonal antibody against recombinant mLOX

Recombinant mLOX, 2 mg of protein was used for raising polyclonal antibody in rabbit. By intra-peritoneal injection recombinant mLOX conjugated with Freund's complete adjuvant was injected into New Zealand white rabbit and immunized it. Booster doses of the same antigen conjugated with Freund's incomplete adjuvant were given on the 21st, 42^{nd} and 64^{th} days with the collection of bleed on every 14^{th} day from first injection and booster doses. From the immunized rabbit antibody was purified from the antisera by affinity purification. Immunization and purification of antibody was performed at BIOKLONE Company, Chennai. Sensitivity and specificity of the purified antibody was assessed by dot blot, indirect ELISA and immuno fluorescence.

3.2.10.2 Dot blot analysis

It is a modified technique of western blot. First, sample will be directly added to the nitro cellulose membrane without separation by electrophoresis and transfer. Then the protein of interest in the sample will be detected similar to the western blot technique. Here, the purified mLOX (antigen) was immobilized on the nitrocellulose membrane and then blocked with 5% skimmed milk to prevent nonspecific binding. Blot was incubated with in-house LOX antibody for 3 h and washed with PBS thrice and incubated secondary antibody for 1 h at RT, then visualized using Fluorchem FC3.

3.2.10.3 Indirect ELISA (Enzyme Linked Immuno Sorbent Assay)

Here, the antigen will be passively adsorbed to the solid micro titer plate and made to react with the specific antibody in the sample. The enzyme tagged secondary antibody [enzyme like, horseradish peroxidase (HRP) and alkaline phosphatase (AP)] reacts with

the specific substrate and gives rise to the chromogenic product. The intensity of the chormogen is proportionate to the concentration of antibody in the sample.

Reagents:

- Carbonate buffer, pH 9.6
- Phosphate buffered saline, pH 7.4 (PBS)
- Substrate solution: 4 mg of ABTS [(2,2'-Azino-di-3-ethyl benzthiazoline sulfonate) di ammonium salt] dissolved in 11 mL of 0.1 M citric acid with 10 µL of 30% hydrogen peroxide.
- Stopping solution: 0.1 % SDS (sodium dodecyl sulphate)

Protocol:

Each micro titer plate was coated with 500 ng of purified LOX (antigen) and was incubated at 4 °C overnight. The unbound antigen was removed by washing with PBS twice and blocked with 5% skimmed milk for 1 h at RT and washed twice with. Purified primary LOX antibody was added and incubated for 4 h at 37 °C, then washed twice with PBS and incubated with HRP conjugated secondary antibody (anti rabbit raised in goat, Santa Cruz) for 1 hr at RT. Blot was washed with PBST five times and finally with PBS. The HRP substrate, ABTS was added and kept in dark for 10 min and the reaction was stopped by adding 0.1 % SDS. The colour developed was read at 405 nm using fluorescent plate reader Spectramax M2^{e}.

3.2.10.4 Immuno fluorescence for LOX

Immuno fluorescence for the LOX protein was performed in HeLa cells. To check the sensitivity of in-house purified LOX antibody, immuno fluorescence was performed for LOX in HeLa cells at various dilutions and compared against the commercial LOX antibody (Santa Cruz). Protocol followed was as explained in the previous section 3.2.10.3.

3.2.10.5 Co-Immunoprecipitation (IP) for LOX

Using the in-house produced antibody, co immuno precipitation was performed to identify the interacting partners of LOX. Co-IP pull down assay was performed in the control human serum sample and in the cultured HUVECs' lysate.

Materials required:

- Co – IP kit – Pierce (26149)
- HUVECs' lysate
- Control human serum sample.

Principle: Co- immunoprecipitation (Co-IP) approach is used for studying protein-protein interactions, using a specific antibody to immunoprecipitate the antigen (bait protein) and co-immunoprecipitate any interacting proteins (prey proteins). This method allows pull down of interacting proteins under native condition without the antibodies as their light and heavy chain mask the protein of interest. Unlike tradition pull down assay where antibody is coupled to an agarose resin, in this method the antibody is cross linked covalently to an amine reactive bead thus making this technique more efficient and easy.
The pull down assay was started with the initial protein concentration of 500 μg in both the cases (serum and HUVEC lysate). Then the pull down assay was performed as per the instructions given by the manufacturer. After the pull down, the eluted protein was subjected to tryptic digestion and analyzed by MS as described in the section

3.2.11 Peptide designing

ClustalW2 is an EMBL-EBI developed online software [153]. It aligns multiple sequences of protein or DNA. The conserved sequences among the protein can be identified through the multi align program. Identified sequence may have similar structure and functional properties. FASTA format of all the members of LOX family was inputted and multi align program was run. From the multi align, conserved regions were identified and designed the following peptides (Table 3.10).

Table 3.10: LOX derived Peptide

S.No.	Sequence	Sequence position in LOX	Peptide name
1	WEWHSCHQHYH (11 mer)	Copper binding domain (286 - 296 amino acids)	M1
2	HSCHQHYH (8 mer)	Copper binding domain (289 – 296 amino acids)	M2
3	VAEGHKASFCLED (13 mer)	CRL domain (315 – 328 amino acids)	C1
4	ESDYTNNVVRCD (12 mer)	CRL domain (387 – 399 amino acids)	C2
5	DIDCQWIDITDV (12 mer)	CRL domain (358 – 370 amino acids)	C3

3.2.11.1 Peptide purity check using HPLC

LOX derived peptides were commercially procured from USV company. Peptides were prepared in the concentration of 1 mg/ mL in Milli-Q water and 10 µg was injected into HPLC (Agilent 110). Buffer A (0.1 % trifluoroacetic acid in Milli-Q water) and buffer B (0.1 % trifluoroacetic acid in 80 % of acetonitrile) were prepared. Buffers were filtered using 0.22 µ filter and degassed by ultra-sonication for 15 min. Linear gradient elution from 0 to 90 % was performed. HPLC column (Jupiter C18 column, particle size: 5 µm and pore size of 300 Å), flow rate of 0.5 ml/ min was used for peptide detection at 215 nm using variable wavelength detector for 1 h time point. All the peptides of 10 µg concentrations were injected in HPLC and analysis was performed.

LOX derived peptides were synthetically produced (USV peptides, India) and were tested for purity using Agilent HPLC system. All the peptides of 10 µg concentrations were injected in HPLC showed a single peak in VWD detector indicating the purity of the synthesized peptides.

3.2.11.2 Circular Dichroism (CD) spectroscopy for LOX derived peptides

Peptides were prepared at the concentration of 3 mg / mL in Milli-Q water. CD spectra were collected for free peptide and peptide treated with 100 µM copper chloride as described in the section 3.2.10.1.

3.2.11.3 Analysis of copper Binding property of designed peptide using Mass Spectroscopy

Cu binding experiments were performed using Xevo G2-S QTof mass spectrometer (Waters). Experiment was performed by direct infusion with a flow rate of 2.0 µL/min. The experiment was done in positive ion mode with resolution of 30,000. Peptides were reconstituted in 0.1% formic acid with 50% acetonitrile and infused at the final concentration of 10 µM. Mass spectra were collected for free peptide and peptide treated with copper. All spectra were measured at a scan rate of 0.014 s with the capillary voltage and cone voltage set at 3.0 kV and 30 V, respectively. The source temperature and the desolvation temperature were 80 °C and 150 °C, respectively and the flow rates were maintained at 50.0 l/h for cone gas flow and 600.0 l/h for desolvation gas flow. The acquired spectra (ranged between 50 and 2000 m/z) were analyzed as centroid data to establishing for the purity of the peptides and for studying copper binding property.

3.2.11.4 Effect of the designed peptide on recombinant mLOX activity

The designed peptides were incubated with recombinant mLOX and their effect on the enzymatic activity was assessed by Amplex red assay method.

3.2.12 Structure prediction of mLOX by *in silico* method

Three dimensional structural details from X-ray crystallography and NMR are not available for LOX and its family members. To develop a basic understanding about LOX structural details, we attempted to predict the 3D structure of mature LOX with its ligand, copper ion by *in silico* approach. With the predicted structure docking studies were done.

Sequence Retrieval: The amino acid sequence of human LOX was retrieved from the UniProtKB server (The Universal Protein Resource (UniProt) is a comprehensive resource for protein sequence and annotation data)[154] LOX UniProt accession ID: **P28300**

The 3 regions of amino acid sequence of LOX containing 417 residues are ,

- Signal peptide region : 1- 21
- Propeptide region : 22 -168
- Active chain region : 169 - 417

In order to study the function and interaction of the active enzyme, we selected the active chain region from 169 – 417 residues for our 3D structure prediction studies. Below represented is the amino acid sequence of pre pro-LOX with the mLOX sequence in "bold font"**:**

*MRFAWTVLLLGPLQLCALVHCAPPAAGQQQPPREPPAAPGAWRQQIQWENNGQVFS LLSLGSQYQPQRRRDPGAAVPGAANASAQQPRTPILLIRDNRTAAARTRTAGSSGVTAG RPRPTARHWFQAGYSTSRAREAGASRAENQTAPGEVPALSNLRPPSRVDGMVG**DDPY NPYKYSDDNPYYNYYDTYERPRPGGRYRPGYGTGYFQYGLPDLVADPYYIQASTQ KMSMYNLRCAAEENCLASTAYRADVRDYDHRVLLRFPQRVKNQGTSDFLPRYW EWHSCHQHYHSMDEFSHYDLLDANTQRRVAEGHKASFCLEDTSCDYGYHRFA CTAHTQGLSPGCYDTYGADIDCQWIDITDVKPGNYILKVSVNPSYLVPESDYTNN VVRCDIRYTGHHAYASGCTISPY***

3.2.12.1 Secondary structure prediction of mLOX by PSIPRED

Secondary structure of mLOX sequence was predicted using the **PSIPRED** online tool [155]. It works based on the PSI-BLAST (Position Specific Iterated – BLAST). Here query protein sequence will be aligned pairwise against the iterated profile by PSI-BLAST. PSIPRED output has the highest accuracy when compared to the available algorithms.

3.2.12.2 Modelling of mLOX

Amino acid sequence of mLOX was aligned against PDB (Protein Data Bank) using BLAST (Basic Local Alignment Search Tool). With the current PDB database, mLOX share the sequence similarity of less than 25 %. Thus, there is no reliable template protein structure available to perform homology modelling to predict mLOX structure. So we attempted the alternative method, *Ab initio* modelling to predict structure of mLOX.

3.2.12.3 *Ab initio* structure modelling of mLOX

In this study, we submitted the mLOX sequence to the ROBETTA server (an online automated structure prediction tool [156]. When there is no template model available, it follows the *de novo* structure prediction. Modelling will be performed in two stages: 1) Monte Carlo fragment assembly - where protein sequence will be fragmented into 3 - 9 mers and a local conformation will be derived from PDB. Then the fragment will be inserted based on the protein-like feature scores. From these ten thousand decoys will be generated for the query and was clustered based on C^{α}- root-mean-square deviation (RMSD). 2) then knowledge based atomic refinement will be applied; refinement will be based on van der Waals forces, pair wise solvation free energy, back bone dihedral angles and hydrogen bonding potential.

3.2.12.4 MODELLER

It is a programming software, which generates structure models from the provided template structure [157]. It builds the model within the allowed stereo chemical property based on an inbuilt database, which has calculated spatial arrangement from resources like NMR experiments, site directed mutagenesis and etc.,. Finally, model is optimized with molecular probability density function. Thus, MODELLER used for comparative protein structure modelling. In this work we used the MODELLER 9.10 version. The following MODELLER scripts were used in this study:

1) To generate 3D models from the identified template structures
2) To generate disulfide bonds between the assigned cysteine residues
3) To improve the spatial arrangement of specific regions by using loop refinement script.

Model generated by ROBETTA was used as a template and generated 1000 models with different conformations using MODELLER 9.10. Among these 1000 models, the best model with a significant QMEAN scores [158] and stereo chemical properties were analyzed by using the Ramachandran plot. The selected model was proceeded further.

3.2.12.5 Generation of Copper co-ordination bonds in predicted mLOX structure

In LOX, copper acts as the cofactor for its activity and is thought to play a stabilizing role in its structure. So we attempted to fix the copper and to create co-ordinate bonds with the specific residues. In copper binding domain, LOX has 4 histidine residues (289, 292, 294 and 296) of which histidine residues (292, 294 and 296) were involved in the co-ordinate bonding with copper ion. The model was optimized for protonation state and orientations of histidine were performed using Maestro 9.3 (Maestro, Version 9.3, Schrödinger, LLC, New York, NY, 2012). Histidine residues were flipped to achieve optimal geometry.

Orientation of histidine residues (292, 294 and 296) in the optimized model was visualized using Maestro 9.3. The proximity and spatial arrangement of the imidazole

rings of specific histidine residues were taken care that they favor copper binding. Hence, we implemented constrained molecular dynamics simulation coupled with multiple cycles of energy minimization by OPLS 2005 force field towards achieving the orientation favoring copper ion binding in LOX. Further, we summed up the Cartesian co-ordinates of copper binding histidine atoms (292N$^{\delta}$, 294N$^{\epsilon}$ and 296N$^{\epsilon}$) and the mean average for X, Y and Z positions were assigned to Cartesian coordinates for the Cu^{2+} ion as described in the following equation:

$$X_0 = \frac{X_1 + X_2 + X_3}{3}$$

Where;

X_0 =Cartesian coordinate value of copper for X axis
X_1 =Cartesian coordinate value of His 292N$^{\delta}$ at X axis
X_2 =Cartesian coordinate value of His 294N$^{\epsilon}$ at X axis
X_3 =Cartesian coordinate value of His 296N$^{\epsilon}$ at X axis

The Cartesian coordinates for Y_0 and Z_0 were also similarly derived and assigned to the copper ion. A water molecule was added to the copper ion to satisfy the valence and also to achieve the tetrahedral symmetry as discussed by Ryvkin et al [159]. Further, the copper ion fixed model was subjected to bond length analysis in order to validate the permitted range of distance (1.9 – 2.1 Å) [160].

3.2.12.6 Model Validation and Refinement of the predicted mLOX structure

The geometry of the copper ion fixed model was assessed for stereo chemical qualities through PROCHECK [161] and 3D check validation servers [162]. Overall protein topology and domain architecture were also analyzed using the PDBsum server [163] .

3.2.12.7 Molecular Dynamics (MD) simulation for predicted mLOX structure

Molecular dynamics is a computational way of understanding the motion and conformational changes of the macromolecule in stipulated conditions. MD is based on the Newton's second law i.e. force on an object is equal to its mass and acceleration (F =

ma). During simulation macromolecule will be experience the in vivo condition by application of stereo chemical properties through computational algorithms. Thus simulation will provide us some information about behavior of macromolecule.

The stability of the copper fixed mLOX model was studied by MD. Constrained MD simulations were carried out using the Desmond package (Desmond Molecular Dynamics System, version 3.1, D. E. Shaw Research, New York, NY, 2012; Maestro-Desmond Interoperability Tools, version 3.1, Schrödinger, New York, NY, 2012) with an inbuilt OPLS 2005 (Optimized Potentials for Liquid Simulation) force field. The atoms involved in the coordination binding to copper and copper was constrained and simulation was carried out. As an initial step, the system was prepared for simulation using a predefined water model (simple point charge, SPC) as a solvent in a cubic box with 18 Å x 18 Å x 18 Å dimension as periodic boundary condition. Further, the system was neutralized by adding two Na^{+} counter ions and energy minimized. Finally, the production run was initiated under NPT ensemble conditions for 4 nano seconds. The temperature was set to 300K and maintained throughout by implementing Nose–Hoover thermostat with the pressure set to 1 atm and maintained through Martyna–Tobias Klein pressure bath [164]. Smooth Particle Mesh Ewald method [165] was applied to analyze the electrostatic interactions with a cut-off value of 9.0 Å distance. The Cu^{2+} ion, histidine residues involved in Cu^{2+} ion interactions and the water molecule bound to Cu^{2+} ion were completely constrained during the simulation process. The trajectory sampling was done at an interval of 1.0 pico seconds.

3.2.12.8 Electrostatic potential calculations and Binding pocket prediction for predicted mLOX structure

Illustration of the charge distributions of molecular structures is typically rendered through electrostatic potential maps. These maps aid in the identification of sites within the structure to facilitate molecular recognition. The electrostatic interactions between the molecules are generally resolved by the classical Poisson–Boltzmann (PB) equation. In this study, the potential surface for the copper ion fixed model was generated by

implementing PB equation through Schrödinger maestro interface. Further, the active site residues were predicted using CASTp server [166]. Finally, contour map for the modelled protein was generated and analyzed for hydrophobic and hydrophilic regions spanning the active site.

3.2.12.9 Induce Fit Docking (IFD) of predicted mLOX structure with known ligands

The 2D structural coordinates of DAP, a pseudo-substrate for LOX [53], was obtained from PUBCHEM in Mol2 format. Similarly, the structural coordinates of reported LOX inhibitors, such as βAPN [94], Hcys [167] and HCTL [168], were also procured. Further, these structures were prepared for docking using LigPrep 2.6 (Schrödinger, LLC, New York, NY, 2012) module of Schrödinger suite, which verifies proper ionization states, tautomeric forms, stereochemistry, ring conformation and chirality.

Final protein model with optimal geometry was imported into Maestro 9.3. Here, the atoms of the active cavity residues (predicted by CASTp) were set as flexible and were assigned as binding site for grid box generation. The ligands were prepared using LigPrep and were docked to the receptor by soften-potential docking with van der Waals radii scaling of 0.70 Å. The resulting 20 best docked conformations with at least one atom within the distance of 5 Å were selected and subjected to geometry optimization, conformational searches and energy minimization. The active cavity residues beyond the range of 5Å, in terms of ligand interactions were set as rigid and those within the 5Å range were set as flexible. Further, the 20 best ligand poses conformations sampled in the initial docking step were re-docked on to the flexible residues within the range of 5Å as followed above. This re-docking was performed using Glide (Extra Precision) XP by soften-potential docking with van der Waals radii scaling of 1.0. Finally, docking score based on OPLS 2005 force field was used to infer the binding affinity of selected small molecules to the receptor.

Additionally, Molecular Mechanics Generalized Born Surface Area (MMGBSA) was also calculated to measure the binding free energy (ΔG_{bind}) of small molecules to the

LOX model using Prime/MM–GBSA method [169]. Binding free energy was calculated using the equation:

$\Delta G_{bind} = \Delta E_{MM} + \Delta G_{solv} + \Delta G_{SA}$

Where, ΔE_{MM} is the difference in minimized energies of LOX and inhibitor bound complex and the sum of total energies of LOX - Inhibitor in free form. ΔG_{solv} is the difference in GB_{SA} solvation energies of LOX-Inhibitor bound complex and the sum of solvation energies of LOX and inhibitor in free form. Here, ΔG_{SA} refers the difference in surface area for unbound LOX and inhibitors.

CHAPTER 4 - RESULTS

Objective 1: To isolate, purify and characterise human LOX protein

4.1 Purification of LOX from bovine aorta

LOX was purified from bovine aorta. Aorta protein was extracted and separated using DEAE-cellulose column. LOX activity was observed in various eluted fractions (Figure 4.1). These fractions were pooled, concentrated and activity was assessed again. The yield in these pooled fractions were found to be 50 % lesser than the initial crude extract (Table 4.1).

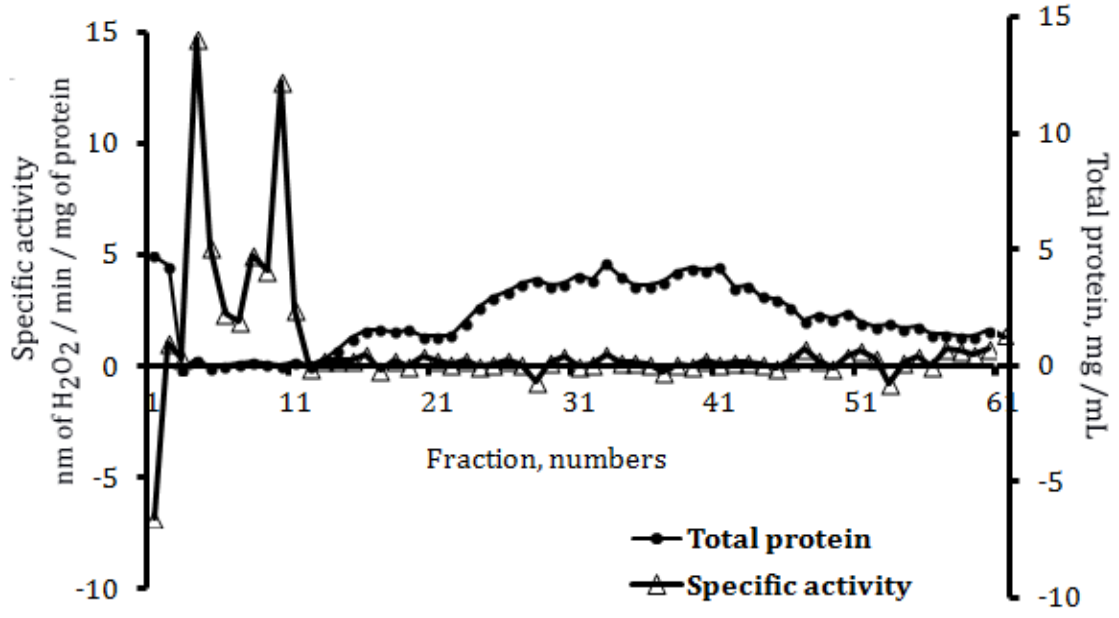

Figure 4.1: Chromatogram of LOX Purification from bovine aorta using DEAE-cellulose. Bovine aorta extract was subjected to DEAE-cellulose ion exchange chromatography. Protein was eluted from the column with 0.4 M NaCl by linear gradient. Fractions were pooled based on the activity peak, pooled fraction 1(fractions 2 – 5); pooled fraction 2(fractions 7 – 9); pooled fraction 3 (fractions 10 -12).

Apart from low yield, the following drawbacks were observed:

1) Initial protein extraction from aorta was difficult because of its fibrous nature.
2) Multiple fractions showed activity, possibly due to the presence of other isoforms of LOX.
3) Activity in the purified fractions was not retained.

Due to these drawbacks, recombinant cloning technique was followed as an alternative strategy for conventional purification technique to purify LOX.

Table 4.1: Purification table of LOX from bovine aorta – DEAE cellulose chromatography

Purification process	Total protein (mg)	Total activity (unit¶)	Specific activity (unit mg)	Yield (% activity)	Purification fold
Aorta extract	677	4648.94	6.49	100	1
Dialysate	125	339.85	6.75	7.3	1.04
Pooled fraction 1	8.9	104.27	14.7	2.24	2.26
Pooled fraction 2	15.3	119.44	7.68	2.56	1.18
Pooled fraction 3	11.5	128.83	9.58	2.77	1.47

¶ One unit is defined as nano moles of hydrogen peroxide released per minute

4.1.2 Cloning of human mature LOX (mLOX)

4.1.2.1 Construction of pQE-30 XA + mLOX vector

Infusion cloning method was implemented to get the purified recombinant mLOX. The mLOX DNA insert was synthesized by PCR amplification from the template cDNA of HUVECs. The synthesized mLOX gene was inserted into the bacterial expression vector, pQE-30 Xa using the restriction enzymes, S*tu*I and H*in*dIII.

4.1.2.2 PCR amplification of mLOX

From HUVECs cDNA, mLOX gene was PCR amplified using infusion primers. Agarose gel electrophoresis of PCR product revealed a single band at 750 base pairs; this corresponds to the molecular size of mLOX gene. The band was eluted from the gel and was used for infusion reaction. The cDNA integrity was confirmed using GAPDH (Figure 4.2).

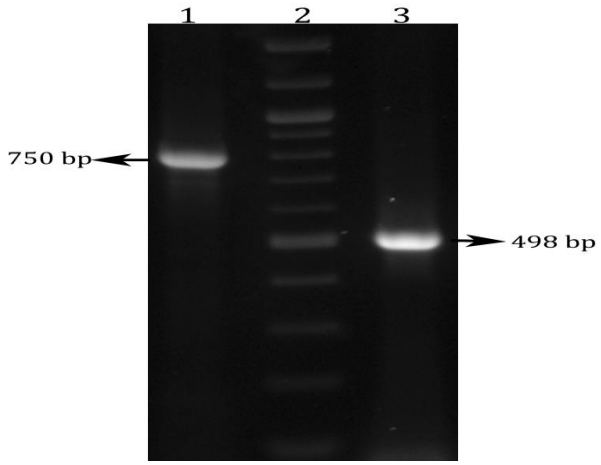

Figure 4.2: Agarose gel electrophoresis for PCR amplified mLOX DNA insert. Lane 1: PCR amplified mLOX DNA insert (750 bp); Lane 2: Molecular size marker (100 – 1000 bp); Lane 3: GAPDH (498 bp)

4.1.2.3 Linearization of pQE-30 Xa vector

Circular pQE-30 Xa vector was treated with *Stu*I and *Hin*dIII restriction enzymes overnight at 37 °C. The digested product was subjected to agarose electrophoresis and visualized. The specific band at 3500 bp was gel eluted and was used for infusion reaction.

4.1.2.4 Infusion reaction

Infusion reaction was performed with eluted mLOX DNA and linearized pQE 30-Xa vector. The resulted infusion product was transfected into competent M15 (pREP4) cells. The transformed cells were inoculated on to selective LB agar plate containing kanamycin (30 µg / mL) and ampicillin (100 µg / mL) then incubated overnight at 37 °C. Colonies grown in the selective LB plate were further confirmed for complete vector construct.

4.1.2.5 Confirmation of pQE-30 Xa + mLOX vector construct

Colonies were randomly picked from the selective plate and were inoculated into LB media (Contains kanamycin and ampicillin) and incubated overnight. Plasmid DNA from the overnight culture was isolated and restriction digestion was performed with *Stu*I and *HindIII* restriction enzymes. Restriction digestion product showed two bands at 3500 bp and 750 bp respective to the molecular size of linearized vector and mLOX DNA insert (Figure 4.3). Thus the transformed M15 (pREP4) *E.coli* contains the complete pQE – 30 Xa + mLOX construct as depicted in the figure 3.2 (page 39). This was further confirmed by gene sequencing.

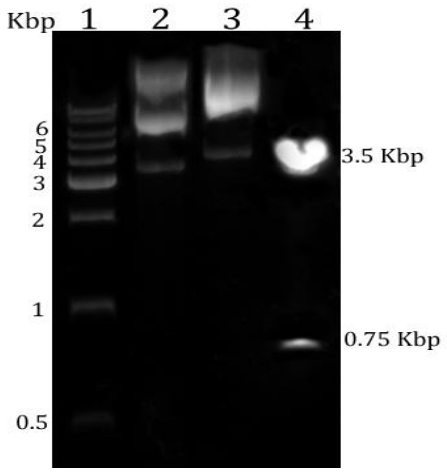

Figure 4.3: Agarose gel electrophoresis of pQE-30Xa+mLOX vector digested using restriction enzymes *Stu*I and *Hind*III. Lane 1: Molecular size marker (500 bp – 10 Kbp); Lane 2: pQE-30Xa vector; Lane 3: pQE-30Xa + mLOX vector undigested; Lane 4: pQE-30Xa + mLOX vector digested.

4.1.2.6 Sequencing of mLOX gene in pQE 30-Xa + mLOX vector constructs

The mLOX gene insert in the pQE-30Xa + mLOX plasmid was sequenced with 3100-Avant Genetic analyzer. Output sequence was analyzed using Bio Edit software tool. Resulted sequence was 100 % identity to the reference LOX sequence in NCBI database with no mutation. Thus, transformed M15 (pREP4) *E.coli* (clone) strain harbours the complete pQE-30 Xa + mLOX plasmid construct. Glycerol stocks of the transformed cells were prepared and stored at -80 °C for future.

4.1.3 Expression of recombinant mLOX in bacterial system

4.1.3.1 Optimization of IPTG induction for expression recombinant mLOX

As a first step IPTG concentration from 0.2 – 1 mM were screened. Cloned cells showed maximal expression of mLOX when induced with 1 mM of IPTG (Figure 4.4).

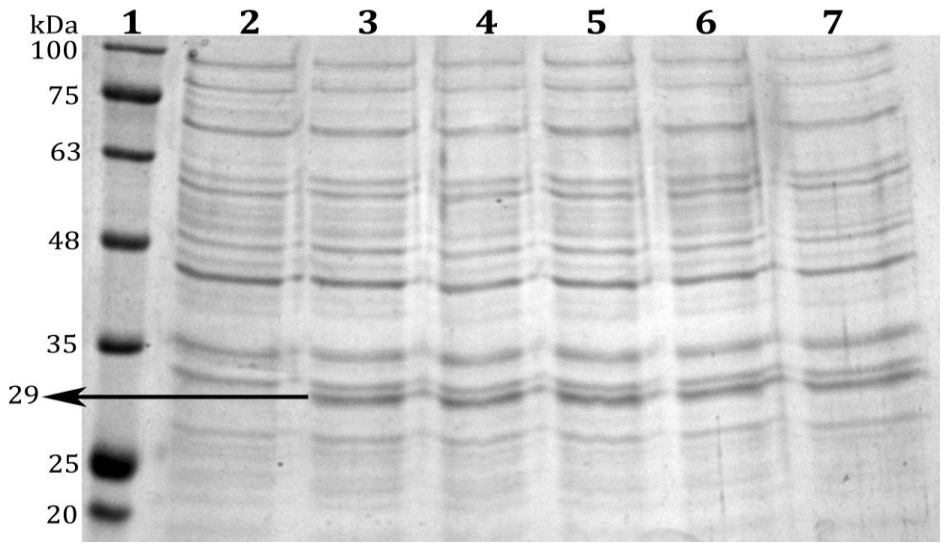

Figure 4.4: Optimization of IPTG concentration for expression of recombinant mLOX. Cloned M15 cells were induced with various concentration of IPTG. After induction lysed and subjected to 10 % SDS-PAGE. Lane 1: Molecular weight marker Lane 2; Uninduced cells; Lane 3: 0.2 mM IPTG induced; Lane 4: 0.4 mM IPTG induced; Lane 5: 0.6 mM IPTG induced; Lane 6: 0.8 mM IPTG induced; Lane 7: 1 mM IPTG induced. Cloned cells induced with IPTG 1 mM showed intense band at 29 kDa (respective to the size of mLOX) and good overall protein profile compared to the other concentrations.

As a second step the different time points (2, 4, 6 and 16 h) were tested and maximum expression of mLOX was found at 4 h time point (Figure 4.5). These optimized conditions were followed for protein over expression and purification experiments.

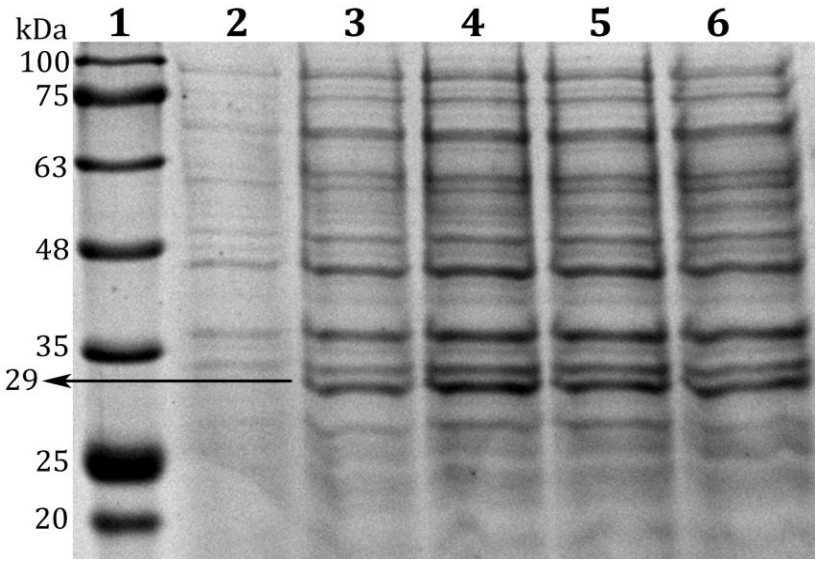

Figure 4.5: Optimization of IPTG induction time for expression of recombinant mLOX. Cloned M15 cells were induced with 1 mM of IPTG for various time points. After induction lysed and subjected to 10 % SDS-PAGE. Lane 1: Molecular weight marker Lane 2; Uninduced cells; Lane 3: IPTG induced for 2 h; Lane 4: IPTG induced for 4 h; Lane 5: IPTG induced for 6 h; Lane 6: IPTG induced for 16 h. Cloned cells induced with IPTG 1 mM for 4 h showed intense band at 29 kDa (respect to the size of mLOX) and good overall protein profile compared to the other time points.

4.1.3.2 Purification of recombinant mLOX using Ni-NTA affinity chromatography

Cloned cells were induced with IPTG and mLOX protein was over expressed and purified using Ni-NTA agarose beads. After induction induced cells were pelleted down and suspended in phosphate buffer containing 8 M urea. Bacterial cells and its inclusion bodies were lysised upon treatment with 8 M urea and sonciation. Then protein was extracted in the denaturing buffer and purified by affinity displacement method, mLOX was eluted from Ni-NTA and purification was assessed by SDS-PAGE. The elution resulted in 29 kDa single band (Figure 4.6), corresponding to the molecular weight of mLOX. Purification yield was about 7 - 9 mg per litre of broth.

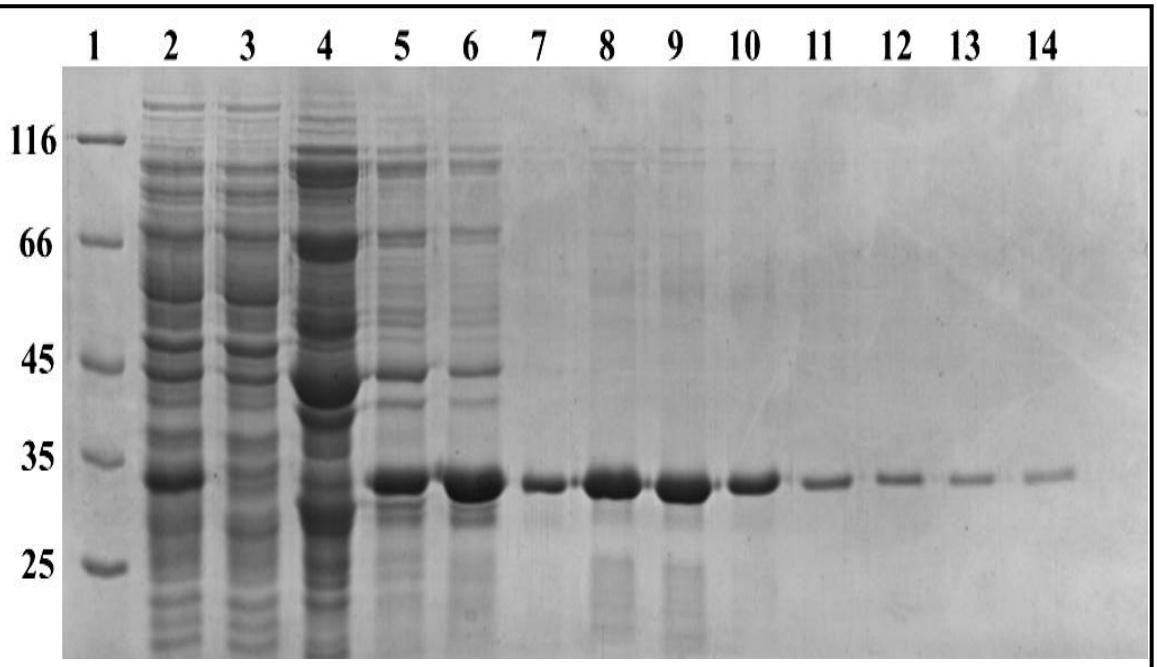

Figure 4.6: Silver stained 10% SDS-PAGE gel showing the Ni-NTA affinity purification. Lane 1: Molecular size marker; Lane 2: Crude cell lysate; Lane 3: Ni-NTA unbound fraction; Lanes 4 – 6: fractions from 25 mM imidazole wash 1-3; Lanes 7 – 14: 250 mM imidazole eluted fraction from 2 to 8.

4.1.3.3 Confirmation of recombinant mLOX

Ni-NTA purified recombinant mLOX was further confirmed by Western blotting and mass spectroscopy.

4.1.3.3.1 Western blot analysis of recombinant mLOX

Purified protein was subjected to Western blot and was probed with His tag and LOX primary antibodies. A single band 29 at kDa was observed in both, the LOX and His tag blots, which confirms the purity of Ni-NTA purified recombinant mLOX (Figure 4.7).

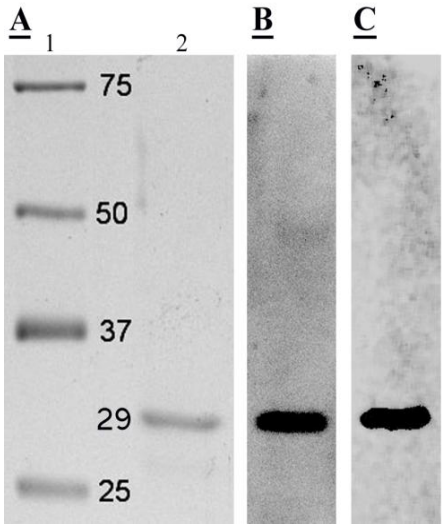

Figure 4.7: Confirmation of recombinant mLOX by Western blot. A) Silver stained 10 % SDS PAGE showing single band at 29 kDa of Ni-NTA purified mLOX (lane 2) and with molecular weight marker (lane 1). B & C showing the western blot for purified recombinant mLOX probed with LOX and His tag antibodies.

4.1.3.3.2 Mass spectroscopy analysis of recombinant mLOX

Purity was further confirmed with MS analysis by in-gel and in-sol tryptic digestion, as follows

1) Silver stained gel showing single band at 29 kDa region was excised and given for MS analysis (ESI-MS) after in-gel tryptic digestion.

2) In-sol tryptic digestion was also performed directly with Ni-NTA elute.

Mature LOX sequence contains 19 cleavage sites for trypsin enzyme. Purified mLOX was reduced, alkylated and treated with trypsin overnight at 37 °C. The peptides were then analysed in positive mode by 2D Nano-ESI-MS (Figure 4.8). Analysis was done with PLGS 2.5.3 software using UniProt protein database. PLGS result output showed a single hit of LOX (UniProt ID p28300) and with peptide coverage of 85 % for mature LOX region. Peptides identified by MS analysis were within the mature LOX region, which indicates that recombinant mLOX preparation was pure (Figure 4.9 & Table 4.2). The results were similar for both the methods of tryptic digestion (in-sol and in-gel).

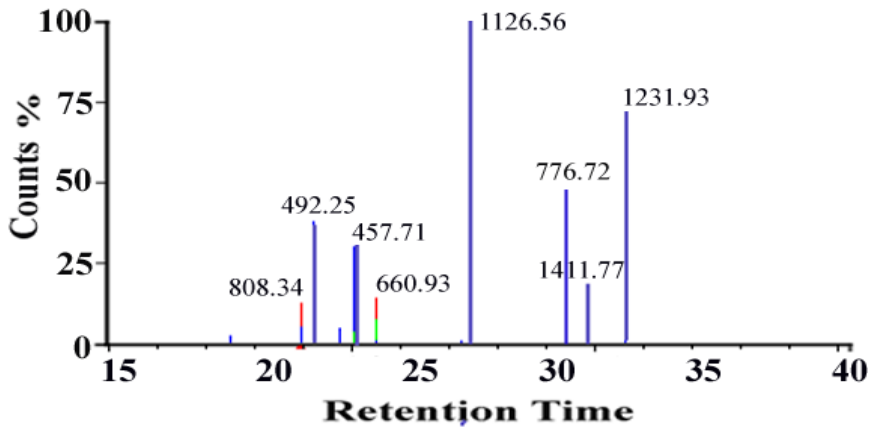

Figure 4.8: MS spectrum of peptide derived from tryptic digestion of recombinant mLOX. X-axis: Retention time of peptides in UPLC, minutes; Y-axis: Peptide intensity represented in counts percentage. Value on each peak denotes the m/z ratio of the peptide.

Figure 4.9: Peptide map of mLOX identified by MS analysis Green colour indicates fully matched, purple colour indicates fully matched with modifications and grey colour indicates partially matched peptides with reference to the Uniprot database.

Table 4.2: Sequence of peptides identified by MS from mLOX tryptic digest

Peptide Sequence	Retention time (min)	Score	Mz
ASFCLEDTSCDYGYHR	23.4166	9.7458	660.9335
VSVNPSYLVPESDYTNNVVR	27.0876	9.9412	1126.5631
NQGTSDFLPSRPR	20.8254	9.1141	492.2524
CAAEENCLASTAYR	20.3571	9.7912	808.3458
MSMYNLR	22.8115	8.7106	457.7148
YTGHHAYASGCTISPY	20.349	9.0308	595.5951
FACTAHTQGLSPGCYDTYGADIDCQWIDITDVKPGNYILK	31.0718	9.4174	1141.7768
YRPGYGTGYFQYGLPDLVADPYYIQASTYVQK	32.2981	9.3146	1231.933
YSWEWHSCHQHYHSMDEFSHYDLLDANTQR	31.4626	7.4797	776.7281
YSDDNPYYNYYDTYERPRPGGR	23.1449	7.3326	691.0533

By infusion cloning method, pQE 30-Xa + mLOX construct was prepared and over expressed in the M15 (pREP4) expression system. Over expressed recombinant mLOX was purified by Ni-NTA affinity method and purity was confirmed with SDS-PAGE, western blot and MS. This purified recombinant mLOX was used for characterization experiments.

4.1.4 Refolding of recombinant mLOX

LOX protein forms amorphous aggregate in the absence of urea, so mLOX was purified with buffer containing 8 M urea. With the presence of urea the structural properties of LOX cannot be studied. So after purification attempted to remove urea and maintain the mLOX in soluble form. Screening was performed with various buffer systems (Table 3.9) and identified the glycine-NaOH buffer, pH 8.0 with 10% glycerol.

4.1.5 Dialysis - removal of urea from recombinant mLOX

By dialysis, urea was removed from the purified mLOX. Purified mLOX was dialyzed against glycine-NaOH buffer and urea concentration was reduced step wise (7 – 6 – 5 – 4 – 3 – 2 – 1 – 0, in molarity). Dialysis was performed for 8 h at 4 °C against each buffer.

The dialysate was inspected for protein aggregates by centrifugation (10,000 rpm for 30 min) at the end of each buffer change.

4.1.6 His Tag Cleavage from recombinant mLOX

Recombinant mLOX contains His tag at its N-terminal, which might interfere with the enzymatic activity of LOX. So it was cleaved using factor Xa protease. Cleaved product did not show any band when probed against His tag antibody but showed band at 29 kDa, when probed against LOX antibody by WB (Figure 10). For both the blots uncleaved purified mLOX was used as control. Cleavage efficiency was about 50 – 70 %. Further experiments were performed with His tag removed recombinant mLOX.

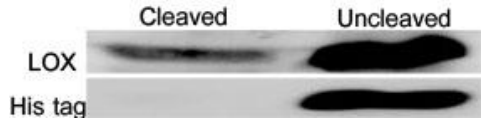

Figure 4.10: Western Blot of His tag removed recombinant mLOX.

4.1.7 Estimation of copper in recombinant mLOX

Estimation of copper was carried out using AAS method. Initially instrument was calibrated with 0.2 % nitric acid and background value for solvents (MQ and buffer) used were determined taken into account during calculation. Standard graph was plotted using elemental copper. From the standard graph it was calculated that 50 % of recombinant mLOX found in the copper bound state. Experiment was performed in triplicate and calculated.

4.1.8 Functional characterization of recombinant mLOX

4.1.8.1 Comparison of various substrates for recombinant mLOX activity

Enzymatic action of recombinant mLOX (100 ng) were tested against natural substrates, elastin and collagen (10 and 100 µg) and pseudo substrate DAP (10 and 100 mM). Among the three substrate used DAP showed maximal activity and dose dependent increase with the increasing concentration (10 mM: 1.1 5 ± 0.4 units and 100 mM: 4.7 ± 0.4 units). Whereas elastin and collagen showed least activity (elastin 100 µg: 1.59 ± 0.7 units and collagen 100 µg: 1.37 ± 0.4 units). Hence DAP was used as the substrate for the rest of the experiments (Figure 4.11).

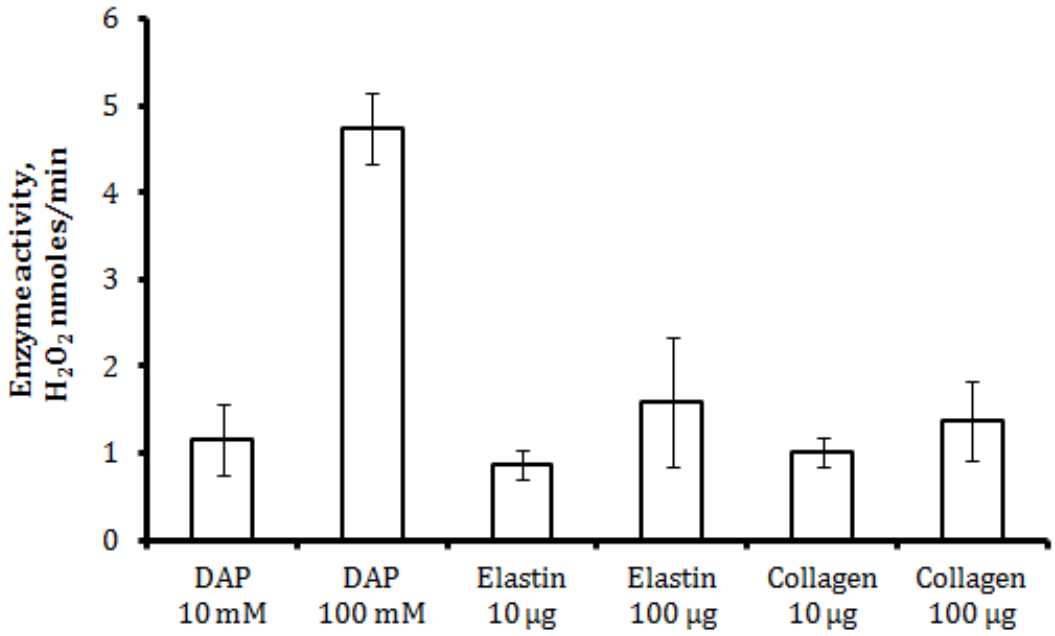

Figure 4.11: Comparison of various substrates on recombinant mLOX activity. Recombinant mLOX and respective substrates were pre-incubated at 37^{o}C for 5 min and the reaction mixture was added and readings were taken fluorimetrically (Excitation 563 nm; Emission 587 nm). Data shown represent mean ± SD from three independent experiments.

4.1.8.2 Effect of pH on recombinant mLOX activity

To examine the effect pH on recombinant mLOX activity, a pH range of 6.5 to 10 was selected. Maximal LOX activity (8.4 ± 0.5 units) was found at the pH of 8. Enzyme activity was found to be decreasing above the pH of 8.5 (7.7 ± 0.4 units) and below the pH of 7.5 (5.6 ± 0.5 units). The optimum pH of the recombinant mLOX was found to be at the pH 8.0 and used for rest of the characterisation experiments (Figure 4.12).

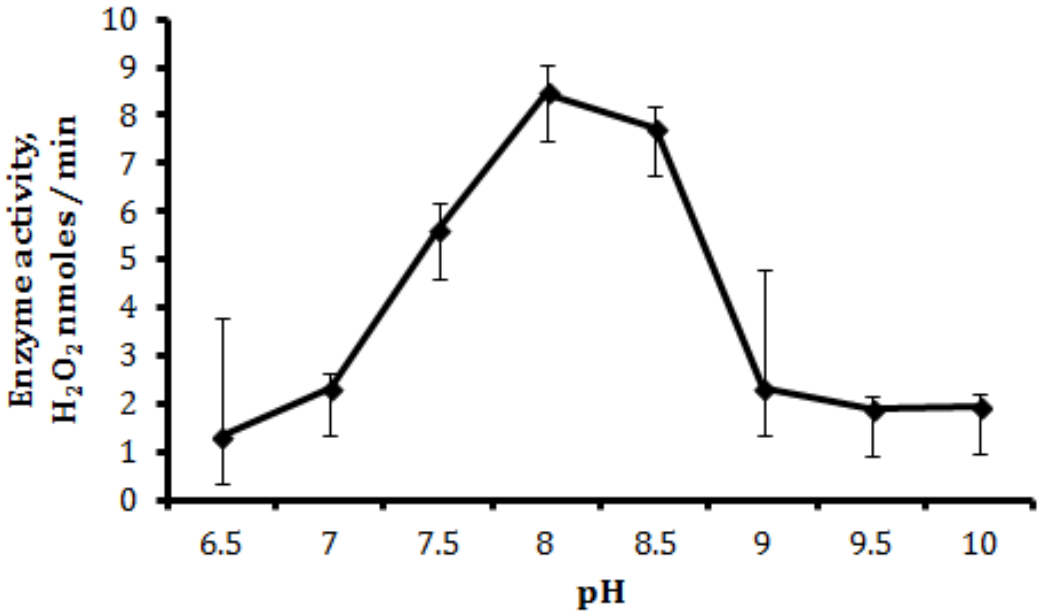

Figure 4.12: Effect of pH on recombinant mLOX activity. Different pH buffers (100 mM) were used: Phosphate buffer (pH 6.5, 7.5), Borax Buffer (pH 8, 8.5) and glycine-NaOH buffer (9, 9.5, 10). Recombinant mLOX 100 ng and 100 mM of DAP was incubated at 37^{o}C for 5 min in the respective buffers and the reaction mixture was added and readings were taken fluorimetrically (Excitation 563 nm; Emission 587 nm). Data shown represent mean ± SD from three independent experiments.

4.1.8.3 Effect of temperature on recombinant mLOX activity

Temperature dependence of recombinant mLOX activity was examined at 25°C, 37 °C, 50°C and 75 °C. Temperature dependence profile showed the activity of recombinant mLOX was increasing with increase the temperature. With the current experimental set up optimum temperature for mLOX activity was not determined. For the further experiments physiological temperature 37 °C was followed (Figure 4.13).

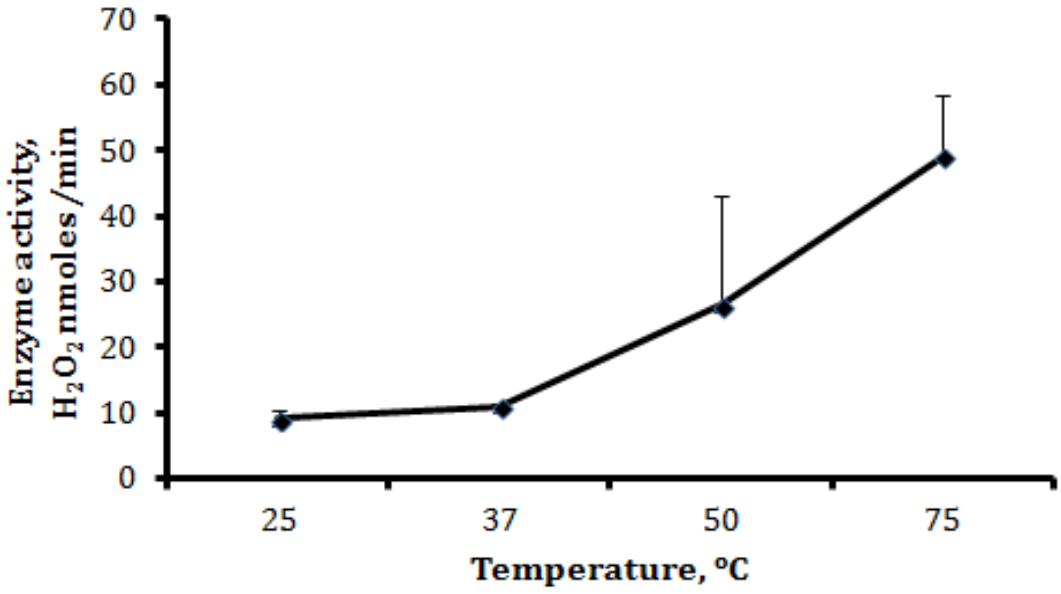

Figure 4.13: Effect of temperature on recombinant mLOX activity. Recombinant mLOX 100 ng and DAP 100 mM were incubated for 15 min at designated temperatures and cooled to room temperature. The reaction mixture was added and incubated for 5 min at 37^{o}C and readings were taken fluorimetrically (Excitation 563 nm; Emission 587 nm). Data shown represent mean ± SD from three independent experiments.

4.1.8.4 Effect of substrate concentration on recombinant mLOX activity

Substrate range of 10 - 400 mM of DAP was used to determine the enzyme kinetics of recombinant mLOX. The activity of recombinant mLOX increased from the 10 – 200 mM DAP concentration. With higher DAP concentration (>200 mM) the activity was found to be saturated (Figure 4.14). With the substrate saturation graph of LOX against DAP used to plot **Michaelis-Menten (MM) and Lineweaver-Burk plot** (LB) plot (Figure 4.15). From MM and LB plot maximum rate of reaction (V_{max}) of recombinant mLOX and its affinity of DAP substrate (K_m) was determined (Table 4.3).

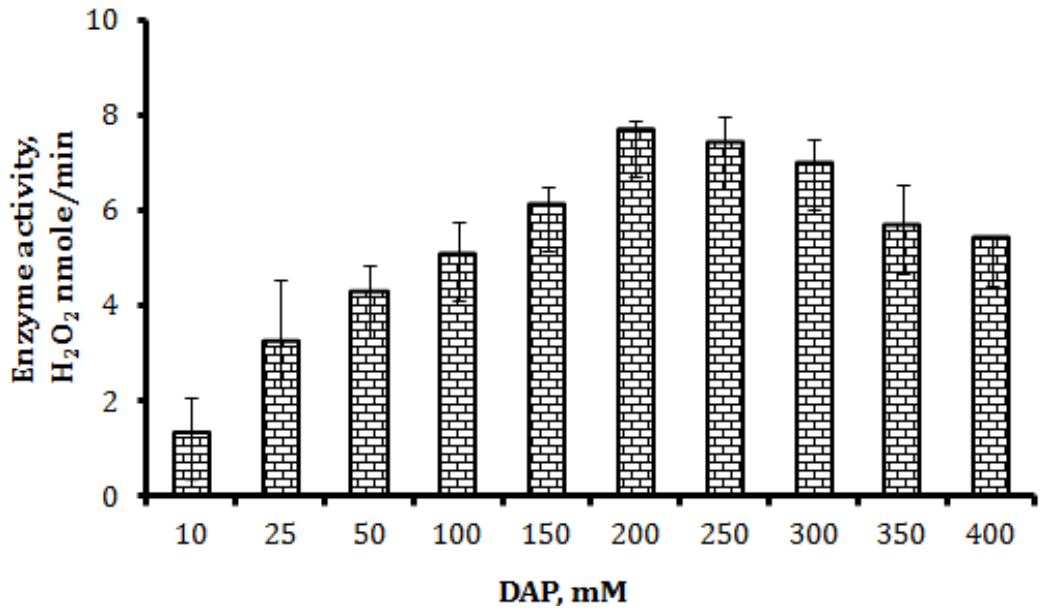

Figure 4.14: Effect of substrate concentration on recombinant mLOX activity. Recombinant mLOX 100 ng was preincubated for 5 min at 37 °C with various concentrations DAP. Then reaction mixture was added and readings were taken fluorimetrically (Excitation 563 nm; Emission 587 nm). Data shown represent mean ± SEM from three independent experiments.

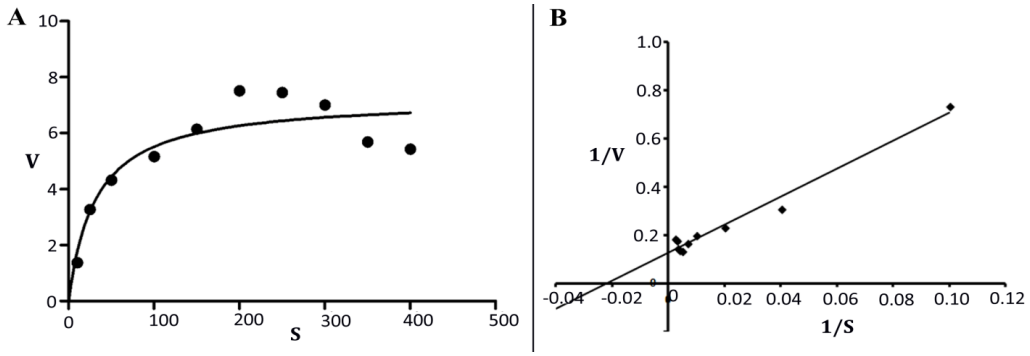

Figure 4.15: Michaelis-Menten and Lineweaver-Burk plot for recombinant mLOX against the substrate DAP. Using the substrate concentration value, A) Michaelis-Menten and B) Line weaver-Burk plots were plotted for recombinant mLOX using Graph pad 5.0 software. From the plot, V_{max} and K_m values were derived. Here V, Velocity of reaction rate (nm of H_2O_2 released / minute / µg of mLOX) and S, substrate concentration in mM. 1/V and 1/S were reciprocal value of V and S.

Table 4.3 : Enzyme kinetics values of recombinant mLOX against DAP

Method	**V_{max} (nm of H_2O_2 released / minute / µg of mLOX)**	**K_m (mM)**
Michaelis-Menten plot	70.44	31.64
Lineweaver-Burk plot	76.74	44.16

4.1.8.5 *In vitro* enzymatic activity of recombinant mLOX

LOX is known to increase collagen cross-linking by its enzymatic action. So collagen cross linking action of recombinant mLOX was tested in ARPE-19 cells. Here ARPE-19 cells were treated with various concentrations (1 to 1000 ng/ mL) for 72 h and stained for collagen by immuno fluorescence (Figure 4.16 C-F). TGF-β the known to induce the collagen and LOX synthesis and used as positive control with the concentration of 2.5 ng/mL (Figure 4.16 B).Staining of collagen revealed long and thick bundles of collagen with increasing concentration of mLOX when compared to control cells. Staining pattern of cells reserved 1000 ng/ mL mLOX and TGF-β was comparable. Hence the enzymatic action of recombiannt mLOX was proved at in vitro condtions.

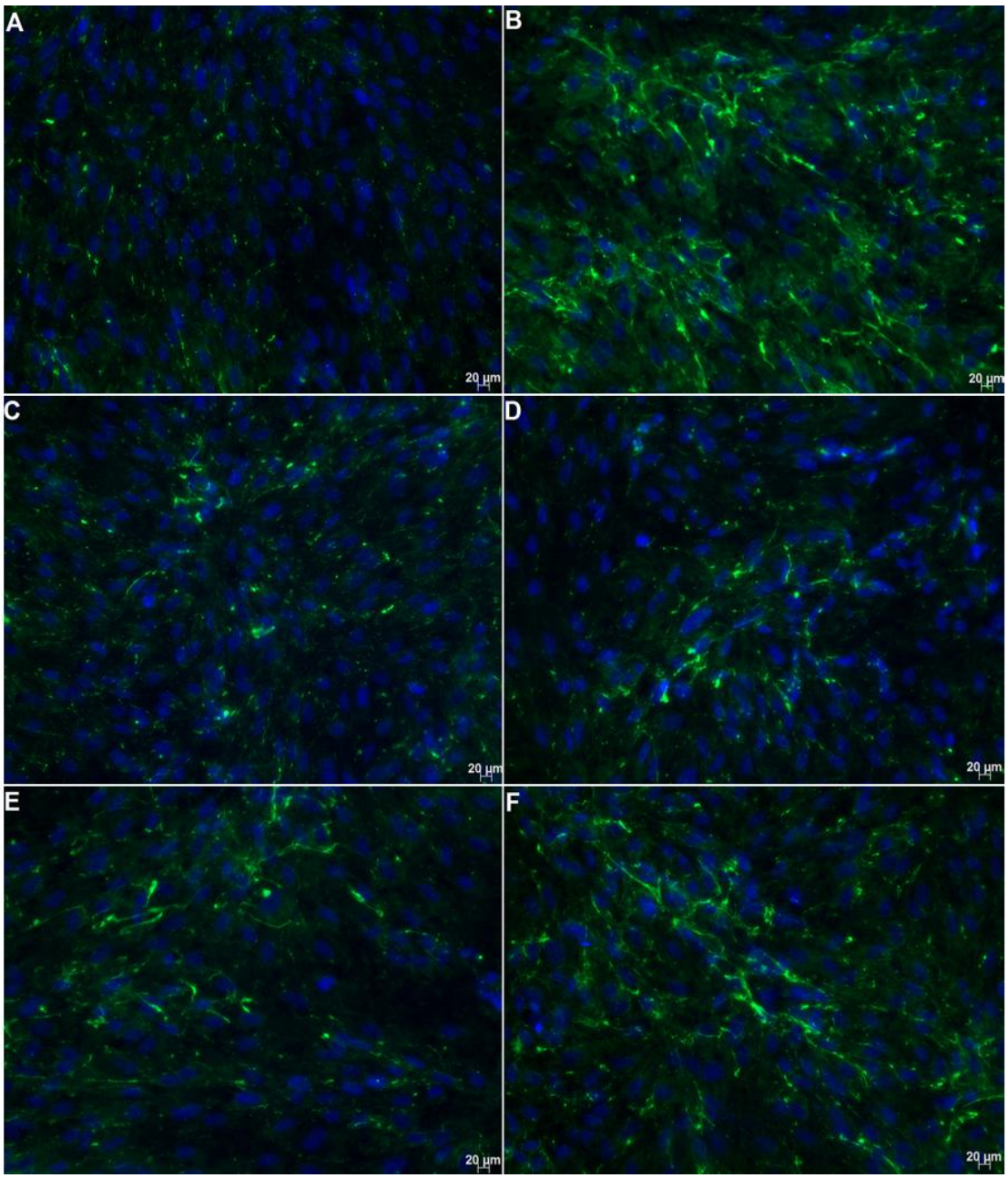

Figure 4.16: Immuno fluorescence staining for collagen in ARPE-19 cells. ARPE-19 cells were exposed to various concentrations of recombinant mLOX (1, 10, 100 & 1000 ng/mL) from (**C – F)** for 72 h. Cells exposed to TGF-β (2.5 ng/mL) serve as positive control (**B**) and control cells (**A**) received only basal media. All images were acquired with 10X objective in Axio-observer microscope.

4.1.9 Structural Characterisation of recombinant mLOX

4.1.9.1 Far UV- CD specturm analysis of recombinant mLOX

The degree of secondary structure for recombinant mLOX was measured in the far UV range, 200 - 240 nm. The collected far UV-CD spectra data were analysed by K2D2 online software. The mLOX suspended in 0.2 M glycine-NaOH buffer with 10 % glycerol buffer showed α-helix of 8.43 % and β-strand of 22 %. The Far-UV CD spectrum correlates with the ratio of secondary struture of predicted mLOX model (13.5 % of α-Helix and 16.4 % of β-Sheet) but there is variation in the percentage of secondary structure.

It is reported that glycerol can increase the thermo stability of the protein upto 50 % with increasing concentration of it [170] [171]. To avoid the cryo-protectant effect of glycerol on recombinant mLOX the percentage of glycerol was reduced from 10 % to 1.5 % and the far UV spectra data was collected at 20°C and 80°C. The mLOX spectrum showed α – helices, 51.86% and 59.98%, β-sheet 9.19% and 5.55%, when exposed to 20 °C and 80 °C, respectively. Thus the CD spectra reveal that there is only minimal change in the secondary structure between mLOX exposed to 20 °C and 80 °C.

The proposition of α-helix and β-strand of recombinant mLOX showed high variance between 10 % and 1.5 %. This variation might have arised due to the alteration in surface tension and interaction of water to the protein. This kind of variation in the secondary structure is due to the co-solvent which was previously reported [172].

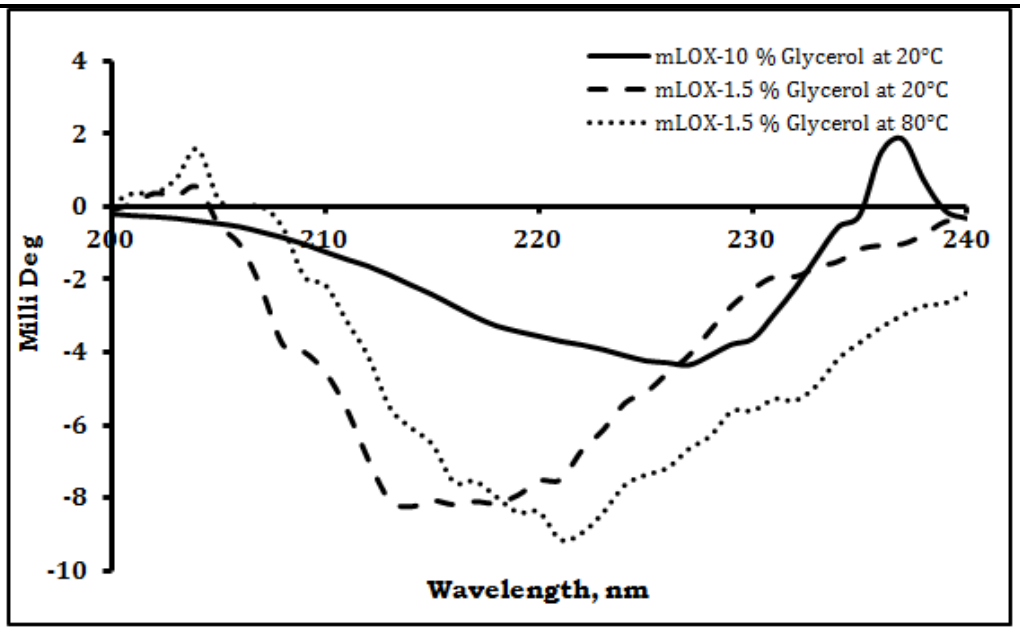

Figure 4.17: Far-UV CD spectrum of recombinant mLOX. Recombinant mLOX was suspended in glycine – sodium hydroxide buffer with 10 % and 1.5 % glycerol at pH 8.0. For temperature analysis recombinant mLOX suspended buffer with 1.5 % glycerol initial spectrum was collected at 20^{o}C and system temperature was gradually increased from 20 °C to 80 °C along with protein in the cuvette and final spectrum was collected at 80^{o}C temperature. Spectrum was collected from 200 nm to 240 nm thrice and cumulative average was taken finally.

4.1.9.2 Tryptophan fluorescence emission of DTT-reduced recombinant mLOX

LOX contains three Tryptophan residues in its structure. The refolded recombinant mLOX was irradiated at 295 nm wavelenght (specifically excite Tryptophan residues alone). Recombinant mLOX showed emission maxima at 304 nm with the fluorescence value of 5000 RFU. This shows that mLOX contain buried tryptophan in its structure When recombinant mLOX was reduced with DTT the emission maxima showed red shift from 304 nm to 308 nm. with increase in the DTT concentration the fluorescence value reduced to 2000 RFU for 100 mM of DTT (Figure 4.18). Decrease in fluorescent yield may be the result of buried tryptophan exposed to aqueous environment.

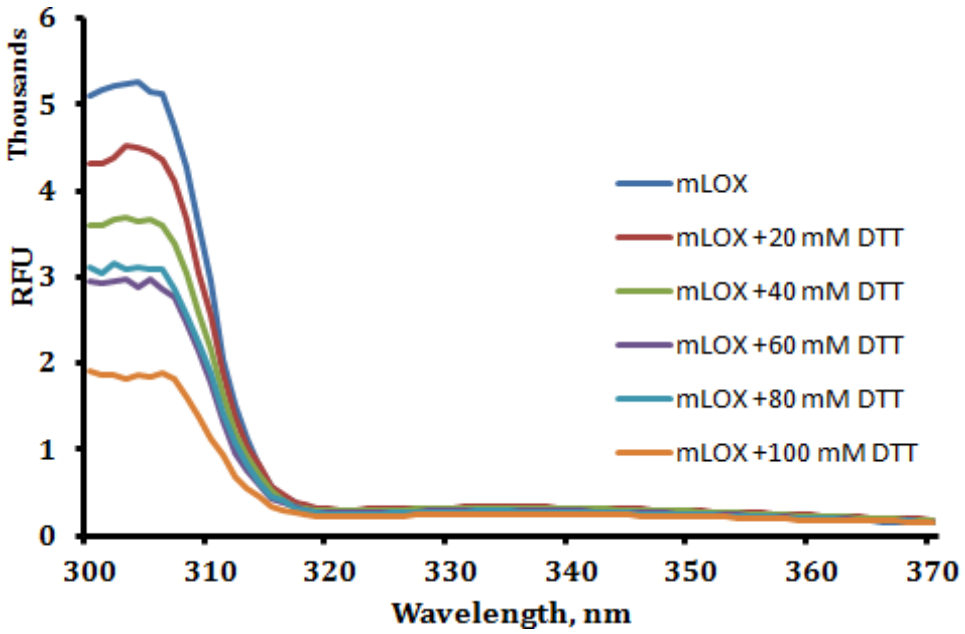

Figure 4.18: Tryptophan fluorescence emission spectrum of native and reduced recombinant mLOX. Recombinant mLOX 3 µM was reduced with different concentrations of DTT (20 – 100 mM) at 60 °C. Intrinsic fluorescence of mLOX was measured by exicting at the wavelength of 295 nm and emission spectrum was collected from 300 to 370 nm with an interval of 1 nm. Data shown represent mean from three independent experiments (RFU–Relative Fluorescence Unit).

4.1.9.3 ANSA binding analysis of reduced and denatured recombinant mLOX

ANSA is a chemical molecule which binds to the exposed hydrophobic patches in a protein surface. Recombinant mLOX showed emission maximum at 450 nm. DTT (100mM) reduced mLOX showed red shift in the emission maxima from 450 nm to 470 nm, this shows the unfolding of the recombinant mLOX. Recombinant mLOX denatured with 2M Guanidinium hydrochloride (GnHcl) did not show much change in the emission spectra. When recombinant mLOX was reduced with DTT (100 mM) and denatured with GnHcl (2 M) the emission spectra showed shift in the emission maxima to 470 nm and increase in the fluorescence value from 250 RFU to 400 RFU. This shows the unfolding and leads exposure of more hydrophobic region of the mLOX, which resulted in increased binding of ANSA (figure 4.19).

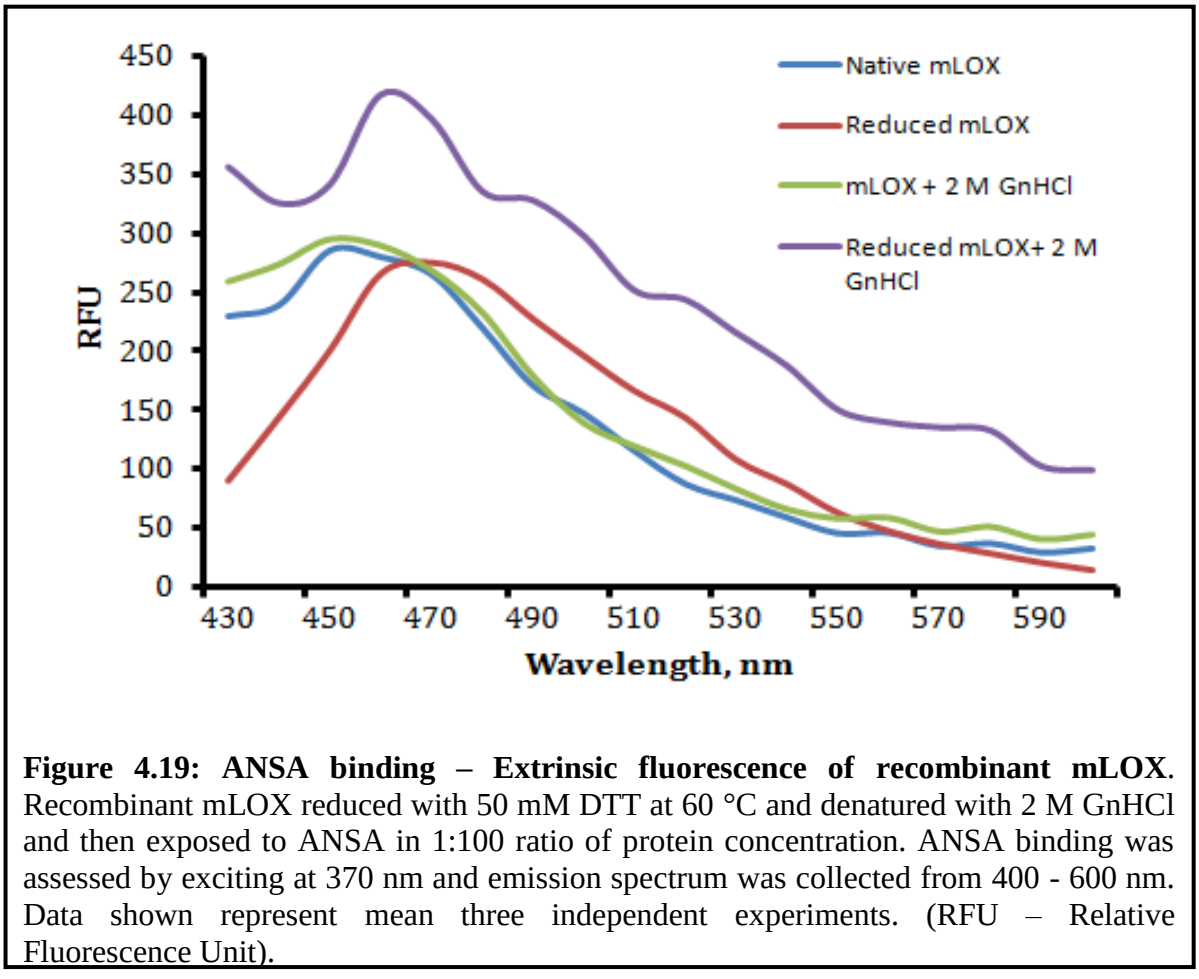

Figure 4.19: ANSA binding – Extrinsic fluorescence of recombinant mLOX. Recombinant mLOX reduced with 50 mM DTT at 60 °C and denatured with 2 M GnHCl and then exposed to ANSA in 1:100 ratio of protein concentration. ANSA binding was assessed by exciting at 370 nm and emission spectrum was collected from 400 - 600 nm. Data shown represent mean three independent experiments. (RFU – Relative Fluorescence Unit).

Objective 2: To determine the structure of LOX by in silico approach

There is no 3D structure of LOX and its family members available in the literature. In this work, 3D structure of LOX was predicted by *ab initio* method. To the predicted structure a copper ion was fixed in the catalytic site of LOX. The copper fixed model was assessed by Ramachandran plot and by molecular dynamic studies. The validated model was docked against the known modulators by induced fit docking (IFD).

4.2 Secondary structure prediction of mLOX by PSIPRED

The amino acid sequence of mature LOX (249 residues) was retrieved from the UniProt database (Accession ID: 28300) and used for structure modelling. Initially to predict the secondary structure mLOX, the sequence was submitted to PSIPRED server. The PSIPRED-predicted secondary structure is given in (Figure 4.20).

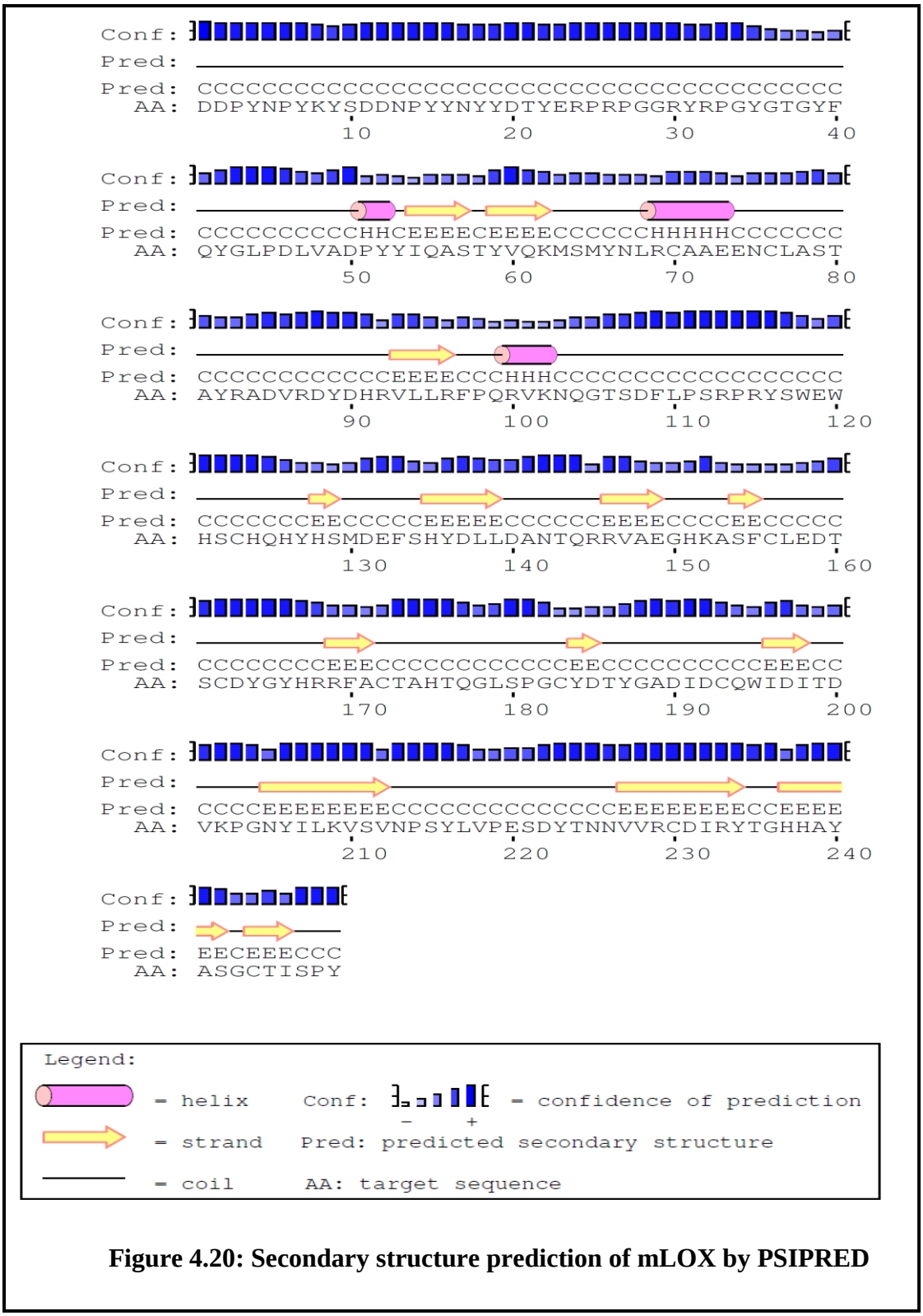

Figure 4.20: Secondary structure prediction of mLOX by PSIPRED

4.2.1 Modelling and refinement of mLOX structure

Mature LOX sequence shares less than 25 % homology with the current PDB database. *ab initio* method was followed to predict the 3D conformation of mLOX (Figure 4.21). The mLOX amino acid sequence was submitted to the ROBETTA online and a template model was acquired. Using ROBETTA template model, thousand models with varied conformations were generated using MODELLER 9.10. The Generated models were validated with Ramachandran plot and QMEAN score. Model with significant QMEAN score 0.602 and 92.6 % in favoured region of Ramachandran plot (figure 4.22) was chosen as the best model and proceeded further.

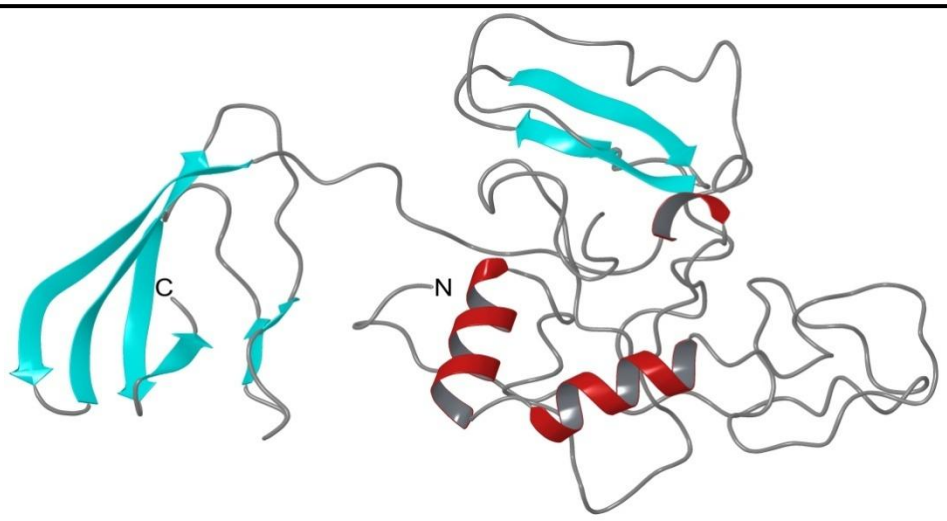

Figure 4.21: Initial predicted model of mLOX. Output from ROBETTA using MODELLER 9.10 version, 1000 decoys were generated with ROBETTA server model as template. The top model was selected based on the QMEAN score and Ramachandran plot. Secondary structure of the top model is represented in different colors (Helices in red, sheets in cyan and loops in gray).

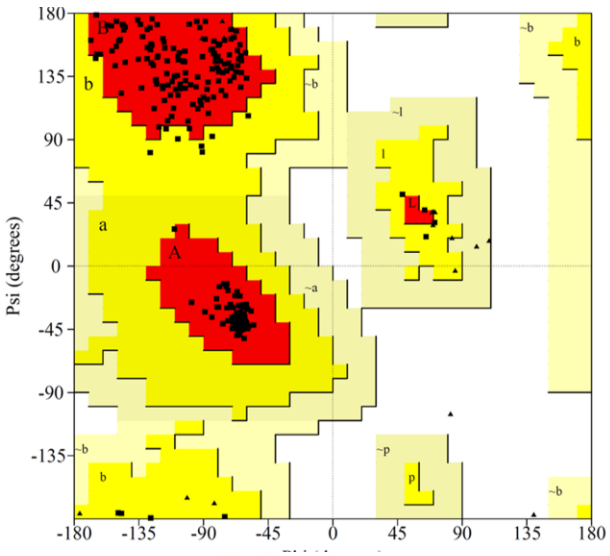

Plot statistics

Residues in most favoured regions [A,B,L]	200	92.6%
Residues in additional allowed regions [a,b,l,p]	16	7.4%
Residues in generously allowed regions [~a,~b,~l,~p]	0	0.0%
Residues in disallowed regions	0	0.0%
Number of non-glycine and non-proline residues	216	100.0%
Number of end-residues (excl. Gly and Pro)	2	
Number of glycine residues (shown as triangles)	15	
Number of proline residues	16	
Total number of residues	249	

Figure 4.22: Ramachandran plot of initial predicted model of mature LOX

4.2.2 Orientation of copper binding histidine in mLOX

The top initial model was subjected to refinement by rectifying stereo chemical errors using Schrodinger suite. Histidine residues (292, 294 and 296) in the copper binding domain of LOX forms coordinate bonding with copper ions. By applying OPLS 2005, multiple steps of manual minimization were performed and these 3 histidine residues were brought to a plane in the spatial arrangement. Histidine residues (His 292N^{δ}, His 294N^{ϵ} and His 296N^{ϵ}) were oriented in such a way that it favors co-ordinate covalent bond with copper in tetrahedral geometry (Figure 4.23 A). Based on the calculated inter atomic space copper ion was placed and co-ordinate bonds were generated between the specific histidines (His 292N^{δ}, His 294N^{ϵ} and His 296N^{ϵ}). Then to satisfy the valence of copper water molecule was added using chimera tool (Figure 4.23 B). The copper-fixed

mLOX model was energy minimization with prime OPLS 2005 force field with constrained applied to the copper ion and its ligand nitrogen molecules. The resultant model was found to have coordinated covalent bond lengths within the allowed distance (1.9 Å-2.2 Å (Figure 4.24).

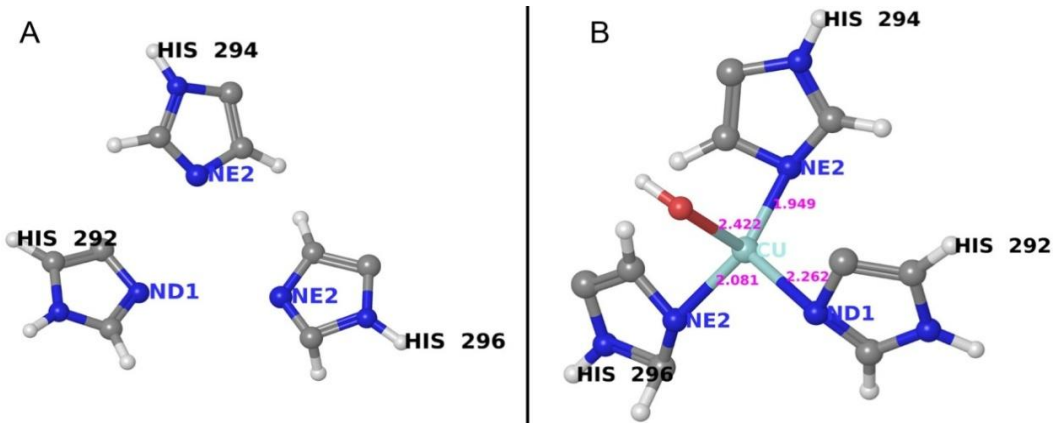

Figure 4.23: Orientation of copper binding histidine in mature LOX. A) Histidine residues flipped and oriented in same plain before copper binding; B) Copper ion was fixed and co-ordinate covalent bond generated between the 292N$^{\delta}$, 294N$^{\epsilon}$ and 296N$^{\epsilon}$ atoms in tetrahedral geometry.

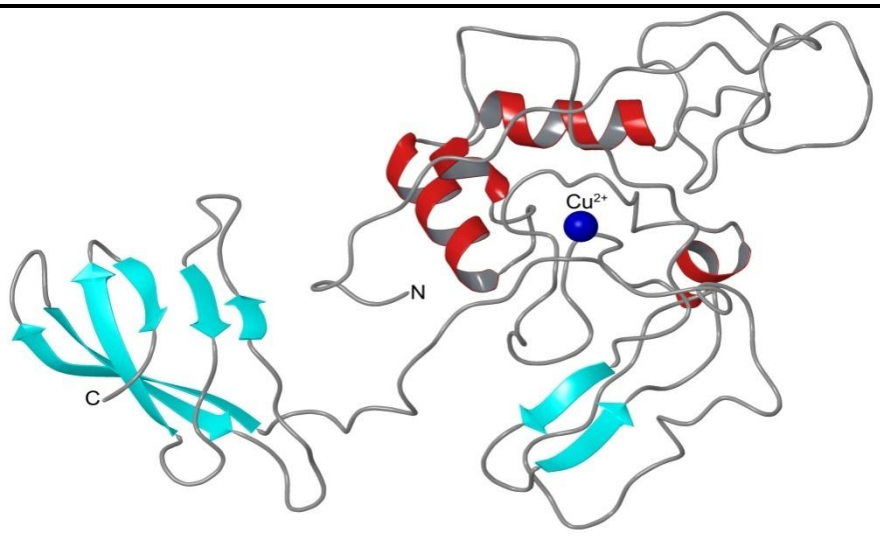

Figure 4.24: Optimized mature LOX model with Cu^{2+} ion. Representation of secondary structure of copper fixed mature LOX model in different colours (Helices in red, sheets in cyan, loop in grey and copper ion as blue sphere).

The copper fixed model was assessed with the Ramachandran plot which showed 90.7 % of residues in favoured region with no residue in disallowed region (Fig 4.25).

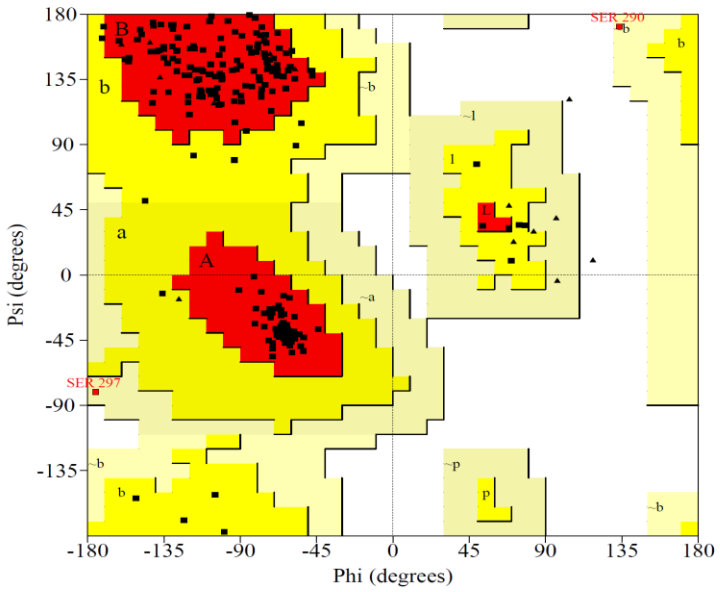

Plot statistics

Residues in most favoured regions [A,B,L]	196	90.7%
Residues in additional allowed regions [a,b,l,p]	18	8.3%
Residues in generously allowed regions [~a,~b,~l,~p]	2	0.9%
Residues in disallowed regions	0	0.0%
Number of non-glycine and non-proline residues	216	100.0%
Number of end-residues (excl. Gly and Pro)	2	
Number of glycine residues (shown as triangles)	15	
Number of proline residues	16	
Total number of residues	249	

Figure 4.25: Ramachandran plot of optimized mature LOX with Cu^{2+} ion

4.2.3 Modelling of disulfide bonds in predicted mLOX structure

Mature LOX sequence contains 10 cysteine residues and is known to form at least 4 disulfide bridges. Using MODELLER 9.10, disulfide script generated 4 disulfide bonds between the specific cysteine residues. After disulfide bonds were generated following observation were made: (1) there was overall loss in the secondary structure, (2) Ramachandran plot showed only 71 % in favoured region after generation of disulphide bonds but Initial model had 90 % in amino acid in favoured region (Ramachandran plot,

Figure 4.26), and (3) the co-ordinate bonds between the copper and histidine residue were lost. Hence, optimized mature LOX structure with Cu^{2+} ion without disulphide bonds was taken for further molecular dynamic studies.

Plot statistics

Residues in most favoured regions [A,B,L]	154	71.3%
Residues in additional allowed regions [a,b,l,p]	51	23.6%
Residues in generously allowed regions [~a,~b,~l,~p]	10	4.6%
Residues in disallowed regions	1	0.5%
	----	------
Number of non-glycine and non-proline residues	216	100.0%
Number of end-residues (excl. Gly and Pro)	2	
Number of glycine residues (shown as triangles)	15	
Number of proline residues	16	

Total number of residues	249	

Figure 4.26: Ramachandran plot statistics for mLOX with disulfide bonds

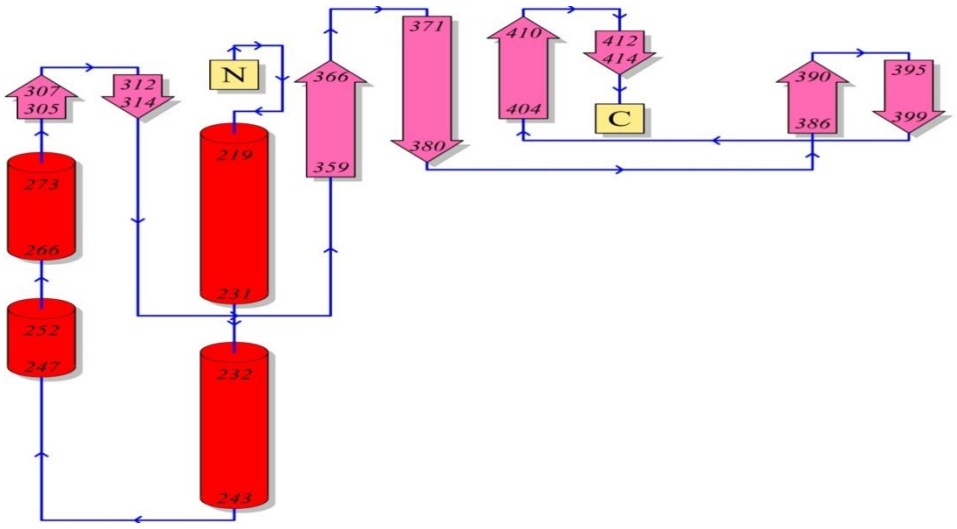

Figure 4.27: Overall topology (N to C terminus) of copper fixed mature LOX generated from PDBsum.

4.2.4 Molecular Dynamic studies of mLOX with Cu^{2+} ion

Further, this model was subjected to constrained molecular dynamics simulation for 4 ns wherein, the copper and its interacting residues were constrained throughout the simulation process. The potential energy of the protein after 4 ns simulation was -307193.771 $kJmol^{-1}$. The RMSD trajectory was stabilized for about 5.5 – 6.0 Å after 2 nano seconds of simulation and did not increase significantly further. This indicates that the system has evolved into a stable state and has reasonably converged over the production run (Figure 4.28 A). The radius of gyration analysis showed a deviation of 0.86 Å, inferring improved relaxation and structural stability of the modelled protein. RMSF graphs also suggest higher flexibility at the C-terminal with few residues showing higher degree of fluctuation (Figure 4.28 B).

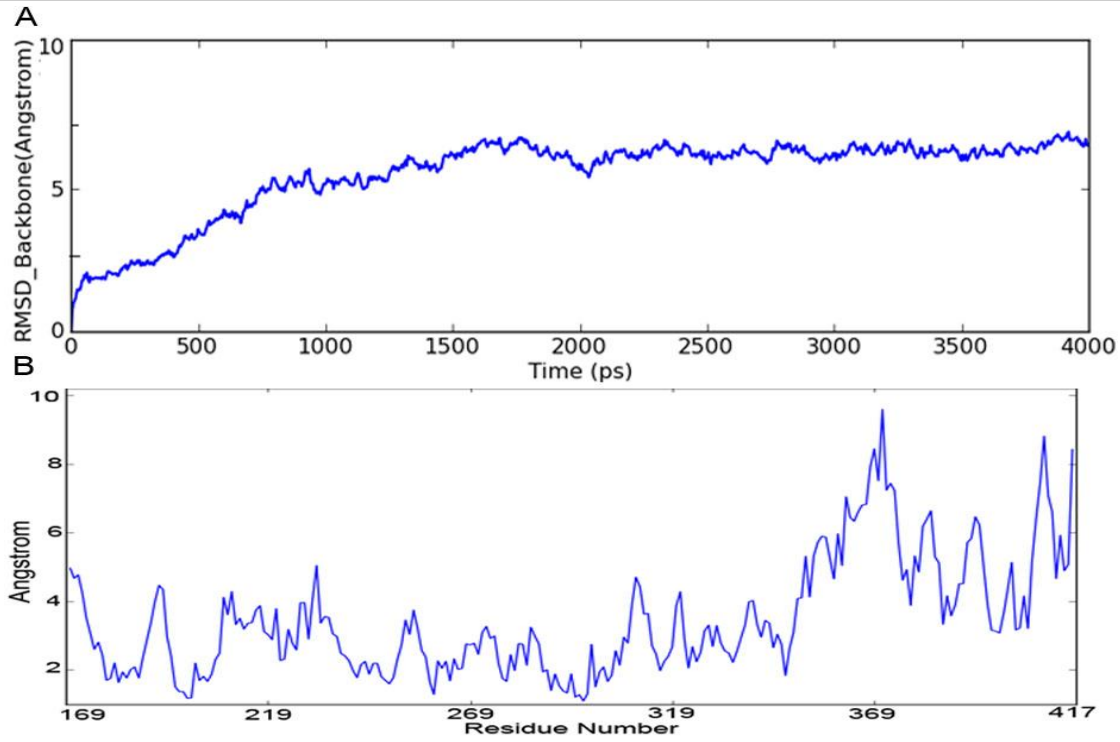

Figure 4.28: Constrained MD simulation results of mature LOX for 4 nano seconds. (A) RMSD plot of carbon - α backbone atoms showing the system stabilized after 2 nano second and remain stable till the end of 4 nano seconds and (B) Time-dependent RMSF fluctuation of individual residues of mature LOX in 4 nano seconds, C-terminal showing maximum fluctuation.

4.2.5 Validation of the predicted model

Backbone of a predicted model is validated through its Psi-Phi angles, Torsion angles, Chi-1/Chi-2 rotamers and bond lengths in WHAT IF server. For the predicted mLOX model Psi-Phi angles are analyzed through Ramachandran plot, which showed 90 % of residues in favoured region, 8.3 % in additional allowed region with 0.9 % in generously allowed region and no residues in the disallowed region. Torsion angle for all the residues are found to be normal. Only eight residues showed deviations in torsion angle but Z-scores for those lie near to the acceptable -2.0. The chi-1/chi-2 angles of the predicted model were found to be normal. Only four residues showed deviation in Tau angle (N-Cα-C) parameter. All other parameter like residue's side chain planarity, chirality, bond angle and bond length in the predicted structure cleared the WHAT IF server checks. This shows that backbone of the predicted structure is valid.

Short interatomic distance in 82 residues with mildest bumps, Tau angle (N-Cα-C) deviation in 4 residues and flipped positions of Aspartic acid (173 and 373), Histidine (343) and Glutamic acid (345) were listed in error. But the predicted model showed no interatomic clashes, tau angle and protonation states of above mentioned residues in protein preparation wizard of Schrödinger suite. Hence these errors cannot be a serious concern. Apart from that these errors protein shows -2.742 score for abnormal average packing environment against the allowed score of -3.0. This is also directly related to Z-score that describes how well this residue feels compared to other similar residues in well refined structures. Thus, as our model passes all Z score criteria this marginal error could be ignored. Predicted LOX model was analyzed through 88 listed parameters of WHAT IF server [4], out of them predicted model passed the 84 parameter with 15 parameters in the warning category and only 4 parameters are listed under the error category. With the available information and limited resource (as no similar protein for homology modeling), the predicted LOX model is highly plausible model. This validated model was further used for docking studies

4.2.6 Electrostatic potential graph of predicted mLOX with Cu^{2+} ion

Electrostatic potential surface of the copper fixed LOX model was calculated by Poisson-Boltzmann equation and was visualized in Maestro. The overall surface charge distribution was found to be negative to neutrally charge. Active cavity identified by the CASTp software showed charge distribution to be profoundly negative charge which would favor the interactions with positively charged substrates (Figure 4.29).

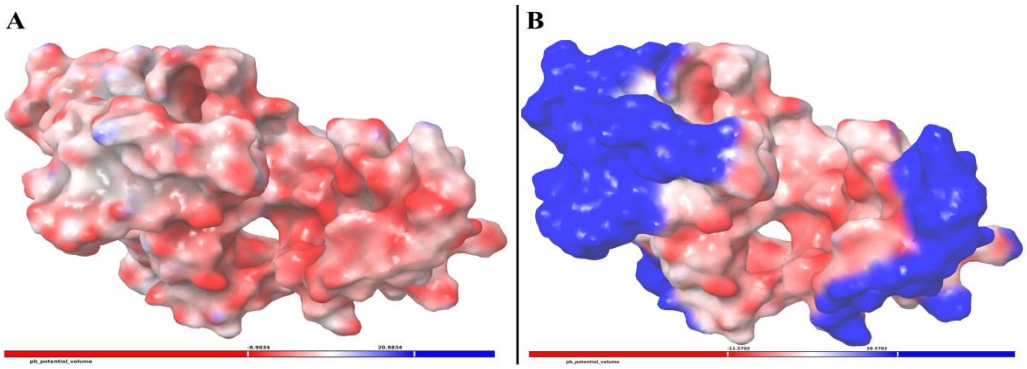

Figure 4.29: Electrostatic potential map of copper fixed mature LOX model. A) Overall surface charge distribution; B) charge distribution in the active cavity alone shown and other areas masked with blue colour.

4.2.7 Induced fit Docking of mLOX with pseudo substrate and inhibitors

Pseudo substrate (DAP) and 3 inhibitors (βAPN, Hcys and HCTL) were docked against the active cavity of copper-fixed LOX model using induced fit docking method. For each molecule, 20 docking poses were generated and the best docking pose was selected. The docked complexes were analyzed for docking score, MMGBSA and molecular interaction maps (Figure 4.30). In the docking results, DAP was to found to be bound with LOX with a significant docking and MMGBSA score of -7.511kcal/mol and -41.381 kcal/mol, respectively. DAP also forms hydrogen bonds with **Asp^{170}, Asp^{169}, Asp^{353}** and **Cys^{351}** of LOX.

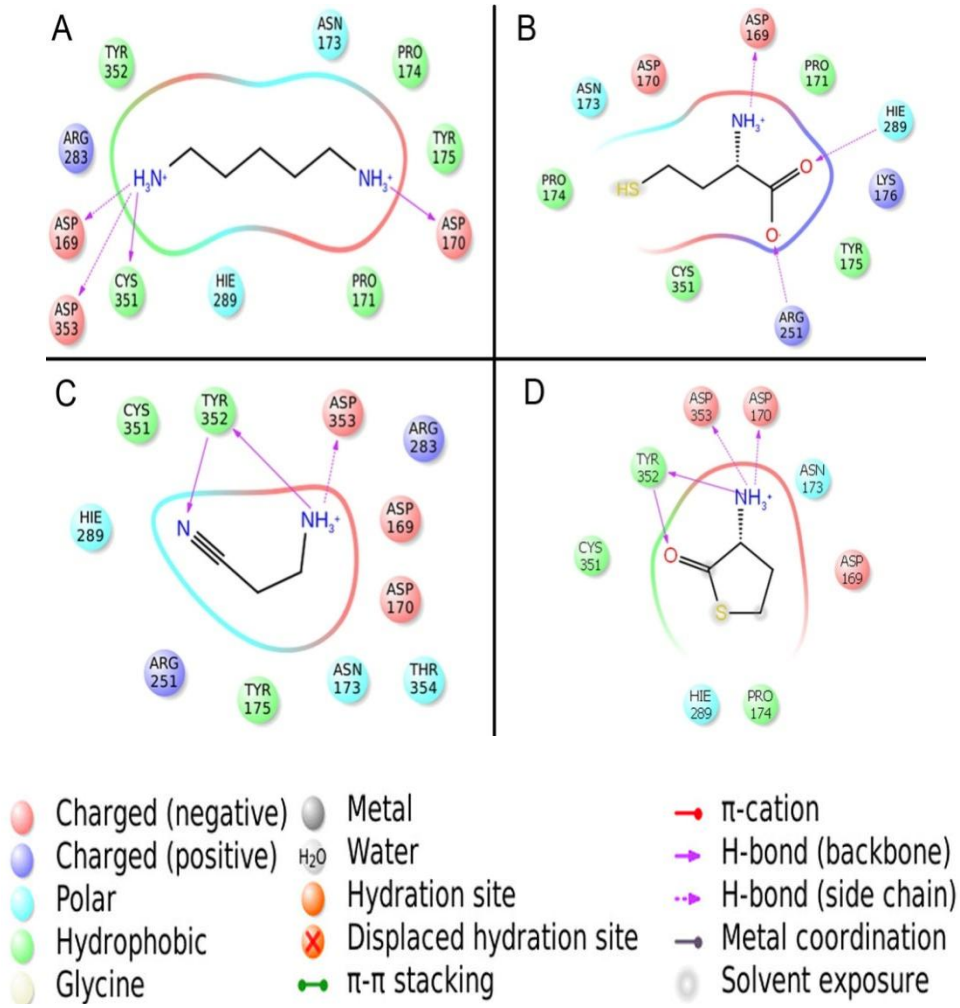

Figure 4.30: 2D interaction graph of mature LOX with its modulators using induced fit docking. (A) Diamino pentane forms hydrogen bonding with the negatively charged Asp[169], Asp[353] & Asp[170] and hydrophobic Cys[351]; (B) Hcys forms hydrogen bond with the negatively charged Asp[169], positively charged Arg[251] and polar His[289]; (C) βAPN forms hydrogen bonds with the negatively charged Asp[353] and hydrophobic Tyr[352]; (D) HCTL forms hydrogen bonds with negatively charged Asp[353] and Asp[170] and hydrophobic Tyr[352].

Table 4.4: IFD score and binding free energies computed using PRIME MM/GBSA

S.No.	PubChem ID: No	Name	Hydrogen bonds	IFD Docking score (kcal/mol)	MMGBSA score (kcal/mol)
1	273	DAP (Pseudo substrate)	Asp^{170}, Asp^{169}, Asp^{353} ,Cys^{351}	-7.51	-41.38
2	778	Hcys	Asp^{169}, Arg^{251} Arg^{251}, HiE^{289}	-9.53	-24.68
3	1667	βAPN	Asp^{353}, Tyr^{352}, Tyr^{352}	-6.29	-22.30
4	107712	HCTL	Asp^{170} ,Tyr^{352}, Asp^{353}	-4.81	-33.53

4.2.8 Validation of the IFD results by Amplex red assay using recombinant mLOX

To validate the IFD results, enzymatic activity of the recombinant mLOX was assessed in the presence of the inhibitors like β-APN, Hcys and HCTL by Amplex red assay (Figure 4. 31). In the initial screening, experiment HCTL showed inconsistent inhibition so it was removed from the future experiments. Hcys serve as a better inhibitor at lower concentration when compared to β-APN.

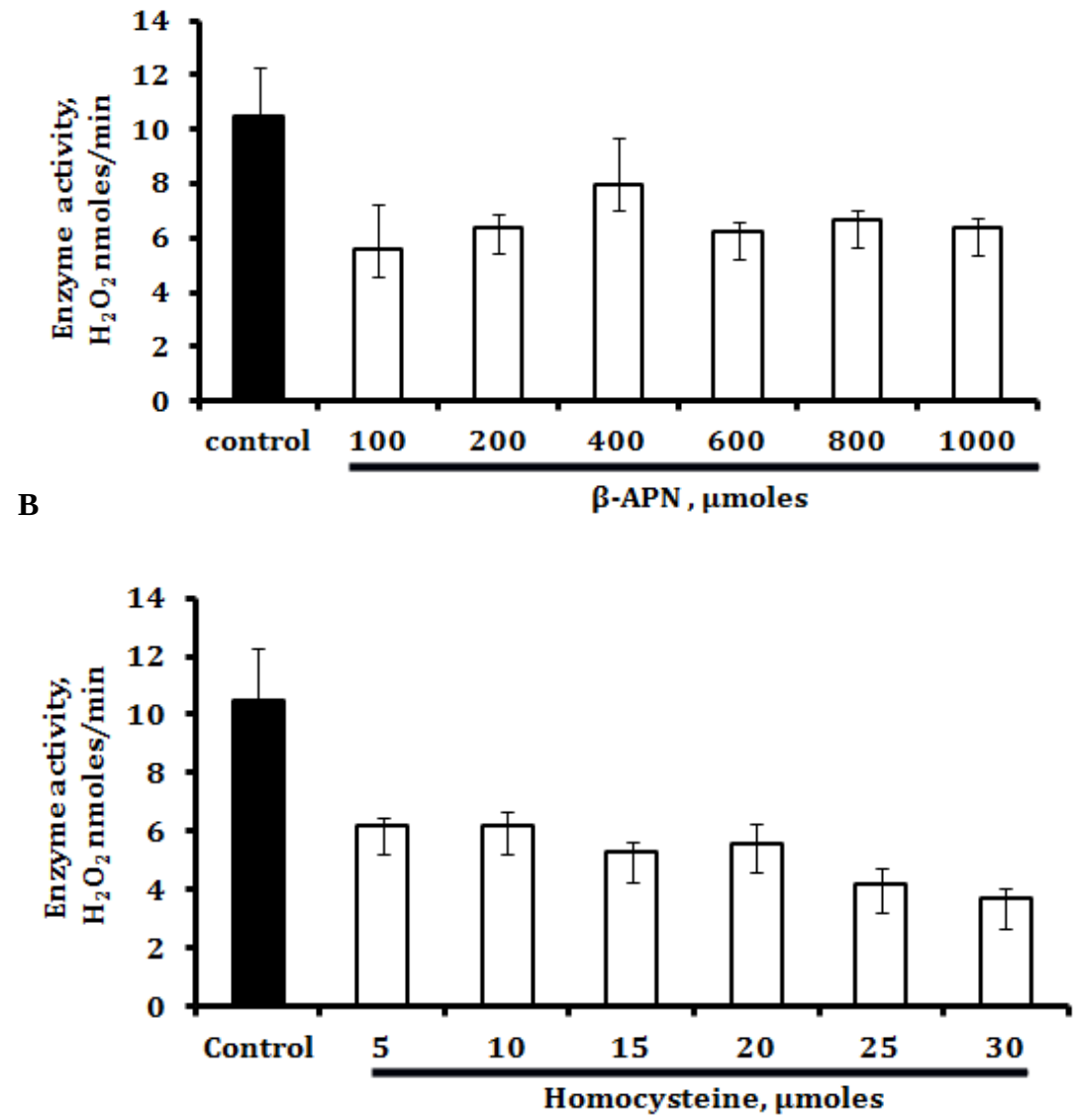

Figure 4.31: Enzyme activity of recombinant mLOX on DAP in the presence of inhibitors. A) β-APN and B) Homocysteine. Recombinant mLOX 100 ng, DAP 100 mM was preincubated at 37^{o}C for 5 min with respective concentration of inhibitors and reaction mixture was added then readings were taken fluorimetrically (Excitation 563 nm; Emission 587 nm). Data shown represent mean ± SD from three independent experiments.

Objective 3: To design LOX modulators to regulate its activity

Identifiying the molecules which can either upregulate or downregulate the LOX activity will have clinical application. Based on the nature of the molecule it can be applied to specific pathological condition. To develop LOX modulators, designed peptides from the conserved domains of LOX family. Peptides namely C1, C2 & C3 from the CRL domain and M1 & M2 from the copper binding region of LOX were designed. Peptides were characterised with CD spectra, mass spectroscopy and influence of the peptide on mLOX activity was assessed by Amplex red assay.

4.3.1 Copper binding analysis of LOX derived peptide using far UV-CD spectra

Secondary structure conformation of free peptide and peptide treated with copper chloride (Cu^{2+}) was studied by far UV-CD spectra. The spectrum of C1 peptide with copper showed incresacd α-helix content compared to the free peptide (Figure 4.32 A). Change in the secondary structure gives the clues that copper bounds to C1 peptide. C2 and C3 showed same degree of secondary structure for free and copper treated conditions (Figure 4.32 B & C). M1 and M2 peptide showed only random coil and no specific secondary struture with addition of copper also there was no change in their conformation (Figure 4.32 D & E). Scrambled peptide didn't showed any change in their secondary strucutre degree with or without copper (Figure 4.32 E).

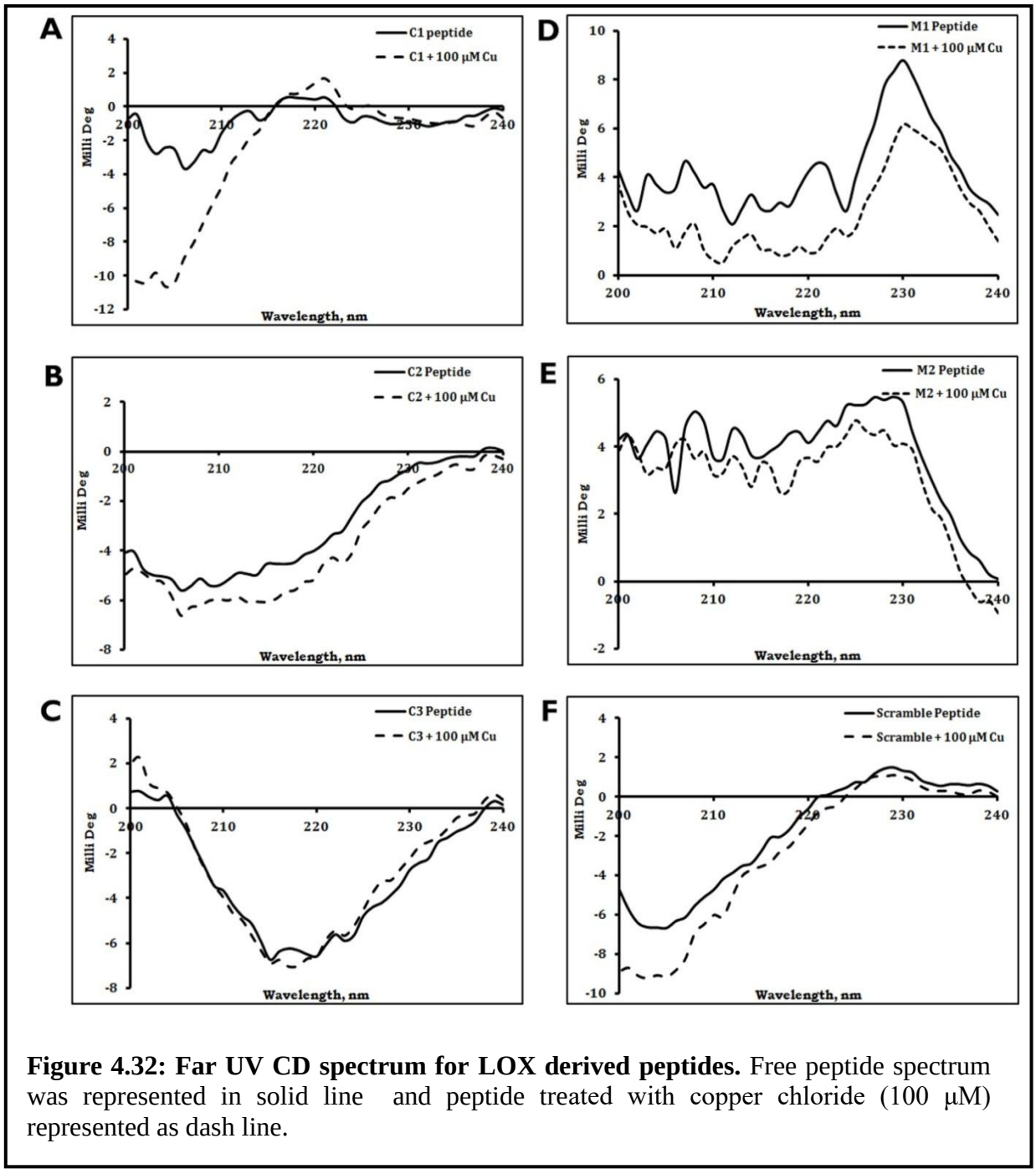

Figure 4.32: Far UV CD spectrum for LOX derived peptides. Free peptide spectrum was represented in solid line and peptide treated with copper chloride (100 µM) represented as dash line.

4.3.2 Copper binding analysis of LOX derived peptides by Mass spectroscopy

LOX derived peptides were analyzed for their Cu binding function. Peptide 10 µM was treated with equimolar concentration of copper chloride and analysis was done in Xevo G2S Qtof MS. C1, M1 and M2 peptide bound to the copper (Figure 4.33 and 4.34). M1 peptide dimerized up on copper bound condition. Other peptides C2, C3 and scramble peptide didn't show any copper binding function.

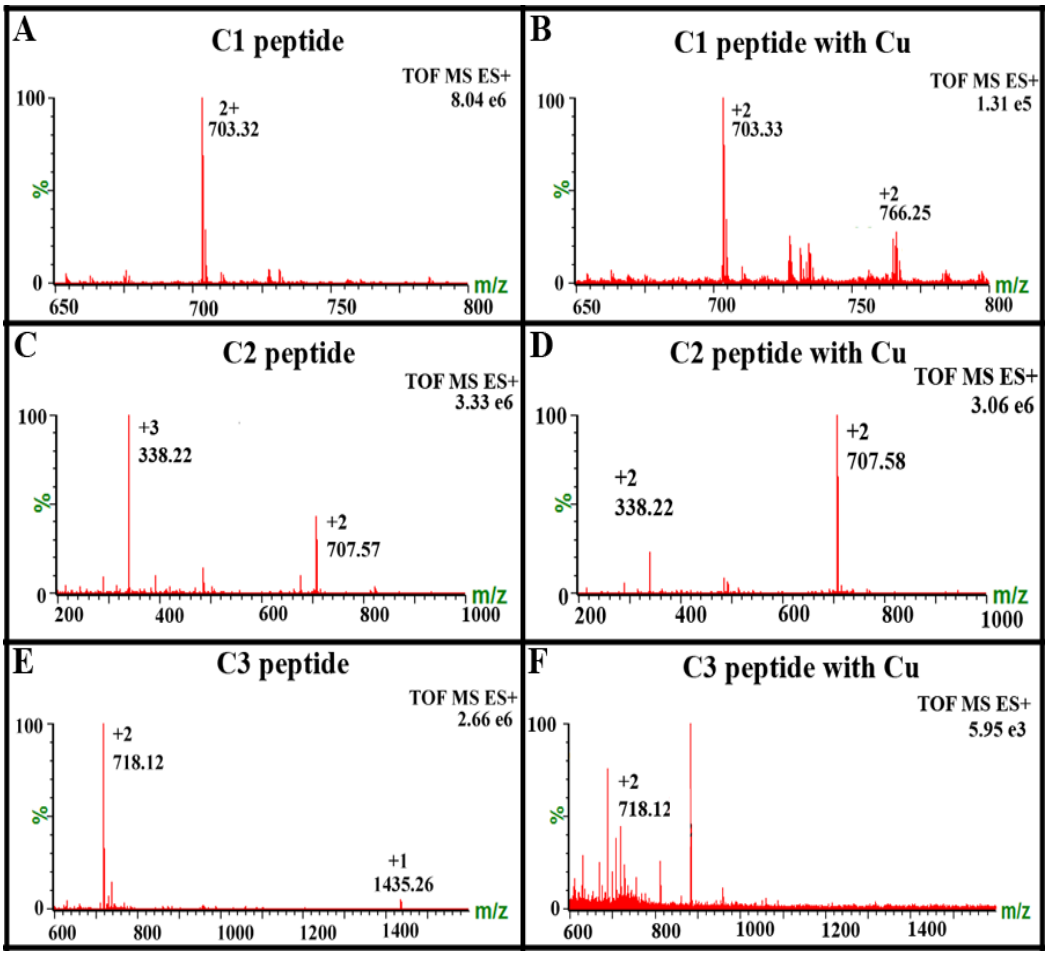

Figure 4.33: Copper binding analysis by mass spectroscopy for C-peptides. Copper binding property of the peptides derived from LOX conserved region were analyzed by MS. MS spectrum was collected for free peptide and peptide treated with equimolar concentration of copper chloride (Cu^{2+}). A) Free C1 peptide showed peak at 703 (2^{+}); B) when C1 peptide treated with copper it showed an additional peak at 766 (2^{+}). This shows that C1 peptide bounds to 2 copper. C) Free C2 peptide showed peak at 707 and 338 with respective to the charge state of +2 and +3; D) No significant change was observed with addition of copper to C2; E) Free C3 peptide; F) No significant change was observed with addition of copper to C3 peptide.

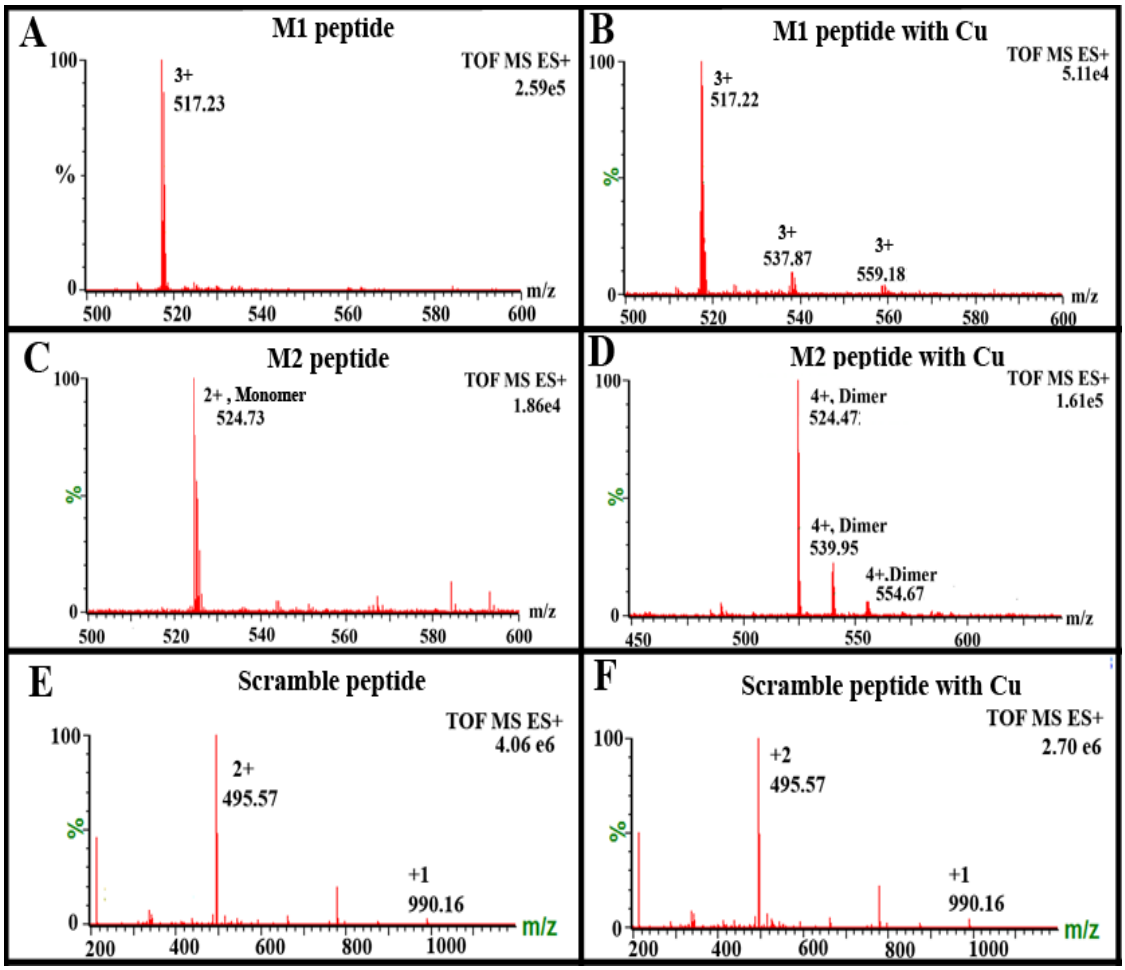

Figure 4.34: Copper binding analysis by mass spectroscopy for M- peptides Copper binding property of the peptides derived from LOX metal binding region were analyzed by MS. A) Free M1 peptide showed peak at 775 (2^+) and 517 (3^+) charge state; B) when M1 peptide treated with copper additional peaks of 537 and 559 (3^+) observed to free M1 peptide, which indicating the binding of one and two copper respectively. C) Free M2 peptide showed peaks at 524 (2^+); D) when M2 peptide treated with copper it showed additional peaks at 539 and 555 (4^+). The additional peaks indicating the binding of one and two copper respectively apart from that swift in the charge state from 2^+ to 4^+ denoting that copper inducing the dimerization of the peptide. E) Scrambled peptide & F) Scrambled peptide with copper, did not show any significant change in the peak pattern observed after addition of copper.

4.3.3 Effect of LOX derived peptides on recombinant mLOX enzymatic activity

LOX activity was assessed in the presence of designed peptide with the activator copper. C1 peptide at 10 nm inhibited 84 % activity (Figure 4.35 A), C2 peptide at 10 nm showed inhibition up to 79 % (Figure 4.35 B), C3 peptide didn't showed consistent results (Figure 4.35 C). M1 peptide at 10 nm showed 64 % inhibition (Figure 4.36 A). M2 peptide showed 62 % of inhibition (Figure 4.36 B). β-APN show only 18 % of inhibition at 500 µM concentration. Scramble peptide did not show any significant inhibition. Percentages of enzyme activity were calculated by keeping activity of mLOX as 100 %.

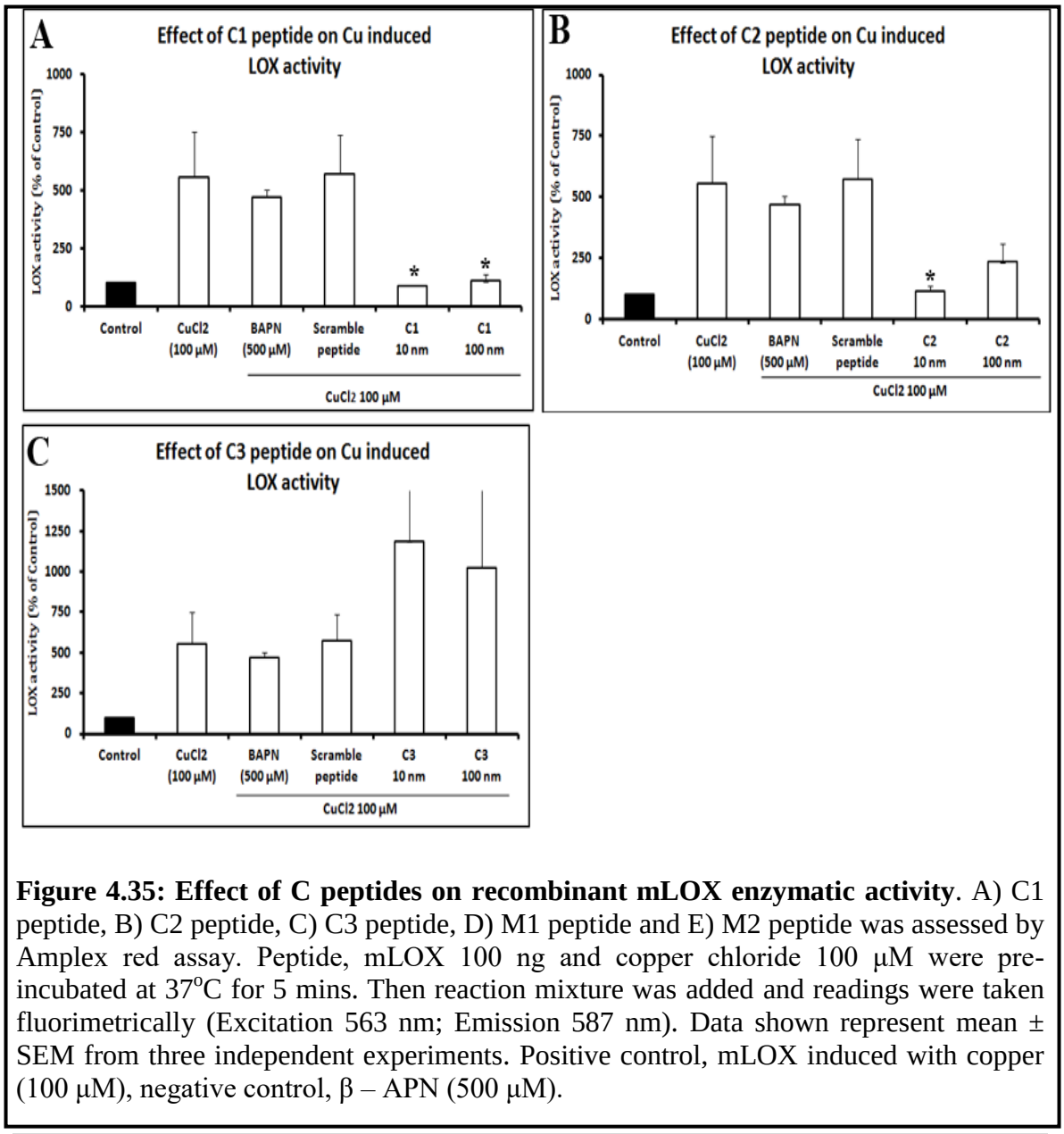

Figure 4.35: Effect of C peptides on recombinant mLOX enzymatic activity. A) C1 peptide, B) C2 peptide, C) C3 peptide, D) M1 peptide and E) M2 peptide was assessed by Amplex red assay. Peptide, mLOX 100 ng and copper chloride 100 µM were pre-incubated at 37^{o}C for 5 mins. Then reaction mixture was added and readings were taken fluorimetrically (Excitation 563 nm; Emission 587 nm). Data shown represent mean ± SEM from three independent experiments. Positive control, mLOX induced with copper (100 µM), negative control, β – APN (500 µM).

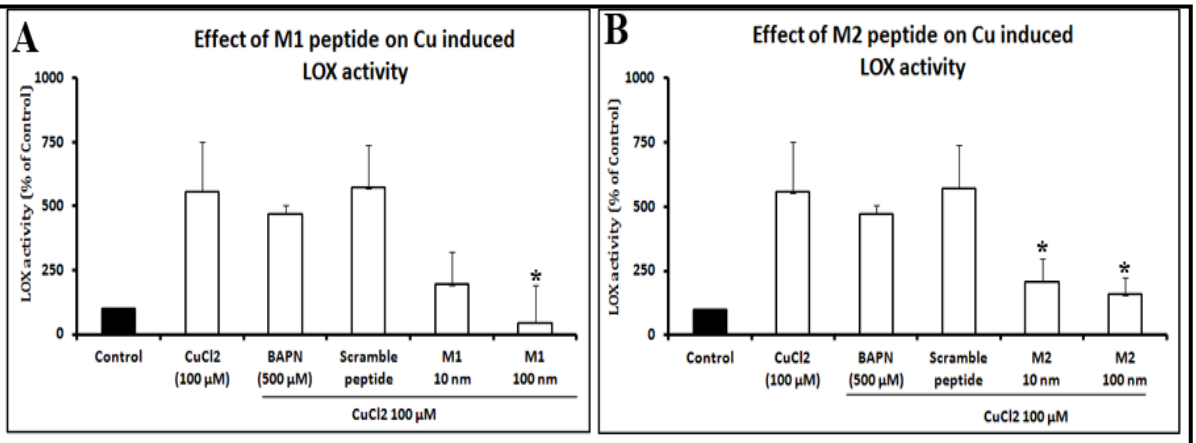

Figure 4.36: Effect of M peptides on recombinant mLOX enzymatic activity. A) M1 peptide and B) M2 peptide, was assessed by Amplex red assay as explained for the C peptides.

4.4 ELISA and Dot blot analysis of in-house developed anti mLOX antibody

The purified mLOX was used to generate antibody. Rabbit was immunized with purified mLOX and polyclonal anti mLOX antibody was purified from the rabbit serum. Sensitivity of the purified mLOX antibody was assessed by dot blot and indirect ELISA. In both the technique dot blot and indirect ELISA technique signal intensity varied with concentration of the antigen. The antibody showed sensitivity up to the concentration of 1.25 µg /ml (0.00125 dilution factor) against the 100 ng of mLOX in both the experiments. For 10 ng of mLOX signal was observed up to 2.5 µg /ml (0.0025 dilution factor). Saturated signal was observed up to the conc. of 10 µg /ml (0.01 dilution factor) for both antigen concentrations (10 and 100 ng) in both the experimental setup.

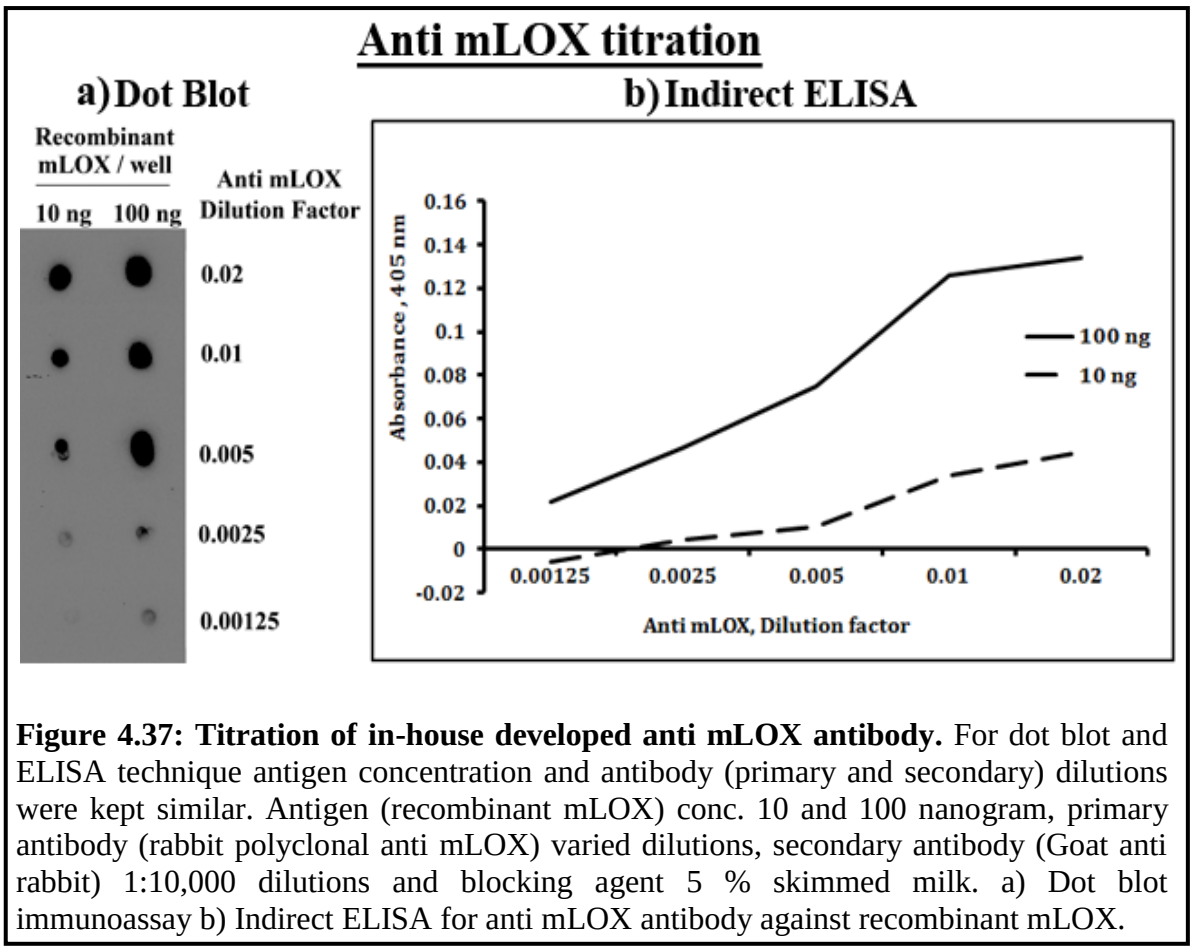

Figure 4.37: Titration of in-house developed anti mLOX antibody. For dot blot and ELISA technique antigen concentration and antibody (primary and secondary) dilutions were kept similar. Antigen (recombinant mLOX) conc. 10 and 100 nanogram, primary antibody (rabbit polyclonal anti mLOX) varied dilutions, secondary antibody (Goat anti rabbit) 1:10,000 dilutions and blocking agent 5 % skimmed milk. a) Dot blot immunoassay b) Indirect ELISA for anti mLOX antibody against recombinant mLOX.

4.4.1 Immuno fluorescence of LOX in HeLa cells using various dilutions of anti mLOX antibody

With the in-house purified polyclonal anti mLOX antibody, HeLa cells were probed for LOX. In-house developed antibody was found to be sensitive up to a dilutions factor of 0.005 (5 µg /ml).

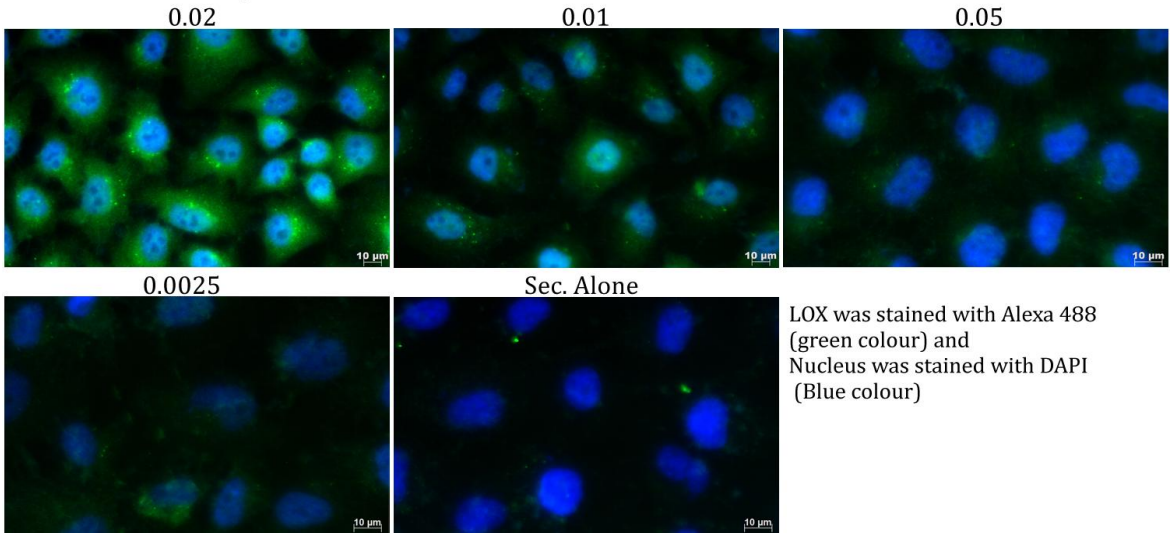

Figure 4.38: Immuno fluorescence of LOX in HeLa cells using various dilutions of anti mLOX antibody. HeLa cells were stained probed with various dilutions of in-house purified anti mLOX antibdoy and stained with FITC-conjugated goat anti rabbit IgG (1:700 dilution). All images were acquired with 20X objective in Axio-observer microscope.

4.4.2 LOX pull down assay using anti mLOX antibody

With the purified polyclonal anti mLOX, LOX pull down assay was performed in normal serum sample to identify its interacting partners. The serum pull down elute was run in a SDS PAGE gel and was silver stained. Visualized bands were excised and subjected to in-gel tryptic digestion and was analyzed using nano LC XEVO G2-S QTof MS.

Table 4.5 lists the proteins identified through LOX IP pull down of serum sample by mass spectroscopy. Mass spectroscopy results showed total hit of 19 proteins from the tryptic digestion of serum IP elute. Of the 19 identified proteins, only 11 proteins with sequence coverage of 5 % are listed in table 4.5 and the bait protein LOX was identified with 5.52% sequence coverage. Ten proteins have been identified in the IP pull down assay of LOX in the human serum. The results are to be validated further using western blotting and co-localization experiments.

Table 4.5: List of proteins identified for LOX pull down assay from human serum using MS

S.No.	Protein Entry	Protein Description	Protein Sequence Coverage (%)	Major function
1	P04792	Heat shock protein beta 1 OS	48.29	Involved in stress resistance and actin organization
2	Q107X0	Putative protein KRIP1 OS	46.27	Expressed abundantly in prostate gland. Function unidentified.
3	Q9UBY9	Heat shock protein beta 7 OS	18.82	Highly expressed in heart muscles and involved in contraction
4	Q8WXA9	Splicing regulatory glutamine lysine rich protein 1	13.19	Present in nucleus and splicesomes. Inhibits the splicing activity of SFRS1, SFRS2 and SFRS6
5	P04792	Heat shock protein beta 1	13.17	Cytoplasmic in inter phase cells and involved in stress resistance and actin organization
6	Q8TE23	Taste receptor type 1 member 2	11.08	Recognizes diverse natural and synthetic sweeteners
7	A6NEQ2	Protein FAM181B	10.8	Function undefined
8	Q13064	Probable E3 ubiquitin protein ligase makorin 3	10.45	Catalyzing the covalent attachment of ubiquitin moieties onto substrate proteins
9	P06733	Alpha enolase	10.14	Involved in glycolysis
10	O75953	DnaJ homolog subfamily B member 5	8.91	Inhibitor of RNA polymerase II promoter
11	**P28300**	**Protein lysine 6 oxidase**	**5.52**	**Cross linking of collagen and elastin**

CHAPTER 5 - DISCUSSION

Extracellular matrix (ECM) plays an important role in both physiological and pathological conditions. Collagen and elastin are the major structural proteins in the ECM [173] and gives structural stability and tensile strength by their insoluble nature. LOX is a copper dependent amine oxidase and the LOX protein family has 5 members- LOX, LOXL1, LOXL2, LOXL3 and LOXL4. The main function of LOX is in solubilisation and stabilisation of extracellular collagen and elastin substrates. It is also known to be involved in functions like tissue development, cell proliferation, cell signalling, cell migration and angiogenesis [174] [175] [55]. Thus, LOX and its isoforms have major role in normal physiological functions and pathophysiological conditions like hypoxia induced tumor metastasis [176] [149], fibrotic disorders [80] and connective tissue disorders [177]. Despite LOX being a vital protein, three dimensional conformations of LOX is not yet elucidated. Information about the functional and structural aspects of LOX is limited.

In this study, primary objective was to characterise LOX in its purified form. Purification of LOX from bovine aorta is performed as described by Kagan et al [119]. Purification resulted in low yield and activity in multiple fractions of anion exchange chromatography (Figure 4.1). Kagan et al had earlier reported purification of LOX from bovine aorta by combination of anion exchange and molecular sieve chromatography, which showed in activity in various fractions (Figure 4.1). This observation may be due to the presence of LOX isoforms in the bovine aorta [119]. Purification of LOX from bovine aorta is a tedious and cumbersome process, and also resulted in low yield (Table 4.1), along with the presence of other isoforms. Presence of other isoforms may lead to ambiguity in further study about LOX enzymatic activity, structure and function. Hence, recombinant protein technique was adopted in the present work obtain mature LOX alone.

5.1 Recombinant mLOX preparation

Earlier, Ouzzine et al attempted to purify LOX in soluble form from periplasmic space and obtained 0.04 mg of purified LOX per litre of broth [125]. Herwald et al purified LOX from the inclusion bodies under denaturing conditions using 8 M urea [126]. In the present work, using infusion cloning technique mature LOX gene was ligated into the pQE-30 Xa vector (Figure 4.3). Vector construct was over expressed in M15 (pREP4) *E.coli* by IPTG induction and purified using one step His-tag affinity purification method under denaturing condition using 8 M urea (Figure 4.6). Purification yield was upto 10 - 15 mg per liter of LB broth, which was comparable with the previous reports [127] [26].

5.2 Refolding of LOX

LOX protein will form amorphous aggregate in aqueous solution immediately though the 60 % amino acid sequence is made of hydrophilic residues [178]. Possible reason for this nature that is N-terminal of mature LOX contains more hydrophobic tyrosine residues; this region might trigger the polymerization and leads to aggregation of the purified LOX [178]. At least 2 M urea requirement has been reported for LOX purification either by conventional or recombinant techniques [119] [94]. However, Herwald et al reported recombinant LOX was soluble in 10 mM of potassium phosphate buffer [126], which resulted in protein aggregation in the present study. Therefore it became necessary to screen various buffers. The glycine-NaOH buffer (pH 8.0) with 10% glycerol was identified here as an ideal buffer (Table 3.9) which does not have the above mentioned shortcomings.

The recombinant mLOX was purified under denaturing condition (buffer containing 8 M urea), after purification by step wise dialysis against the buffer glycine – NaOH buffer pH of 8.0 with 10% glycerol with stepwise reduction in the urea concentration. Denatured protein can be refolded by step wise dialysis and reducing the denaturant concentration [179]. Glycine acts as protein stabilizing agent by preferential exclusion mechanism and thereby reduces the surface tension. Also glycine prevents the change in pH while freezing, by its bulking action [180]. Glycerol acts as a co-solvent in protein

stabilization, by pushing the hydrophobic region of a protein into it and preventing inter-molecular interactions. Glycerol also gives compactness and rigidity to protein structure [181]. Probably, synergistic action of glycine and glycerol maintained the purified mLOX in solution state stably [182].

5.3 His tag removal

His tag is widely tagged with recombinant protein for purification because of its low immunogenicity and low interference with protein of interest [183] [184] [185]. But variation in the activity of recombinant chlorocatechol 1,2-dioxygenase with and without His tag has been reported [186]. Interference of His tag on the structure and activity depends on the individual proteins nature and structure [187]. As LOX is a copper dependent protein and His residues are known to bind with the copper. In order to prevent interference in LOX activity, His tag was removed using endoprotease factor Xa with an efficiency of about 50 % (Figure 4.10). This is the first work to show removal of His tag from the recombinant mLOX. Previous reports [127] [126] [188] that have demonstrated over expressed and purified LOX had retained the His tag.

5.4 Enzymatic characterisation

Enzymatic activity of mLOX was assessed by the hydrogen peroxide coupled Amplex red assay [189] [54]. The recombinant mLOX showed maximum activity at the pH of 7.5 to 8.5 (Figure 4.12). It is reported that LOX oxidises basic globular proteins with pI value of > 8.0 and not the neutral and acidic proteins. LOX purified from the *Dosidicus gigas* showed maximum activity between the pH of 8 to 8.2 [190]. Torres-Arreola et al showed *Dosidicus gigas* LOX showed activity up to 90 °C [190]. In this study too, the recombinant mLOX was stable at 20 °C and 80 °C with minimal change in secondary structure (8.12 % in α-helices and 3.64 % in β- sheet) (Figure 4.17), which coincided with increased enzyme activity in the range of temperatures between 20 °C and 80 °C (Fig. 4.13).

At temperature of 37 °C and pH 8.0, recombinant mLOX enzyme showed maximum enzyme activity of 70 nmoles of DAP/ min / μg of recombinant mLOX (Table 4.3), when saturated with the non peptidyl diamine substrate DAP. Herwald et al showed 0.31 U /mg (1 Unit = 1 n mol of DAP / min) of recombinant LOX activity using Amplex red assay [126]. Jung et al purified LOX by cloning and showed activity of 0.097 U/mg (1 Unit = 1 μmol of benzyl amine / min) using amine oxidase activity assay [188]. The activity of purified recombinant mLOX in this study was higher than the previous reports. In both the previous reports, recombinant LOX was assayed with His tagged protein, unlike the present study where the His tag was removed.

Recombinant mLOX showed affinity for DAP was 44 mM (Table 4.3) where as Palamkumbura et al determined Km for LOX towards DAP to be 0.5 mM [54]. The possible reasons for this difference may be: (a) Difference in enzyme source, here purified recombinant mLOX and in the reported work LOX was purified from bovine aorta, (b) Only 50 % of recombinant mLOX found to be in copper bound state (c) drawbacks of dialysis method in refolding the protein.

Kothapalli et al showed that exogenously added LOX can increase the elasin synthesis and its cross linking in rat smooth muscle cells [191]. In 2014 Makris et al expremental showed that collagen cross linking and its tensile strenght can be improved by exogenous LOX addition, both in in vitro and in vivo condtions [192]. In this study ARPE-19 cells showed increased collagen cross linking in dose dependent manner to exogenously added recombinant mLOX (Figure 4.16). This shows that recombinant mLOX purifed in this study was enzymatically active.

5.5 *In silico* structure prediction of human mLOX

So far crystallized structure of LOX is not available to understand its tertiary arrangement. One report by site directed mutagenesis cloning method determined the histidine which is involved in the copper binding [26] and another one using multiple endoprotease determined the cysteine residues pairs involved in disulphide bond

formation [127]. Lynch and Ryvkin reported the three dimension structure of human LOX by homology modelling, despite LOX sharing less than 25 % homology with the current PBD database [193]. Due to this variation reliability of their predicted LOX structure is uncertain [193]. Other than these reports, tertiary conformation of LOX was not explained neither by *in silico* nor *in vitro* studies. In this study, predicted the 3D structure of human mature LOX by *ab initio* method (Figure 4.21) and also fixed the optimal coordinated covalent interactions of Cu^{2+} at the copper binding region (Figure 4.23). The predicted structure was found to be a valid model as per SAVES evaluation (http: //nihserver.mbi.ucla.edu /SAVES/) (Figure 4.24).

5.6 Generation of copper coordination in mLOX

Copper belongs to the transition metal and exists in two ionic state; cuprous [Cu^{1+} with $3d^{10}$ electronic configuration] and cupric [Cu^{2+} with $3d^{9}$ electronic configuration] in biological systems. Generally, in amine oxidase copper present in cupric ionic state and classified under type 2 copper proteins, based on their spectroscopic property. Nitrogen atom of the histidine moiety acts as the ligand in the type 2 copper proteins [194]. Gacheru et al in 1990, with EPR spectroscopic analysis demonstrated that three histidine moiety act as the ligand for copper [25]. Lopez and Frederick identified the histidine residues 292, 294 and 296 as the copper ligand in LOX protein by site directed mutagenic analysis [26]. In cupric state, copper exist majorly in the octahedral or square pyramidal geometry in copper proteins [195]. It is hypothesized that in LOX, copper exist in the octahedral geometry and distorted in tetragonal symmetry[24] [25]. In the present study, with the predicted LOX structure attempted to generate coordinate covalent bonds between copper ion [Cu^{2+}] and specified histidine residues (292, 294 and 296) as mentioned in literature [196]. Copper binding region of LOX was predicted to be random coil in nature and will exhibit a talon shaped loop structure with copper to be positioned at the centre of the loop [24]. Copper binding site of present predicted LOX structure displayed loop structure with a shape of talon; this is in agreement with the previous reports [24] [196]. By Cartesian coordinate calculation positioned the copper ion and generated the coordinate covalent between copper and histidine atoms ($292N^{\delta}$, $294N^{\epsilon}$

and 296N$^{\epsilon}$) with the bond length of 1.9 – 2.2 Å as explained in the methodology section 3.2.12.5. Tetrahedral geometry was completed with one water molecule in the fourth position of the copper bond (Figure 4.23 B) similar copper geometry was reported in crystal structure of *E.coli* amine oxidase [160].

5.7 MD simulation

The Root Mean Square Deviation (RMSD) of the recombinant mLOX showed Cα-backbone displacement within a range of 0.5 Å after 2 ns (figure 4.28 A) and maintained till the end of production run which suggests the stability of the predicted model. Moreover, the radius of gyration plot also infers the compactness of the model of protein backbone. RMSF (Root Mean Square Fluctuation) of the model shows, residues in C-terminal are highly flexible (figure 4.28 B).

5.8 Induced Fit Docking

Using induced fit docking (IFD), binding mode of pseudo substrate DAP and inhibitors (β-APN, Hcys and HCTL) are analyzed in this study. Beta-amino propionitrile (β-APN) is described as molecule which disturbs the formation of collagen and elastin. It was reported that, 14 day chick embryo administrated with βAPN led to negligible elastin aggregation and fiber formation which resulted in structural abnormalities [197]. In both *in vitro* and *in vivo* studies, β-APN showed inhibition of LOX enzymatic activities and impaired maturation of elastin and collagen [198] [199] [200] [149]. In previous report from our lab demonstrated that elevated level of Hcys inhibits the activity of LOX in the PDR vitreous samples [167]. Another report stated that HCTL compete with DAP substrate for LOX and inhibits its activity [201]. Based on this experimental proof, these molecules where selected and their binding ability was analyzed by Induced fit docking and LOX activity assay.

In amine oxidases, the substrate binding and positioning are mainly guided by charge – charge interactions. These substrates are generally cationic and found to interact with the

key anionic residues at active cavity [202]. Similarly, the active cavity of the modelled LOX structure was observed to be anionic. Further, the proton abstraction is usually catalyzed by aspartic acid in case of all amine oxidases [203] [204]**.** In this study, the IFD results for copper fixed LOX model with pseudo substrate DAP and all the inhibitors showed hydrogen bonding with aspartic acid residues. Copper amine oxidases follow the ping pong catalytic mechanism [205], in the first half of the oxidative reaction, proton from α-carbon of the substrate is removed by aspartic acid present in the catalytic cavity [203] [206] [32]. Here, DAP showed interaction with aspartic acid residue (Asp 353), which is conserved among all the members of LOX (Table 4.4). This aspartic acid (Asp 353) present near the tyrosine (Tyr 355) which proposed to form carbonyl cofactor (LTQ) with lysine (Lys 320) by cross linking. Possibly this aspartic acid (Asp 353) will act as catalytic base in human LOX. Inhibitors βAPN and HCTL also showed interaction with Asp 353 except HCys, which might have different mode of inhibition. The docking score showed binding affinity of inhibitors toward LOX in the following order Hcys> βAPN>HCTL. The docking results are validated by the *in vitro* Amplex red assay using recombinant mLOX against these inhibitors with DAP as substrate. HCys showed 50 % of enzyme inhibition activity against mLOX at 30 μM concentrations where as βAPN showed only 20 % of enzyme inhibition at milli molar concentration (Figure 4.31 A and B). HCTL showed inconsistent results. Thus, *in vitro* result correlates with *in silico* IFD results. Here, both *in vitro* and *in silico* results show that βAPN has less potent enzyme inhibitor effect on LOX, when compared to the homocysteine. The mechanism of inhibition has to be further studied.

This is the first study to predict and validate the 3D conformation of mature LOX with proper co-ordination of copper. Overall spatial arrangement of the predicted model correlates with the available literature and docking studies results go in agreement with the *in vitro* experiments of this study. However the present model lacks the carbonyl cofactor (LTQ) and disulphide bonds, which are reported to be present in the LOX structure. Hence these limitations are to be considered while understanding and interpreting of the results derived from this structure. Nevertheless this model can serve as valid structure in understanding the binding nature of LOX and to design small modulators to regulate its activity. With the current available facility, LOX structure has

been predicted, copper coordinates are generated with specified ligand and docking studies are performed with the known substrate and inhibitor.

5.9 Spectroscopic analysis

Based on the environment fluorescence profile of tryptophan varies [207] and this property is used to investigate the folding of proteins [208]. Azurin is a small blue copper protein (15 kDa) with single tryptophan. In folded state the tryptophan in azurin is completely buried in apolar environment and shows emission maxima at 307 nm [209]. Mature LOX contains 3 tryptophan residues (286, 288 and 363), among them 2 residues (286 and 288) present in the conserved copper binding site. Tryptophan emission spectra of recombinant mLOX showed heterogeneous emission, emission peak at 304 nm with major contribution and emission peat at 333-336 nm with minimal contribution in the total emission (Figure 4.18). In the predicted structure, tryptophan (286 and 288) present in buried state along with the copper binding region and tryptophan 363 found in the surface (Figure 5.1). *In vitro* and *in silico* results suggest heterogeneous condition of these tryptophan's in LOX structure. Considering the predicted structure and recombinant mLOX is near to native folded condition, the emission peak of tryptophan at 304 (Figure 8.18) was raised due buried environment and surrounded by the energy acceptors like histidine [152] residues and copper [210].

Iriarte et al using DTNB method showed that LOX will contain at least four disulphide bridges and stated that disulphide bonds gives thermo stability for LOX [211]. In 2011, using mass spectroscopy method mapped the cysteine pairs (238-244, 291- 340, 324-330, 351-361 and 398-412 specified cysteine residues) involved in the disulphide bonding of LOX [127]. To address this issue, DTT reduced recombinant mLOX showed shift in the tryptophan emission to 307 nm and ANSA fluorescence maxima shifted from 460 to 470 nm (Figure 4.19). Apart from this binding of ANSA to recombinant mLOX increased with guanidinium hydrochloride after reducing with DTT. Jana et al demonstrated streptomycin adenyltransferase structure is stabilized by disulphide bonds using tryptophan emission and ANSA binding analysis [212]. Chen et al stated that disulphide

bonds render rigid and high resistance to denaturant [127] for LOX and observation made in this study is supports this statement.

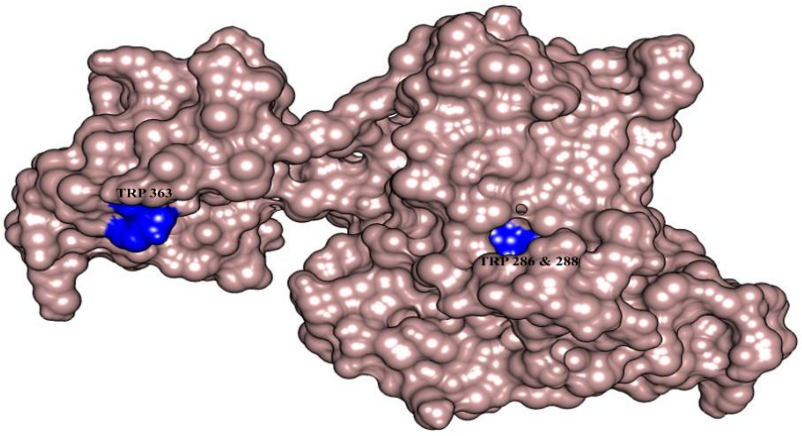

Figure 5.1: Localization of the tryptophan in the predicted LOX model. Over all surface of the protein is shown in grey colour and tryptophan residues (286, 288 and 363) are shown in blue colour.

5.10 LOX interacting proteins

Interacting protein of LOX is poorly understood, particularly with respect to serum. In this study**,** LOX IP pull down assay was performed from normal human serum to identify the interacting partner of LOX using mass spectroscopy analysis (Table 4.5). In-house developed anti mLOX antibody was used for the IP pull down assay. By pull down assay, most of the identified proteins belong to heat shock family proteins. In the biosynthesis of collagen, HSP involved in the folding and modification of translated tropocollagen in the intracellular and LOX involved in the maturation of tropocollagen in extra cellular. In liver fibrosis, miR-29b shown inhibit the ECM formation through down regulation of LOX and HSP 47 [213]. With the identified protein using GENEMANIA (online open software) putative pathway was derived based on the co-expressed proteins and proteins to have physical interaction (Figure 5.2). In putative pathway showed HIF1α and NFκB proteins, these two proteins are reported to involve in the LOX expression and activity [81] [83]. Erler showed, hypoxia inducible factor regulates the LOX expression in the breast and head and neck tumours [62]. The interacting partners identified in the

present study are in agreement with the cited literatures but these results should be further validated by other experiments like far western and FRET analysis.

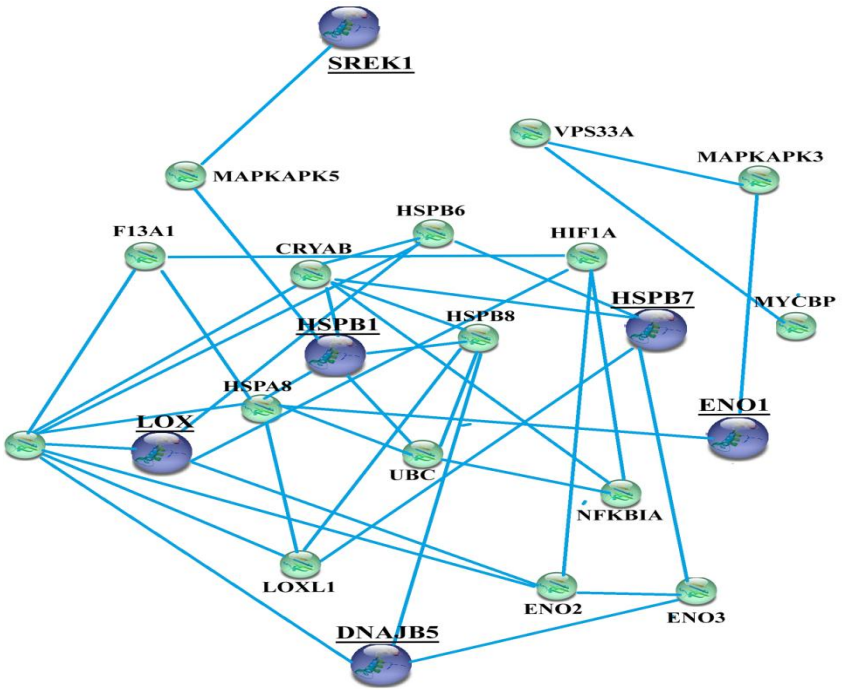

Figure 5.2: Putative interaction map of LOX build - using GENEMANIA. Proteins identified by MS were representing in blue spheres. Green spheres are the interacting proteins build by GENEMANIA software.

5.11 Inhibitory effect of the LOX derived peptides

The modern era of drug development aims to regulate proteins by small molecules which show high potential with low side effect and immunogenicity [214]. Peptide gained importance in the field of drug development due its stability, low immunogenicity, improved bioavailability with additional delivery methods [215], [216]. Regulation of LOX expression and activity by small chemical molecules, siRNA, and antibody are reported in literature. In this study, 5 peptides designed from the conserved metal binding region (M1 & M2) and CRL (C1, C2 and C3) domain of the LOX family members. ESI MS result of peptides M1, M2 and C1 showed copper binding properties (Figure 4.33 and 4.34). Copper binding property of M1 and M2 peptide are attributed to presence of three

histidine residues as Sankararamakrishnan et al demonstrated the binding of copper in ATCUN motif through three histidine residues [217]. C1 peptide contains the GHK (glycyl-L-histidyl-L-lysine) in its sequence. Naturally human tissues and organ contain this GHK tripeptide, which possess high copper binging property [218], [219]. LOX is a copper dependent enzyme and these peptides inhibited the activity of recombinant mLOX up to 80 % (Figure 4.35). This inhibition is attributed to the copper sequestering nature of these peptides. Elevated levels of copper have been reported in various types of human cancer including breast, colon, lungs and brain [220][221]. LOX expression was found to be high in hypoxic human tumor cells and prior studies concluded that LOX has a major role in hypoxia induced metastasis [78] [149]. Chelators like penicillamine, and tetrathiomolybdate are used to chelate copper from the angiogenic environment [222]. Copper chelating therapeutic treatments are in wide use in the combating cancer [223]. Another peptide C2 showed inhibition of recombinant LOX up to 70 % but the exact mechanism of action of this peptide is not understood clearly (Figure 4.35 B). The inhibitor effect of these peptides were studied in HUVECs using in vitro angiogenesis assay, migration assay and enzymatic activity of LOX in the cultured medium in another study of our department. Peptides designed in this study can be used to inhibit LOX activity and tumor progression. Further in vivo experiments are needed to understand its exact mechanism of these peptides.

CHAPTER 6 – CONCLUSION

Lysyl Oxidase (LOX) an enzyme implicated in the construction of the ECM. Importance of LOX enzyme is elucidated in connective tissue pathological conditions like Menkes' disease, occipital horn syndrome, lathyrism and fibrotic disorders. LOX also involved in the cancer progression and migration of tumor cells during metastasis conditions. Since understanding the LOX structure and function will help in combating the diseases.

In the present study, mature LOX enzyme was over-expressed and purified by cloning method. The purified recombinant protein was refolded and solubilized in the glycine-NaOH buffer pH 8.0 with 10 % glycerol. The enzymatic activity of the recombinant mLOX was shown by *in vitro* enzymatic analysis by Amplex red assay and increase collagen fibers in the cultured ARPE-19 cells. The folding of the mLOX was confirmed by far UV-CD spectroscopy analysis, tryptophan fluorescence emission spectra and ANSA binding analysis. Thermo stability of the LOX was demonstrated by CD spectra. Importance of disulphide bonds in structure stability of LOX was demonstrated by increased ANSA binding, in DTT reduced recombinant mLOX and shift in the emission maxima.

By *in silico* approach, 3D structure of mature LOX was predicted. To the predicted LOX structure, coordinated covalent bonds were generated between specified histidine residues and copper ion in tetrahedral geometry. The predicted structure was validated by Ramachandran plot. By molecular dynamic (MD) simulations, stability of the predicted structure was confirmed. Active cavity was predicted by CASTp and docking was performed using Induced Fit docking (IFD) for the known inhibitors. IFD results was validated by in vitro Amplex red assay, in both the in silico and in vitro results showed homocysteine to be the potent inhibitor for LOX activity when compared to β-APN and homocysteine thiolactone.

From the conserved regions of LOX family, 5 peptides were designed. The secondary structures of the peptides were studied by CD spectra. The copper binding property of C1, M1 and M2 peptides were demonstrated using CD spectra and mass spectroscopy. These peptides showed inhibition of LOX activity at nano molar concentration, where established β-APN show inhibition at milli molar concentration.

CHAPTER 7- SPECIFIC CONTRIBUTIONS

- Properties of LOX like its optimum pH, K_m and V_{max} have been identified in this study.

- Contribution of disulphide bond in stability of LOX structure was shown experimentally.

- Structure of LOX was predicted by *ab initio* and generated proper copper coordination in allowed bond length. Predicted structure was validated with the *in vitro* experiments.

- Identified homocysteine can be potent inhibitor for LOX by IFD and also validated the same by *in vitro* enzymatic assay.

- Peptide designed from conserved regions of LOX showed inhibitory action on LOX enzymatic activity at nanomoles concentration.

CHAPTER 8 - LIMITATIONS AND FUTURE SCOPE

- Crystal structure of LOX is not elucidated due its inherent aggregating property using the buffer identified in this work can be used for elucidating the structure of LOX by X-ray crystallography.

- Steady state fluorescence only performed in this study, to have better understanding on LOX structure time resolved fluorescence should be performed.

- The predicted structure of LOX in this study, lack the co-factor LTQ and disulphide bridges. This limitation can be overcome in the future, which will help in understanding the enzymatic mechanism and binding nature of LOX

- Using predicted LOX structure, virtual docking studies can be performed and lead molecules can be identified to modulate the activity of LOX.

- Compare to the chemical or monoclonal antibody inhibitors of LOX, the identified peptide in this work can be valid inhibitors.

- LOX derived peptides mechanism of action should be studied further and its anti angiogenic properties can be validated with animal studies.

CHAPTER 9 - REFERENCES

[1] J. Rosenbloom, W. R. Abrams, and R. Mecham, "Extracellular matrix 4: the elastic fiber.," *FASEB J.*, vol. 7, no. 13, pp. 1208–18, Oct. 1993.

[2] J. K. Mouw, G. Ou, and V. M. Weaver, "Extracellular matrix assembly: a multiscale deconstruction," *Nat. Rev. Mol. Cell Biol.*, vol. 15, no. 12, pp. 771–785, 2014.

[3] A. Sampath Narayanan, R. C. Siegel, and G. R. Martin, "On the inhibition of lysyl oxidase by β-aminopropionitrile," *Biochem. Biophys. Res. Commun.*, vol. 46, no. 2, pp. 745–751, Jan. 1972.

[4] H. E. Barker, T. R. Cox, and J. T. Erler, "The rationale for targeting the LOX family in cancer.," *Nat. Rev. Cancer*, vol. 12, no. 8, pp. 540–52, Aug. 2012.

[5] K. Csiszar, "Lysyl oxidases: a novel multifunctional amine oxidase family.," *Prog. Nucleic Acid Res. Mol. Biol.*, vol. 70, pp. 1–32, Jan. 2001.

[6] F. Buffoni and G. Ignesti, "The copper-containing amine oxidases: biochemical aspects and functional role.," *Mol. Genet. Metab.*, vol. 71, no. 4, pp. 559–64, Dec. 2000.

[7] S. R. Pinnell and G. R. Martin, "The cross-linking of collagen and elastin: enzymatic conversion of lysine in peptide linkage to alpha-aminoadipic-delta-semialdehyde (allysine) by an extract from bone.," *Proc. Natl. Acad. Sci. U. S. A.*, vol. 61, no. 2, pp. 708–16, Oct. 1968.

[8] R. C. Siegel, S. R. Pinnell, and G. R. Martin, "Cross-linking of collagen and elastin. Properties of lysyl oxidase.," *Biochemistry*, vol. 9, no. 23, pp. 4486–4492, 1970.

[9] K. Reiser, R. J. McCormick, and R. B. Rucker, "Enzymatic and nonenzymatic cross-linking of collagen and elastin.," *FASEB J.*, vol. 6, no. 7, pp. 2439–49, Apr. 1992.

[10] H. Kuivaniemi, L. Ala-Kokko, and K. I. Kivirikko, "Secretion of lysyl oxidase by cultured human skin fibroblasts and effects of monensin, nigericin, tunicamycin and colchicine.," *Biochim. Biophys. Acta*, vol. 883, no. 2, pp. 326–334, 1986.

[11] D. L. Layman, A. S. Narayanan, and G. R. Martin, "The production of lysyl oxidase by human fibroblasts in culture.," *Arch. Biochem. Biophys.*, vol. 149, no. 1, pp. 97–101, Mar. 1972.

[12] P. M. Royce, J. Camakaris, and D. M. Danks, "Reduced lysyl oxidase activity in skin fibroblasts from patients with Menkes' syndrome.," *Biochem. J.*, vol. 192, no. 2, pp. 579–86, Nov. 1980.

[13] P. C. Trackman, A. M. Pratt, A. Wolanski, S. S. Tang, G. D. Offner, R. F. Troxler, and H. M. Kagan, "Cloning of rat aorta lysyl oxidase cDNA: complete codons and predicted amino acid sequence.," *Biochemistry*, vol. 29, no. 20, pp. 4863–4870, May 1990.

[14] P. C. Trackman, A. M. Pratt, A. Wolanski, S. S. Tang, G. D. Offner, R. F. Troxler, and H. M. Kagan, "Cloning of rat aorta lysyl oxidase cDNA: complete codons and predicted amino acid sequence.," *Biochemistry*, vol. 30, no. 33, p. 8282, Aug. 1991.

[15] P. C. Trackman, D. Bedell-Hogan, J. Tang, and H. M. Kagan, "Post-translational glycosylation and proteolytic processing of a lysyl oxidase precursor," *J. Biol. Chem.*, vol. 267, no. 12, pp. 8666–8671, Apr. 1992.

[16] K. Takahara, G. E. Lyons, and D. S. Greenspan, "Bone morphogenetic protein-1 and a mammalian tolloid homologue (mTld) are encoded by alternatively spliced transcripts which are differentially expressed in some tissues.," *J. Biol. Chem.*, vol. 269, no. 51, pp. 32572–8, Dec. 1994.

[17] M. I. Uzel, I. C. Scott, H. Babakhanlou-Chase, a H. Palamakumbura, W. N. Pappano, H. H. Hong, D. S. Greenspan, and P. C. Trackman, "Multiple bone morphogenetic protein 1-related mammalian metalloproteinases process pro-lysyl oxidase at the correct physiological site and control lysyl oxidase activation in mouse embryo fibroblast cultures.," *J. Biol. Chem.*, vol. 276, no. 25, pp. 22537–43, Jun. 2001.

[18] T. Kosonen, J. Y. Uriu-Hare, M. S. Clegg, C. L. Keen, and R. B. Rucker, "Incorporation of copper into lysyl oxidase.," *Biochem. J.*, vol. 327 (Pt 1, pp. 283–289, Oct. 1997.

[19] P. R. Williamson and H. M. Kagan, "Reaction pathway of bovine aortic lysyl oxidase.," *J. Biol. Chem.*, vol. 261, no. 20, pp. 9477–9482, Jul. 1986.

[20] R. B. Rucker, T. Kosonen, M. S. Clegg, A. E. Mitchell, B. R. Rucker, J. Y. Uriu-Hare, and C. L. Keen, "Copper, lysyl oxidase, and extracellular matrix protein cross-linking.," *Am. J. Clin. Nutr.*, vol. 67, no. 5 Suppl, p. 996S–1002S, May 1998.

[21] A. D. Cronshaw, L. A. Fothergill-Gilmore, and D. J. Hulmes, "The proteolytic processing site of the precursor of lysyl oxidase.," *Biochem. J.*, vol. 306 (Pt 1, pp. 279–284, Feb. 1995.

[22] H. Iguchi, R. Kasai, Okumura, T. Yamamuro, and H. M. Kagan, "Effect of dietary cadmium and/or copper on the bone lysyl oxidase in copper-deficient rats relative to the metabolism of copper in the bone," *Bone Miner.*, vol. 10, no. 1, pp. 51–59, 1990.

[23] H. Iguchi and S. Sano, "Cadmium- or zinc-binding to bone lysyl oxidase and copper replacement.," *Connect. Tissue Res.*, vol. 14, no. 2, pp. 129–139, 1985.

[24] C. J. Krebs and S. A. Krawetz, "Lysyl oxidase copper-talon complex: a model.," *Biochim. Biophys. Acta*, vol. 1202, no. 1, pp. 7–12, Sep. 1993.

[25] S. N. Gacheru, P. C. Trackman, M. A. Shah, C. Y. O'Gara, P. Spacciapoli, F. T. Greenaway, and H. M. Kagan, "Structural and catalytic properties of copper in lysyl oxidase.," *J. Biol. Chem.*, vol. 265, no. 31, pp. 19022–19027, Nov. 1990.

[26] K. M. Lopez and F. T. Greenaway, "Identification of the copper-binding ligands of lysyl oxidase.," *J. Neural Transm.*, vol. 118, no. 7, pp. 1101–9, Jul. 2011.

[27] S. X. Wang, N. Nakamura, M. Mure, J. P. Klinman, and J. Sanders-Loehr, “Characterization of the native lysine tyrosylquinone cofactor in lysyl oxidase by Raman spectroscopy.,” *J. Biol. Chem.*, vol. 272, no. 46, pp. 28841–4, Nov. 1997.

[28] P. R. Williamson, R. S. Moog, D. M. Dooley, and H. M. Kagan, “Evidence for pyrroloquinolinequinone as the carbonyl cofactor in lysyl oxidase by absorption and resonance Raman spectroscopy,” *J. Biol. Chem.*, vol. 261, no. 35, pp. 16302–16305, Dec. 1986.

[29] S. M. Janes, D. Mu, D. Wemmer, A. J. Smith, S. Kaur, D. Maltby, A. L. Burlingame, and J. P. Klinman, “A new redox cofactor in eukaryotic enzymes: 6-hydroxydopa at the active site of bovine serum amine oxidase.,” *Science*, vol. 248, no. 4958, pp. 981–987, May 1990.

[30] S. X. Wang, M. Mure, K. F. Medzihradszky, A. L. Burlingame, D. E. Brown, D. M. Dooley, A. J. Smith, H. M. Kagan, and J. P. Klinman, “A crosslinked cofactor in lysyl oxidase: redox function for amino acid side chains.,” *Science*, vol. 273, no. 5278, pp. 1078–1084, 1996.

[31] P. R. Williamson and H. M. Kagan, “Alpha-proton abstraction and carbanion formation in the mechanism of action of lysyl oxidase.,” *J. Biol. Chem.*, vol. 262, no. 17, pp. 8196–8201, Jun. 1987.

[32] M. A. Shah, C. H. Scaman, M. M. Palcic, and H. M. Kagan, “Kinetics and stereospecificity of the lysyl oxidase reaction,” *J. Biol. Chem.*, vol. 268, no. 16, pp. 11573–11579, Jun. 1993.

[33] H. M. Kagan, “Lysyl oxidase: mechanism, regulation and relationship to liver fibrosis.,” *Pathol. Res. Pract.*, vol. 190, no. 9–10, pp. 910–9, Oct. 1994.

[34] M. Akagawa and K. Suyama, “Characterization of a model compound for the lysine tyrosylquinone cofactor of lysyl oxidase.,” *Biochem. Biophys. Res. Commun.*, vol. 281, no. 1, pp. 193–9, Feb. 2001.

[35] C. Tang and J. P. Klinman, “The catalytic function of bovine lysyl oxidase in the absence of copper.,” *J. Biol. Chem.*, vol. 276, no. 33, pp. 30575–8, Aug. 2001.

[36] J. M. Mäki, “Lysyl oxidases in mammalian development and certain pathological conditions.,” *Histol. Histopathol.*, vol. 24, no. 5, pp. 651–60, May 2009.

[37] B. Fogelgren, N. Polgár, K. M. Szauter, Z. Újfaludi, R. Laczkó, K. S. K. Fong, and K. Csiszar, “Cellular fibronectin binds to lysyl oxidase with high affinity and is critical for its proteolytic activation,” *J. Biol. Chem.*, vol. 280, no. 26, pp. 24690–24697, Jul. 2005.

[38] R. C. Siegel, “Biosynthesis of collagen crosslinks: increased activity of purified lysyl oxidase with reconstituted collagen fibrils.,” *Proc. Natl. Acad. Sci. U. S. A.*, vol. 71, no. 12, pp. 4826–4830, Dec. 1974.

[39] J. Brinckmann, “Collagens at a glance,” *Topics in Current Chemistry*, vol. 247, no. Pt 12. pp. 1–6, 15-Jun-2005.

[40] A. J. Bailey, R. G. Paul, and L. Knott, “Mechanisms of maturation and ageing of collagen.,” *Mech. Ageing Dev.*, vol. 106, no. 1–2, pp. 1–56, Dec. 1998.

[41] M. J. Fazio, M. G. Mattei, E. Passage, M. L. Chu, D. Black, E. Solomon, J. M. Davidson, and J. Uitto, “Human elastin gene: new evidence for localization to the long arm of chromosome 7.,” *Am. J. Hum. Genet.*, vol. 48, no. 4, pp. 696–703, Apr. 1991.

[42] Z. Szabó, S. A. Levi-Minzi, A. M. Christiano, C. Struminger, M. Stoneking, M. A. Batzer, and C. D. Boyd, “Sequential loss of two neighboring exons of the tropoelastin gene during primate evolution.,” *J. Mol. Evol.*, vol. 49, no. 5, pp. 664–671, Nov. 1999.

[43] S. Privitera, C. A. Prody, J. W. Callahan, and A. Hinek, “The 67-kDa enzymatically inactive alternatively spliced variant of beta-galactosidase is identical to the elastin/laminin-binding protein.,” *J. Biol. Chem.*, vol. 273, no. 11, pp. 6319–26, Mar. 1998.

[44] S. L. Chapman, F.-X. Sicot, E. C. Davis, J. Huang, T. Sasaki, M.-L. Chu, and H. Yanagisawa, “Fibulin-2 and fibulin-5 cooperatively function to form the internal elastic lamina and protect from vascular injury.,” *Arterioscler. Thromb. Vasc. Biol.*, vol. 30, no. 1, pp. 68–74, Jan. 2010.

[45] E. Petersen, F. Wågberg, and K.-A. Angquist, “Serum concentrations of elastin-derived peptides in patients with specific manifestations of atherosclerotic disease.,” *Eur. J. Vasc. Endovasc. Surg.*, vol. 24, no. 5, pp. 440–4, Nov. 2002.

[46] P.-P. Kuang, X.-H. Zhang, C. B. Rich, J. A. Foster, M. Subramanian, and R. H. Goldstein, “Activation of elastin transcription by transforming growth factor-beta in human lung fibroblasts.,” *Am. J. Physiol. Lung Cell. Mol. Physiol.*, vol. 292, no. 4, pp. L944–52, Apr. 2007.

[47] V. M. Kähäri, Y. Q. Chen, M. M. Bashir, J. Rosenbloom, and J. Uitto, “Tumor necrosis factor-alpha down-regulates human elastin gene expression. Evidence for the role of AP-1 in the suppression of promoter activity.,” *J. Biol. Chem.*, vol. 267, no. 36, pp. 26134–41, Dec. 1992.

[48] A. Mauviel, Y. Q. Chen, V. M. Kähäri, I. Ledo, M. Wu, L. Rudnicka, and J. Uitto, “Human recombinant interleukin-1 beta up-regulates elastin gene expression in dermal fibroblasts. Evidence for transcriptional regulation in vitro and in vivo.,” *J. Biol. Chem.*, vol. 268, no. 9, pp. 6520–4, Mar. 1993.

[49] S. G. Wise and A. S. Weiss, “Tropoelastin.,” *Int. J. Biochem. Cell Biol.*, vol. 41, no. 3, pp. 494–7, Mar. 2009.

[50] P. Brown-Augsburger, C. Tisdale, T. Broekelmann, C. Sloan, and R. P. Mecham, “Identification of an elastin cross-linking domain that joins three peptide chains. Possible role in nucleated assembly.,” *J. Biol. Chem.*, vol. 270, no. 30, pp. 17778–83, Jul. 1995.

[51] D. R. Eyre, M. A. Weis, and J.-J. Wu, “Advances in collagen cross-link analysis.,” *Methods*, vol. 45, no. 1, pp. 65–74, May 2008.

[52] H. M. Kagan, M. a Williams, P. R. Williamson, and J. M. Anderson, “Influence of sequence and charge on the specificity of lysyl oxidase toward protein and synthetic peptide substrates.,” *J. Biol. Chem.*, vol. 259, no. 18, pp. 11203–7, Sep. 1984.

[53] P. C. Trackman and H. M. Kagan, “Nonpeptidyl amine inhibitors are substrates of lysyl oxidase.,” *J. Biol. Chem.*, vol. 254, no. 16, pp. 7831–7836, Aug. 1979.

[54] A. H. Palamakumbura and P. C. Trackman, “A fluorometric assay for detection of lysyl oxidase enzyme activity in biological samples.,” *Anal. Biochem.*, vol. 300, no. 2, pp. 245–251, Jan. 2002.

[55] H. a Lucero and H. M. Kagan, “Lysyl oxidase: An oxidative enzyme and effector of cell function,” *Cellular and Molecular Life Sciences*, vol. 63, no. 19–20. pp. 2304–2316, Oct-2006.

[56] N. Nagan and H. M. Kagan, “Modulation of lysyl oxidase activity toward peptidyl lysine by vicinal dicarboxylic amino acid residues. Implications for collagen cross-linking,” *J. Biol. Chem.*, vol. 269, no. 35, pp. 22366–22371, Sep. 1994.

[57] A. L. Cronlund, B. D. Smith, and H. M. Kagan, “Binding of lysyl oxidase to fibrils of type I collagen.,” *Connect. Tissue Res.*, vol. 14, no. 2, pp. 109–119, Jan. 1985.

[58] L. Thomassin, C. C. Werneck, T. J. Broekelmann, C. Gleyzal, I. K. Hornstra, R. P. Mecham, and P. Sommer, “The pro-regions of lysyl oxidase and lysyl oxidase-like 1 are required for deposition onto elastic fibers,” *J. Biol. Chem.*, vol. 280, no. 52, pp. 42848–42855, 2005.

[59] M. Giampuzzi, R. Oleggini, and A. Di Donato, “Demonstration of in vitro interaction between tumor suppressor lysyl oxidase and histones H1 and H2: definition of the regions involved.,” *Biochim. Biophys. Acta*, vol. 1647, no. 1–2, pp. 245–51, Apr. 2003.

[60] H. M. Kagan, M. A. Williams, S. D. Calaman, and E. M. Berkowitz, “Histone H1 is a substrate for lysyl oxidase and contains endogenous sodium borotritide-reducible residues.,” *Biochem. Biophys. Res. Commun.*, vol. 115, no. 1, pp. 186–92, Aug. 1983.

[61] W. Li, M. A. Nugent, Y. Zhao, A. N. Chau, S. J. Li, I. N. Chou, G. Liu, and H. M. Kagan, “Lysyl oxidase oxidizes basic fibroblast growth factor and inactivates its mitogenic potential,” *Journal of Cellular Biochemistry*, vol. 88, no. 1. pp. 152–164, 01-Jan-2003.

[62] J. T. Erler, K. L. Bennewith, M. Nicolau, N. Dornhöfer, C. Kong, Q.-T. Le, J.-T. A. Chi, S. S. Jeffrey, and A. J. Giaccia, “Lysyl oxidase is essential for hypoxia-induced metastasis.,” *Nature*, vol. 440, no. 7088, pp. 1222–1226, Apr. 2006.

[63] T. Fujimaki, Y. Hotta, H. Sakuma, K. Fujiki, and A. Kanai, “Large-scale sequencing of the rabbit corneal endothelial cDNA library.,” *Cornea*, vol. 18, no. 1, pp. 109–114, Jan. 1999.

[64] A. Di Donato, G. M. Ghiggeri, M. Di Duca, E. Jivotenko, R. Acinni, J. Campolo, F. Ginevri, and R. Gusmano, "Lysyl oxidase expression and collagen cross-linking during chronic adriamycin nephropathy.," *Nephron*, vol. 76, no. 2, pp. 192–200, Jan. 1997.

[65] Y. Zhao, S. Gao, I. N. Chou, P. Toselli, P. Stone, and W. Li, "Inhibition of the expression of lysyl oxidase and its substrates in cadmium-resistant rat Fetal lung fibroblasts," *Toxicol. Sci.*, vol. 90, no. 2, pp. 478–489, Apr. 2006.

[66] A. M. Boak, R. Roy, J. Berk, L. Taylor, P. Polgar, R. H. Goldstein, and H. M. Kagan, "Regulation of lysyl oxidase expression in lung fibroblasts by transforming growth factor-beta 1 and prostaglandin E2.," *Am. J. Respir. Cell Mol. Biol.*, vol. 11, no. 6, pp. 751–5, Dec. 1994.

[67] P. C. Trackman, R. J. Graham, H. K. Bittner, D. L. Carnes, J. A. Gilles, and D. T. Graves, "Inflammation-associated lysyl oxidase protein expression in vivo, and modulation by FGF-2 plus IGF-1," *Histochem. Cell Biol.*, vol. 110, no. 1, pp. 9–14, Jul. 1998.

[68] R. Koslowski, D. Seidel, E. Kuhlisch, and K.-P. Knoch, "Evidence for the involvement of TGF-beta and PDGF in the regulation of prolyl 4-hydroxylase and lysyloxidase in cultured rat lung fibroblasts.," *Exp. Toxicol. Pathol.*, vol. 55, no. 4, pp. 257–264, Nov. 2003.

[69] R. E. Bronson, S. D. Calaman, A. M. Traish, and H. M. Kagan, "Stimulation of lysyl oxidase (EC 1.4.3.13) activity by testosterone and characterization of androgen receptors in cultured calf aorta smooth-muscle cells.," *Biochem. J.*, vol. 244, no. 2, pp. 317–323, Jun. 1987.

[70] K. Ravid, L. I. Smith-Mungo, Z. Zhao, K. M. Thomas, and H. M. Kagan, "Upregulation of lysyl oxidase in vascular smooth muscle cells by cAMP: role for adenosine receptor activation.," *J. Cell. Biochem.*, vol. 75, no. 1, pp. 177–185, Oct. 1999.

[71] M. L. Casey and P. C. MacDonald, "Lysyl oxidase (ras recision gene) expression in human amnion: ontogeny and cellular localization.," *J. Clin. Endocrinol. Metab.*, vol. 82, no. 1, pp. 167–72, Jan. 1997.

[72] M. Baccarani-Contri, D. Vincenzi, D. Quaglino, G. Mori, and I. Pasquali-Ronchetti, "Localization of human placenta lysyl oxidase on human placenta, skin and aorta by immunoelectronmicroscopy.," *Matrix*, vol. 9, no. 6, pp. 428–436, Jan. 1989.

[73] Y. Kim, C. D. Boyd, and K. Csiszar, "A new gene with sequence and structural similarity to the gene encoding human lysyl oxidase.," *J. Biol. Chem.*, vol. 270, no. 13, pp. 7176–82, Mar. 1995.

[74] H. Ito, H. Akiyama, H. Iguchi, K. I. Iyama, M. Miyamoto, K. Ohsawa, and T. Nakamura, "Molecular Cloning and Biological Activity of a Novel Lysyl Oxidase-related Gene Expressed in Cartilage," *J. Biol. Chem.*, vol. 276, no. 26, pp. 24023–24029, 2001.

[75] A. Borel, D. Eichenberger, J. Farjanel, E. Kessler, C. Gleyzal, D. J. S. Hulmes, P. Sommer, and B. Font, "Lysyl oxidase-like protein from bovine aorta: Isolation and

maturation to an active form by bone morphogenetic protein-1," *J. Biol. Chem.*, vol. 276, no. 52, pp. 48944–48949, Dec. 2001.

[76] Z. Vadasz, O. Kessler, G. Akiri, S. Gengrinovitch, H. M. Kagan, Y. Baruch, O. Ben Izhak, and G. Neufeld, "Abnormal deposition of collagen around hepatocytes in Wilson's disease is associated with hepatocyte specific expression of lysyl oxidase and lysyl oxidase like protein-2," *J. Hepatol.*, vol. 43, no. 3, pp. 499–507, Sep. 2005.

[77] J. E. Lee and Y. Kim, "A tissue-specific variant of the human lysyl oxidase-like protein 3 (LOXL3) functions as an amine oxidase with substrate specificity," *J. Biol. Chem.*, vol. 281, no. 49, pp. 37282–37290, Dec. 2006.

[78] L. Perryman and J. T. Erler, "Lysyl oxidase in cancer research," *Futur. Oncol.*, vol. 10, no. 9, pp. 1709–1717, Jul. 2014.

[79] I. K. Hornstra, S. Birge, B. Starcher, A. J. Bailey, R. P. Mecham, and S. D. Shapiro, "Lysyl oxidase is required for vascular and diaphragmatic development in mice," *J. Biol. Chem.*, vol. 278, no. 16, pp. 14387–14393, Apr. 2003.

[80] B. López, A. González, N. Hermida, F. Valencia, E. de Teresa, and J. Díez, "Role of lysyl oxidase in myocardial fibrosis: from basic science to clinical aspects.," *Am. J. Physiol. Heart Circ. Physiol.*, vol. 299, no. 1, pp. H1–9, Jul. 2010.

[81] S. Jeay, S. Pianetti, H. M. Kagan, and G. E. Sonenshein, "Lysyl oxidase inhibits ras-mediated transformation by preventing activation of NF-kappa B.," *Mol. Cell. Biol.*, vol. 23, no. 7, pp. 2251–63, Apr. 2003.

[82] K. K. Papachroni, C. Piperi, G. Levidou, P. Korkolopoulou, L. Pawelczyk, E. Diamanti-Kandarakis, and A. G. Papavassiliou, "Lysyl oxidase interacts with AGE signalling to modulate collagen synthesis in polycystic ovarian tissue," *J. Cell. Mol. Med.*, vol. 14, no. 10, pp. 2460–2469, Oct. 2010.

[83] A. Guadall, M. Orriols, J. F. Alcudia, V. Cachofeiro, J. Martinez-Gonzalez, and C. Rodriguez, "Hypoxia-induced ROS signaling is required for LOX up-regulation in endothelial cells.," *Front. Biosci. (Elite Ed).*, vol. 3, pp. 955–967, Jan. 2011.

[84] E. D. Harris, "Copper-induced activation of aortic lysyl oxidase in vivo.," *Proc. Natl. Acad. Sci. U. S. A.*, vol. 73, no. 2, pp. 371–4, Feb. 1976.

[85] R. B. Rucker, B. R. Rucker, A. E. Mitchell, C. T. Cui, M. Clegg, T. Kosonen, J. Y. Uriu-Adams, E. H. Tchaparian, M. Fishman, and C. L. Keen, "Activation of chick tendon lysyl oxidase in response to dietary copper.," *J. Nutr.*, vol. 129, no. 12, pp. 2143–2146, Dec. 1999.

[86] W. Opsahl, H. Zeronian, M. Ellison, D. Lewis, R. B. Rucker, and R. S. Riggins, "Role of copper in collagen cross-linking and its influence on selected mechanical properties of chick bone and tendon.," *J. Nutr.*, vol. 112, no. 4, pp. 708–716, Apr. 1982.

[87] N. Romero-Chapman, J. Lee, D. Tinker, J. Y. Uriu-Hare, C. L. Keen, and R. R. Rucker, "Purification, properties and influence of dietary copper on accumulation and functional activity of lysyl oxidase in rat skin.," *Biochem. J.*, vol. 275 (Pt 3, pp. 657–662, May 1991.

[88] R. B. Rucker, N. Romero-Chapman, T. Wong, J. Lee, F. M. Steinberg, C. McGee, M. S. Clegg, K. Reiser, T. Kosonen, J. Y. Uriu-Hare, J. Murphy, and C. L. Keen, "Modulation of lysyl oxidase by dietary copper in rats.," *J. Nutr.*, vol. 126, no. 1, pp. 51–60, Jan. 1996.

[89] S. G. Kaler, "Metabolic and Molecular Bases of Menkes Disease and Occipital Horn Syndrome," *Pediatr. Dev. Pathol.*, vol. 1, no. 1, pp. 85–98, Jan. 1998.

[90] J. Chelly, Z. Tümer, T. Tønnesen, A. Petterson, Y. Ishikawa-Brush, N. Tommerup, N. Horn, and A. P. Monaco, "Isolation of a candidate gene for Menkes disease that encodes a potential heavy metal binding protein.," *Nat. Genet.*, vol. 3, no. 1, pp. 14–9, Jan. 1993.

[91] C. D. Vulpe and S. Packman, "Cellular copper transport.," *Annu. Rev. Nutr.*, vol. 15, pp. 293–322, Jan. 1995.

[92] S. Das, B. Levinson, C. Vulpe, S. Whitney, J. Gitschier, and S. Packman, "Similar splicing mutations of the Menkes/mottled copper-transporting ATPase gene in occipital horn syndrome and the blotchy mouse.," *Am. J. Hum. Genet.*, vol. 56, no. 3, pp. 570–6, Mar. 1995.

[93] R. C. Siegel and G. R. Martin, "Collagen cross-linking. Enzymatic synthesis of lysine-derived aldehydes and the production of cross-linked components.," *J. Biol. Chem.*, vol. 245, no. 7, pp. 1653–1658, 1970.

[94] S. S. Tang, P. C. Trackman, and H. M. Kagan, "Reaction of aortic lysyl oxidase with beta-aminopropionitrile," *J. Biol. Chem.*, vol. 258, no. 7, pp. 4331–4338, Apr. 1983.

[95] C. Rodríguez, J. F. Alcudia, J. Martínez-González, A. Guadall, B. Raposo, S. Sánchez-Gómez, and L. Badimon, "Statins normalize vascular lysyl oxidase down-regulation induced by proatherogenic risk factors.," *Cardiovasc. Res.*, vol. 83, no. 3, pp. 595–603, Aug. 2009.

[96] C. Rodríguez, B. Raposo, J. Martínez-González, L. Casaní, and L. Badimon, "Low density lipoproteins downregulate lysyl oxidase in vascular endothelial cells and the arterial wall," *Arterioscler. Thromb. Vasc. Biol.*, vol. 22, no. 9, pp. 1409–1414, Aug. 2002.

[97] S. Pushpakumar, S. Kundu, and U. Sen, "Endothelial dysfunction: the link between homocysteine and hydrogen sulfide.," *Curr. Med. Chem.*, vol. 21, no. 32, pp. 3662–72, Jan. 2014.

[98] B. Raposo, C. Rodríguez, J. Martínez-González, and L. Badimon, "High levels of homocysteine inhibit lysyl oxidase (LOX) and downregulate LOX expression in vascular endothelial cells.," *Atherosclerosis*, vol. 177, no. 1, pp. 1–8, Nov. 2004.

[99] S. H. Phan, "Genesis of the Myofibroblast in Lung Injury and Fibrosis," *Proceedings of the American Thoracic Society*, vol. 9, no. 3. pp. 148–152, Jul-2012.

[100] R. Bataller and D. A. Brenner, “Liver fibrosis.,” *J. Clin. Invest.*, vol. 115, no. 2, pp. 209–18, Feb. 2005.

[101] S.-Y. Lee, S. Il Kim, and M. E. Choi, “Therapeutic targets for treating fibrotic kidney diseases,” *Transl. Res.*, vol. 165, no. 4, pp. 512–30, Apr. 2014.

[102] P. Kong, P. Christia, and N. G. Frangogiannis, “The pathogenesis of cardiac fibrosis,” *Cellular and Molecular Life Sciences*, vol. 71, no. 4. pp. 549–574, Feb-2014.

[103] J. L. McPhie, “The activity of lysyl oxidase in experimental hepatic fibrosis.,” *Hepatogastroenterology.*, vol. 28, no. 5, pp. 240–1, Oct. 1981.

[104] O. A. Mesarwi, M.-K. Shin, L. F. Drager, S. Bevans-Fonti, J. C. Jun, N. Putcha, M. S. Torbenson, R. P. Pedrosa, G. Lorenzi-Filho, K. E. Steele, M. A. Schweitzer, T. H. Magnuson, A. O. Lidor, A. R. Schwartz, and V. Y. Polotsky, “Lysyl Oxidase as a Serum Biomarker of Liver Fibrosis in Patients With Severe Obesity and Obstructive Sleep Apnea.,” *Sleep*, Jun. 2015.

[105] K. Kenyon, S. Contente, P. C. Trackman, J. Tang, H. M. Kagan, and R. M. Friedman, “Lysyl oxidase and rrg messenger RNA.,” *Science*, vol. 253, no. 5021, p. 802, Aug. 1991.

[106] S. L. Payne, M. J. C. Hendrix, and D. a Kirschmann, “Paradoxical roles for lysyl oxidases in cancer - A prospect,” *Journal of Cellular Biochemistry*, vol. 101, no. 6. pp. 1338–1354, 15-Aug-2007.

[107] Siddikuzzaman, V. M. B. Grace, and C. Guruvayoorappan, “Lysyl oxidase: a potential target for cancer therapy.,” *Inflammopharmacology*, vol. 19, no. 3, pp. 117–29, Jun. 2011.

[108] S. L. Payne, B. Fogelgren, A. R. Hess, E. A. Seftor, E. L. Wiley, S. F. T. Fong, K. Csiszar, M. J. C. Hendrix, and D. A. Kirschmann, “Lysyl oxidase regulates breast cancer cell migration and adhesion through a hydrogen peroxide-mediated mechanism,” *Cancer Res.*, vol. 65, no. 24, pp. 11429–11436, Dec. 2005.

[109] S. L. Payne, M. J. C. Hendrix, and D. a Kirschmann, “Lysyl oxidase regulates actin filament formation through the p130(Cas)/Crk/DOCK180 signaling complex.,” *J. Cell. Biochem.*, vol. 98, no. 4, pp. 827–837, Jul. 2006.

[110] Z. Urban, O. Agapova, V. Hucthagowder, P. Yang, B. C. Starcher, and M. R. Hernandez, “Population differences in elastin maturation in optic nerve head tissue and astrocytes.,” *Invest. Ophthalmol. Vis. Sci.*, vol. 48, no. 7, pp. 3209–15, Jul. 2007.

[111] U. Schlötzer-Schrehardt, F. Pasutto, P. Sommer, I. Hornstra, F. E. Kruse, G. O. H. Naumann, A. Reis, and M. Zenkel, “Genotype-correlated expression of lysyl oxidase-like 1 in ocular tissues of patients with pseudoexfoliation syndrome/glaucoma and normal patients.,” *Am. J. Pathol.*, vol. 173, no. 6, pp. 1724–1735, 2008.

[112] G. Y. Hyeong, X. Liu, S. Kiss, E. Connolly, E. S. Gragoudas, N. A. Michaud, O. V Bulgakov, M. Adamian, M. M. DeAngelis, J. W. Miller, T. Li, and I. K. Kim, “Increased

choroidal neovascularization following laser induction in mice lacking lysyl oxidase-like 1," *Investig. Ophthalmol. Vis. Sci.*, vol. 49, no. 6, pp. 2599–2605, Jun. 2008.

[113] Y. Bykhovskaya, X. Li, I. Epifantseva, T. Haritunians, D. Siscovick, A. Aldave, L. Szczotka-Flynn, S. K. Iyengar, K. D. Taylor, J. I. Rotter, and Y. S. Rabinowitz, "Variation in the lysyl oxidase (LOX) gene is associated with keratoconus in family-based and case-control studies.," *Invest. Ophthalmol. Vis. Sci.*, vol. 53, no. 7, pp. 4152–7, Jan. 2012.

[114] R. J. Wordinger and A. F. Clark, "Lysyl Oxidases in the Trabecular Meshwork," *J. Glaucoma*, vol. 23, no. 8 Suppl 1, pp. S55–S58, Jan. 2014.

[115] K. Coral, N. Angayarkanni, J. Madhavan, M. Bharathselvi, S. Ramakrishnan, K. Nandi, P. Rishi, N. Kasinathan, and S. Krishnakumar, "Lysyl oxidase activity in the ocular tissues and the role of LOX in proliferative diabetic retinopathy and rhegmatogenous retinal detachment.," *Invest. Ophthalmol. Vis. Sci.*, vol. 49, no. 11, pp. 4746–52, Nov. 2008.

[116] H. M. Kagan, N. A. Hewitt, L. L. Salcedo, and C. Franzblau, "Catalytic activity of aortic lysyl oxidase in an insoluble enzyme-substrate complex.," *Biochim. Biophys. Acta*, vol. 365, no. 1, pp. 223–34, Sep. 1974.

[117] E. D. Harris, W. A. Gonnerman, J. E. Savage, and B. L. O'Dell, "Connective tissue amine oxidase II. Purification and partial characterization of lysyl oxidase from chick aorta," *Biochim. Biophys. Acta - Enzymol.*, vol. 341, no. 2, pp. 332–344, Apr. 1974.

[118] R. E. Jordan, P. Milbury, K. A. Sullivan, P. C. Trackman, and H. M. Kagan, "Studies on lysyl oxidase of bovine ligamentum nuchae and bovine aorta.," *Adv. Exp. Med. Biol.*, vol. 79, pp. 531–542, Jan. 1977.

[119] H. M. Kagan, K. A. Sullivan, T. A. Olsson, and A. L. Cronlund, "Purification and properties of four species of lysyl oxidase from bovine aorta.," *Biochem. J.*, vol. 177, no. 1, pp. 203–14, Jan. 1979.

[120] S. T. Kalinowski, P. W. Hedrick, and P. S. Miller, "No inbreeding depression observed in Mexican and red wolf captive breeding programs," *Conserv. Biol.*, vol. 13, no. 6, pp. 1371–1377, Jun. 1999.

[121] J. J. Shieh and K. T. Yasunobu, "Purification and properties of lung lysyl oxidase, a copper-enzyme.," *Adv. Exp. Med. Biol.*, vol. 74, pp. 447–63, Jan. 1976.

[122] A. S. Narayanan, L. B. Sandberg, K. Jones, S. S. Coleman, and R. A. Bagley, "Lysyloxidase activities of male and female turkey aortae.," *Exp. Mol. Pathol.*, vol. 36, no. 1, pp. 107–117, Feb. 1982.

[123] H. Kuivaniemi, E. R. Savolainen, and K. I. Kivirikko, "Human placental lysyl oxidase. Purification, partial characterization, and preparation of two specific antisera to the enzyme," *J. Biol. Chem.*, vol. 259, no. 11, pp. 6996–7002, Jun. 1984.

[124] R. Ferrera, B. Faris, P. J. Mogayzel, W. A. Gonnerman, and C. Franzblau, “A micromethod for the purification of lysyl oxidase.,” *Anal. Biochem.*, vol. 126, no. 2, pp. 312–317, Nov. 1982.

[125] M. Ouzzine, A. Boyd, and D. J. S. Hulmes, “Expression of active, human lysyl oxidase in Escherichia coli,” *FEBS Lett.*, vol. 399, no. 3, pp. 215–219, Dec. 1996.

[126] S. E. Herwald, F. T. Greenaway, and K. M. Lopez, “Purification of high yields of catalytically active lysyl oxidase directly from Escherichia coli cell culture,” *Protein Expr. Purif.*, vol. 74, no. 1, pp. 116–121, Nov. 2010.

[127] X. Chen and F. T. Greenaway, “Identification of the disulfide bonds of lysyl oxidase,” in *Journal of Neural Transmission*, 2011, vol. 118, no. 7, pp. 1111–1114.

[128] J. L. Hartley, “Cloning technologies for protein expression and purification,” *Current Opinion in Biotechnology*, vol. 17, no. 4. pp. 359–366, 2006.

[129] J. R. Luft, J. Newman, and E. H. Snell, “Crystallization screening: the influence of history on current practice.,” *Acta Crystallogr. Sect. F, Struct. Biol. Commun.*, vol. 70, no. Pt 7, pp. 835–53, Jul. 2014.

[130] A. McPherson, “Introduction to protein crystallization.,” *Methods*, vol. 34, no. 3, pp. 254–65, Nov. 2004.

[131] N. E. Chayen and E. Saridakis, “Protein crystallization: from purified protein to diffraction-quality crystal.,” *Nat. Methods*, vol. 5, no. 2, pp. 147–53, Feb. 2008.

[132] I. I. Rabi, J. R. Zacharias, S. Millman, and P. Kusch, “A New Method of Measuring Nuclear Magnetic Moment,” *Phys. Rev.*, vol. 53, no. 4, pp. 318–318, Feb. 1938.

[133] E. M. Purcell, H. C. Torrey, and R. V. Pound, “Resonance Absorption by Nuclear Magnetic Moments in a Solid,” *Phys. Rev.*, vol. 69, no. 1–2, pp. 37–38, Jan. 1946.

[134] F. Bloch, W. W. Hansen, and M. Packard, “Nuclear Induction,” *Phys. Rev.*, vol. 69, no. 3–4, pp. 127–127, Feb. 1946.

[135] B. J. C. Edwards and D. Ph, “Principles of NMR,” 1946.

[136] S. Biology, “Protein Ligation : Applications in NMR Studies of Proteins,” vol. 24, pp. 129–146, 2007.

[137] G. Wider and G. Wider, “Structure Determination of Biological Macromolecules in Solution Using NMR Spectroscopy,” *Bio Tech.*, vol. 29, pp. 1278–1294, 2000.

[138] M. From, T. H. E. Premier, T. H. E. Minister, F. O. R. Local, O. Of, T. Guidelines, T. H. E. Objectives, O. F. C. Planning, A. C. For, S. Planning, A. S. Guide, and C. Information, “Cultural Planin,” *Chem. Commun. (Camb).*, vol. 48, no. 15, pp. 2043–2054, 2012.

[139] M. Möller and A. Denicola, “Protein tryptophan accessibility studied by fluorescence quenching,” *Biochemistry and Molecular Biology Education*, vol. 30, no. 3. pp. 175–178, 2002.

[140] R. W. Alston, M. Lasagna, G. R. Grimsley, J. M. Scholtz, G. D. Reinhart, and C. N. Pace, “Peptide sequence and conformation strongly influence tryptophan fluorescence.,” *Biophys. J.*, vol. 94, no. 6, pp. 2280–2287, 2008.

[141] W. Jiskoot, V. Hlady, J. J. Naleway, and J. N. Herron, “Application of fluorescence spectroscopy for determining the structure and function of proteins.,” *Pharm. Biotechnol.*, vol. 7, pp. 1–63, Jan. 1995.

[142] A. O. Grillo, K. L. T. Edwards, R. S. Kashi, K. M. Shipley, L. Hu, M. J. Besman, and C. R. Middaugh, “Conformational origin of the aggregation of recombinant human factor VIII,” *Biochemistry*, vol. 40, no. 2, pp. 586–595, Jan. 2001.

[143] D. Matulis, C. G. Baumann, V. A. Bloomfield, and R. E. Lovrien, “1-anilino-8-naphthalene sulfonate as a protein conformational tightening agent.,” *Biopolymers*, vol. 49, no. 6, pp. 451–8, May 1999.

[144] W. R. Kirk, E. Kurian, and F. G. Prendergast, “Characterization of the sources of protein-ligand affinity: 1-sulfonato-8-(1’)anilinonaphthalene binding to intestinal fatty acid binding protein.,” *Biophys. J.*, vol. 70, no. 1, pp. 69–83, Jan. 1996.

[145] A. Fiser, M. Feig, C. L. Brooks, and A. Sali, “Evolution and physics in comparative protein structure modeling.,” *Acc. Chem. Res.*, vol. 35, no. 6, pp. 413–421, Jun. 2002.

[146] D. Baker and A. Sali, “Protein structure prediction and structural genomics.,” *Science*, vol. 294, no. 5540, pp. 93–6, Oct. 2001.

[147] T. L. Blundell and M. S. Johnson, “Catching a common fold,” *Protein Sci.*, vol. 2, no. 6, pp. 877–883, Jun. 1993.

[148] J. W. Chien, T. J. Richards, K. F. Gibson, Y. Zhang, K. O. Lindell, L. Shao, S. K. Lyman, J. I. Adamkewicz, V. Smith, N. Kaminski, and T. O’Riordan, “Serum lysyl oxidase-like 2 levels and idiopathic pulmonary fibrosis disease progression.,” *Eur. Respir. J.*, vol. 43, no. 5, pp. 1430–8, May 2014.

[149] T. Osawa, N. Ohga, K. Akiyama, Y. Hida, K. Kitayama, T. Kawamoto, K. Yamamoto, N. Maishi, M. Kondoh, Y. Onodera, M. Fujie, N. Shinohara, K. Nonomura, M. Shindoh, and K. Hida, “Lysyl oxidase secreted by tumour endothelial cells promotes angiogenesis and metastasis.,” *Br. J. Cancer*, vol. 109, no. 8, pp. 2237–47, Oct. 2013.

[150] D.-J. Cheon and S. Orsulic, “Ten-gene biomarker panel: a new hope for ovarian cancer?,” *Biomark. Med.*, vol. 8, no. 4, pp. 523–6, Jan. 2014.

[151] B. Zhu, G. Cai, E. O. Hall, and G. J. Freeman, “In-Fusion assembly: seamless engineering of multidomain fusion proteins, modular vectors, and mutations,” *Biotechniques*, vol. 43, no. 3, pp. 354–359, 2007.

[152] Y. Chen and M. D. Barkley, “Toward understanding tryptophan fluorescence in proteins.,” *Biochemistry*, vol. 37, no. 28, pp. 9976–82, Jul. 1998.

[153] H. McWilliam, W. Li, M. Uludag, S. Squizzato, Y. M. Park, N. Buso, A. P. Cowley, and R. Lopez, “Analysis Tool Web Services from the EMBL-EBI.,” *Nucleic Acids Res.*, vol. 41, no. Web Server issue, pp. W597–600, Jul. 2013.

[154] “The Universal Protein Resource,” *Nucleid Acid Res.*, vol. 36, no. Database issue, pp. D190–D195, Jan. 2008.

[155] D. W. A. Buchan, F. Minneci, T. C. O. Nugent, K. Bryson, and D. T. Jones, “Scalable web services for the PSIPRED Protein Analysis Workbench.,” *Nucleic Acids Res.*, vol. 41, no. Web Server issue, pp. W349–57, Jul. 2013.

[156] D. E. Kim, D. Chivian, and D. Baker, “Protein structure prediction and analysis using the Robetta server.,” *Nucleic Acids Res.*, vol. 32, no. Web Server issue, pp. W526–31, Jul. 2004.

[157] M. A. Martí-Renom, A. C. Stuart, A. Fiser, R. Sánchez, F. Melo, and A. Sali, “Comparative protein structure modeling of genes and genomes.,” *Annu. Rev. Biophys. Biomol. Struct.*, vol. 29, pp. 291–325, Jan. 2000.

[158] P. Benkert, M. Biasini, and T. Schwede, “Toward the estimation of the absolute quality of individual protein structure models.,” *Bioinformatics*, vol. 27, no. 3, pp. 343–50, Feb. 2011.

[159] F. Ryvkin and F. T. Greenaway, “Modeling Cu(II) binding to peptides using the extensible systematic force field.,” *Bioinorg. Chem. Appl.*, vol. 2010, p. 724210, Jan. 2010.

[160] M. R. Parsons, M. A. Convery, C. M. Wilmot, K. D. Yadav, V. Blakeley, A. S. Corner, S. E. Phillips, M. J. McPherson, and P. F. Knowles, “Crystal structure of a quinoenzyme: copper amine oxidase of Escherichia coli at 2 å resolution.,” *Structure*, vol. 3, no. 11, pp. 1171–84, Nov. 1995.

[161] R. A. Laskowski, J. A. Rullmannn, M. W. MacArthur, R. Kaptein, and J. M. Thornton, “AQUA and PROCHECK-NMR: programs for checking the quality of protein structures solved by NMR.,” *J. Biomol. NMR*, vol. 8, no. 4, pp. 477–86, Dec. 1996.

[162] J. U. Bowie, R. Lüthy, and D. Eisenberg, “A method to identify protein sequences that fold into a known three-dimensional structure.,” *Science*, vol. 253, no. 5016, pp. 164–70, Jul. 1991.

[163] T. A. P. de Beer, K. Berka, J. M. Thornton, and R. A. Laskowski, “PDBsum additions.,” *Nucleic Acids Res.*, vol. 42, no. Database issue, pp. D292–6, Jan. 2014.

[164] G. Martyna, “Remarks on ‘“Constant-temperature molecular dynamics with momentum conservation,”’” *Phys. Rev. E*, vol. 50, no. 4, pp. 3234–3236, Oct. 1994.

[165] T. Darden, L. Perera, L. Li, and L. Pedersen, “New tricks for modelers from the crystallography toolkit: the particle mesh Ewald algorithm and its use in nucleic acid simulations.,” *Structure*, vol. 7, no. 3, pp. R55–60, Mar. 1999.

[166] J. Dundas, Z. Ouyang, J. Tseng, A. Binkowski, Y. Turpaz, and J. Liang, “CASTp: computed atlas of surface topography of proteins with structural and topographical mapping of functionally annotated residues.,” *Nucleic Acids Res.*, vol. 34, no. Web Server issue, pp. W116–8, Jul. 2006.

[167] K. Coral, N. Angayarkanni, N. Gomathy, M. Bharathselvi, R. Pukhraj, and R. Rupak, “Homocysteine levels in the vitreous of proliferative diabetic retinopathy and rhegmatogenous retinal detachment: its modulating role on lysyl oxidase.,” *Invest. Ophthalmol. Vis. Sci.*, vol. 50, no. 8, pp. 3607–12, Aug. 2009.

[168] G. Liu, K. Nellaiappan, and H. M. Kagan, “Irreversible inhibition of lysyl oxidase by homocysteine thiolactone and its selenium and oxygen analogues. Implications for homocystinuria.,” *J. Biol. Chem.*, vol. 272, no. 51, pp. 32370–7, Dec. 1997.

[169] P. D. Lyne, M. L. Lamb, and J. C. Saeh, “Accurate prediction of the relative potencies of members of a series of kinase inhibitors using molecular docking and MM-GBSA scoring.,” *J. Med. Chem.*, vol. 49, no. 16, pp. 4805–8, Aug. 2006.

[170] T. A. K. Nubovets, J. O. H. N. J. O. Sterhout, P. E. J. C. Onnolly, and A. L. M. K. Libanov, “Structure , thermostability , and conformational flexibility of hen egg-white lysozyme dissolved in glycerol,” *Proc. Natl. Acad. Sci*, vol. 96, no. February, pp. 1262–1267, 1999.

[171] K. Shiraki, K. Nishikawa, and Y. Goto, “Trifluoroethanol-induced Stabilization of the a -Helical Structure of b -Lactoglobulin : Implication for Non-hierarchical Protein Folding,” *J. Mol. Biol.*, vol. 245, pp. 180–194, 1995.

[172] A. Dongs, “Effects of Dimethyl Sulfoxide , Glycerol , and Ethylene Glycol on Secondary Structures of Cytochrome c and Lysozyme As Observed by Infrared Spectroscopy,” *J Pharm Sci.*, vol. 84, no. 4, pp. 387–392, 1995.

[173] D. R. Senger and G. E. Davis, “Angiogenesis,” *Cold Spring Harb. Perspect. Biol.*, vol. 3, no. 8, pp. 1–19, 2011.

[174] L. I. Smith-Mungo and H. M. Kagan, “Lysyl oxidase: properties, regulation and multiple functions in biology.,” *Matrix Biol.*, vol. 16, no. 7, pp. 387–98, Feb. 1998.

[175] H. M. Kagan and W. Li, “Lysyl Oxidase : Properties , Specificity , and Biological Roles Inside and Outside of the Cell,” vol. 672, no. September 2002, pp. 660–672, 2003.

[176] J. T. Erler and A. J. Giaccia, “Lysyl oxidase mediates hypoxic control of metastasis.,” *Cancer Res.*, vol. 66, no. 21, pp. 10238–41, Nov. 2006.

[177] J. M. Mäki, “Lysyl oxidases in mammalian development and certain pathological conditions,” *Histology and Histopathology*, vol. 24, no. 5. pp. 651–660, 2009.

[178] D. E. Birk and P. Br, *The Extracellular Matrix: an Overview*. Berlin, Heidelberg: Springer Berlin Heidelberg, 2011.

[179] Y. Maeda, H. Koga, H. Yamada, T. Ueda, and T. Imoto, "Effective renaturation of reduced lysozyme by gentle removal of urea.," *Protein Eng.*, vol. 8, no. 2, pp. 201–5, Feb. 1995.

[180] V. Vagenende, M. G. S. Yap, and B. L. Trout, "Mechanisms of protein stabilization and prevention of protein aggregation by glycerol," *Biochemistry*, vol. 48, no. 46, pp. 11084–11096, 2009.

[181] A. L. M. K. Libanov, "Correct protein folding in glycerol," vol. 94, no. December, pp. 13520–13523, 1997.

[182] R. Sousa, "Use of glycerol, polyols and other protein structure stabilizing agents in protein crystallization.," *Acta Crystallogr. D. Biol. Crystallogr.*, vol. 51, no. Pt 3, pp. 271–7, May 1995.

[183] X.-Q. Zhu, S.-X. Li, H.-J. He, and Q.-S. Yuan, "On-column Refolding of an Insoluble His6-tagged Recombinant EC-SOD Overexpressed in Escherichia coli," *Acta Biochim. Biophys. Sin. (Shanghai).*, vol. 37, no. 4, pp. 265–269, Apr. 2005.

[184] M. Ito, K. Nagata, Y. Kato, Y. Oda, S. Yamagoe, K. Suzuki, and M. Tanokura, "Expression, oxidative refolding, and characterization of six-histidine-tagged recombinant human LECT2, a 16-kDa chemotactic protein with three disulfide bonds.," *Protein Expr. Purif.*, vol. 27, no. 2, pp. 272–8, Feb. 2003.

[185] S. H. J. Smits, A. Mueller, and K. Manfred, "crystallization communications Coenzyme- and His-tag-induced crystallization of octopine dehydrogenase crystallization communications," pp. 836–839, 2008.

[186] G. Oliva, R. C. Garratt, O. Ca, L. M. Beltramini, and D. De Gene, "Influence of the Histidine Tail on the Structure and Activity of Recombinant Chlorocatechol 1 , 2-Dioxygenase," vol. 484, pp. 480–484, 2000.

[187] A. Freydank, W. Brandt, and B. Dra, "Protein structure modeling indicates hexahistidine-tag interference with enzyme activity ¨," no. October 2007, pp. 173–183, 2008.

[188] S. T. Jung, M. S. Kim, J. Y. Seo, H. C. Kim, and Y. Kim, "Purification of enzymatically active human lysyl oxidase and lysyl oxidase-like protein from Escherichia coli inclusion bodies," *Protein Expr. Purif.*, vol. 31, no. 2, pp. 240–246, Oct. 2003.

[189] P. C. Trackman, C. G. Zoski, and H. M. Kagan, "Development of a peroxidase-coupled fluorometric assay for lysyl oxidase.," *Anal. Biochem.*, vol. 113, no. 2, pp. 336–342, May 1981.

[190] W. Torres-Arreola, J. M. Ezquerra-Brauer, C. G. Figueroa-Soto, E. M. Valenzuela-Soto, G. Garcia-Sanchez, E. Marquez-Rios, and R. Pacheco-Aguilar, "Lysyl oxidase from

jumbo squid (Dosidicus gigas) muscle: detection and partial purification," *Int. J. Food Sci. Technol.*, vol. 46, no. 8, pp. 1711–1715, May 2011.

[191] C. R. Kothapalli and A. Ramamurthi, "Lysyl oxidase enhances elastin synthesis and matrix formation by vascular smooth muscle cells.," *J. Tissue Eng. Regen. Med.*, vol. 3, no. 8, pp. 655–61, Dec. 2009.

[192] E. A. Makris, D. J. Responte, N. K. Paschos, J. C. Hu, and K. A. Athanasiou, "Developing functional musculoskeletal tissues through hypoxia and lysyl oxidase-induced collagen cross-linking.," *Proc. Natl. Acad. Sci. U. S. A.*, vol. 111, no. 45, pp. E4832–41, Nov. 2014.

[193] M. Lynch and F. Ryvkin, "Investigation into Structural Changes of the Copper Binding Site in Lysyl Oxidase upon Substrate and Inhibitor Docking," *ISRN Inorg. Chem.*, vol. 2013, no. Ii, 2013.

[194] R. H. Holm, P. Kennepohl, and E. I. Solomon, "Structural and Functional Aspects of Metal Sites in Biology.," *Chem. Rev.*, vol. 96, no. 7, pp. 2239–2314, Nov. 1996.

[195] C. Ramakrishnan and Y. S. Geetha, "Analysis of the coordination geometry in copper complexes," *Proc. Indian Acad. Sci. - Chem. Sci.*, vol. 102, no. 4, pp. 481–496, 1990.

[196] F. Ryvkin and F. T. Greenaway, "Modeling Cu(II) binding to peptides using the extensible systematic force field.," *Bioinorg. Chem. Appl.*, vol. 2010, no. Ii, p. 724210, Jan. 2010.

[197] A. Kadar, A. Joos, and H. Jellinek, "Influence of beta-amino-propionitrile on elastogenesis in the chick embryo (light and electron microscopic study).," *Paroi Arterielle*, vol. 4, no. 3, pp. 165–175, Apr. 1978.

[198] K. R. Wilmarth and J. R. Froines, "In vitro and in vivo inhibition of lysyl oxidase by aminopropionitriles.," *J. Toxicol. Environ. Health*, vol. 37, no. 3, pp. 411–23, Nov. 1992.

[199] R. C. Siegel and J. C. Fu, "Collagen cross-linking. Purification and substrate specificity of lysyl oxidase.," *J. Biol. Chem.*, vol. 251, no. 18, pp. 5779–85, Sep. 1976.

[200] A. S. Narayanan, R. C. Siegel, and G. R. Martin, "On the inhibition of lysyl oxidase by -aminopropionitrile.," *Biochem. Biophys. Res. Commun.*, vol. 46, no. 2, pp. 745–751, Jan. 1972.

[201] G. Liu, K. Nellaiappan, and H. M. Kagan, "Irreversible inhibition of lysyl oxidase by homocysteine thiolactone and its selenium and oxygen analogues: Implications for homocystinuria," *J. Biol. Chem.*, vol. 272, no. 51, pp. 32370–32377, 1997.

[202] J. Finney, H. J. Moon, T. Ronnebaum, M. Lantz, and M. Mure, *Human copper-dependent amine oxidases*, vol. 546. Elsevier Inc., 2014.

[203] R. Li, J. P. Klinman, and F. S. Mathews, "Copper amine oxidase from Hansenula polymorpha: the crystal structure determined at 2.4 A resolution reveals the active conformation.," *Structure*, vol. 6, no. 3, pp. 293–307, Mar. 1998.

[204] M. L. Di Paolo, M. Lunelli, M. Fuxreiter, A. Rigo, I. Simon, and M. Scarpa, “Active site residue involvement in monoamine or diamine oxidation catalysed by pea seedling amine oxidase.,” *FEBS J.*, vol. 278, no. 8, pp. 1232–43, Apr. 2011.

[205] H. C. Dawkes and S. E. V Phillips, “Copper amine oxidase: Cunning cofactor and controversial copper,” *Current Opinion in Structural Biology*, vol. 11, no. 6. pp. 666–673, Dec-2001.

[206] M. L. Di Paolo, C. Pesce, M. Lunelli, M. Scarpa, and A. Rigo, “N-alkanamines as substrates to probe the hydrophobic region of bovine serum amine oxidase active site: A kinetic and spectroscopic study,” *Arch. Biochem. Biophys.*, vol. 465, no. 1, pp. 50–60, Sep. 2007.

[207] C. A. Royer, “Fluorescence spectroscopy.,” *Methods Mol. Biol.*, vol. 40, pp. 65–89, Jan. 1995.

[208] E. A. Burstein, N. S. Vedenkina, and M. N. Ivkova, “Fluorescence and the location of tryptophan residues in protein molecules.,” *Photochem. Photobiol.*, vol. 18, no. 4, pp. 263–279, 1973.

[209] E. A. Burstein, E. A. Permyakov, V. A. Yashin, S. A. Burkhanov, and A. Finazzi Agro, “The fine structure of luminescence spectra of azurin.,” *Biochim. Biophys. Acta*, vol. 491, no. 1, pp. 155–9, Mar. 1977.

[210] A. G. Szabo, T. M. Stepanik, D. M. Wayner, and N. M. Young, “Conformational heterogeneity of the copper binding site in azurin. A time-resolved fluorescence study.,” *Biophys. J.*, vol. 41, no. 3, pp. 233–44, Mar. 1983.

[211] A. Iriarte, H. M. Kagan, and M. Martinez-Carrion, *Biochemistry and Molecular Biology of Vitamin B6 and Pqq-Dependent Proteins (Google eBook)*. Basel: Birkhäuser Basel, 2000.

[212] S. Jana, T. K. Chaudhuri, and J. K. Deb, “Effects of Guanidine Hydrochloride on the Conformation and Enzyme Activity of Streptomycin Adenylyltransferase Monitored by Circular Dichroism and Fluorescence Spectroscopy,” *Biochem.*, vol. 71, no. 11, pp. 1230–1237, 2006.

[213] Y. Zhang, M. Ghazwani, J. Li, M. Sun, D. B. Stolz, F. He, J. Fan, W. Xie, and S. Li, “MiR-29b inhibits collagen maturation in hepatic stellate cells through down-regulating the expression of HSP47 and lysyl oxidase.,” *Biochem. Biophys. Res. Commun.*, vol. 446, no. 4, pp. 940–4, Apr. 2014.

[214] D. J. Craik, D. P. Fairlie, S. Liras, and D. Price, “The Future of Peptide-based Drugs,” *Chem. Biol. Drug Des.*, vol. 81, no. 1, pp. 136–147, 2013.

[215] L. Sun, “Peptide-Based Drug Development,” *Mod. Chem. Appl.*, vol. 1, no. 1, pp. 1–2, 2013.

[216] R. Lax, “The Future of Peptide Development in the Pharmaceutical Industry,” *PharManufacturing Int. Pept. Rev.*, no. Sep, pp. 10–15, 2010.

[217] R. Sankararamakrishnan, S. Verma, and S. Kumar, “ATCUN-like metal-binding motifs in proteins: identification and characterization by crystal structure and sequence analysis.,” *Proteins*, vol. 58, no. 1, pp. 211–221, Jan. 2005.

[218] A. Trapaidze and C. Hureau, “Thermodynamic study of Cu 2 + binding to the DAHK and GHK peptides by isothermal titration calorimetry (ITC) with the weaker competitor glycine,” *JBIC J. Biol. Inorg. Chem.*, vol. 17, no. 1, pp. 37–47, 2012.

[219] Y. Zheng, Q. Huo, P. Kele, F. M. Andreopoulos, S. M. Pham, and R. M. Leblanc, “LETTERS A New Fluorescent Chemosensor for Copper Ions Based on Tripeptide Glycyl − Histidyl − Lysine (GHK),” *Org. Lett.*, vol. 3, no. 2, pp. 2–5, 2001.

[220] M. Ebadi and S. Swanson, “The status of zinc, copper, and metallothionein in cancer patients.,” *Prog. Clin. Biol. Res.*, vol. 259, pp. 161–75, Jan. 1988.

[221] B. Floriańczyk, “Copper and metallothioneins in cancer cells.,” *Ann. Univ. Mariae Curie-Skłodowska. Sect. D Med.*, vol. 58, no. 2, pp. 390–3, Jan. 2003.

[222] V. L. Goodman, G. J. Brewer, and S. D. Merajver, “Copper deficiency as an anti-cancer strategy.,” *Endocr. Relat. Cancer*, vol. 11, no. 2, pp. 255–63, Jun. 2004.

[223] S. Brem, S. A. Grossman, K. A. Carson, P. New, J. B. Alavi, T. Mikkelsen, J. D. Fisher, and N. Approaches, “Phase 2 trial of copper depletion and penicillamine as antiangiogenesis therapy of glioblastoma 1 , 2,” *Neuro. Oncol.*, vol. 2005, pp. 246–253, 2005.

Publications

1. ***Bhuvanasundar R***, Arun J, Sulochana KN, K Coral, Deepa PR, Umashankar V. A molecular model of human Lysyl oxidase with optimal copper orientation in the catalytic cavity for induced fit docking studies with potential modulators. *Bioinformation* 2014;10(7): 406-12.

2. M Arun[#], ***R Bhuvanasundar*** [#], K Coral, C Subbulakshmi, KN Sulochana.· Peptides derived from the copper-binding region of lysyl oxidase are antiangiogeneic by inhibiting enzyme activity: an *in vitro* study. *J. Pept Sci.* 2014;20:837-49. (# Equal contribution)

3. Arun M, ***Bhuvanasundar R***, K Coral, Sulochana KN. Peptide derived from n-terminal of lysyl oxidase promote endothelial attachment and migration by inducing enzymatic activity. Int J Pharm Bio Sci 2014; 5(4): (B) 709 – 20

4. Selvi R**, *Bhuvanasundar R***, Saijyothi AV, Sulochana KN, Angayarkanni N. Amino acids potentiate the insulin signaling in CHO-K1 at high glucose conditions. *Arch Med Res*, 2012;43:173-82.

Manuscript under preparation

1. Cloning, over expression and enzymatic characterization of human Lysyl oxidase
2. Anti angiogenic property of Peptide derived from the conserved domain of human Lysyl oxidase
3. Understanding the structure of human mature Lysyl Oxidase: spectroscopic analysis.

Patent filed

1. A Peptide based drug for the inhibition of angiogenesis.
   Patent No: 935/DEL/2014. Inventor: Dr.K.N.Sulochana.
   Co-Inventor: Dr.K.Coral, **R. Bhuvanasundar,** M.Arun.

Posters presented

1. Participated in 81rd SBCI conference, Lucknow. Improved Micro Titre Plate Assay for the Measurement of Lysyl Oxidase Activity in Human Serum.
2. Participated in 83rd SBCI conference, Bhubaneswar. Characterization of human Lysyl Oxidase (LOX) and development of novel peptides to inhibit its activity

Workshops attended:

1. Practical Proteome School by Waters India, 2012.
2. Workshop on Scientific writing 2014- Elite school of optometry.

BRIEF BIODATA OF CANDIDATE

Mr.R.Bhuvanasundar, acquired his Bachelor's degree in Biochemistry from R.K.M.Vivekananda College, Chennai in 2007. He got Master's degree in Medical Laboratory Technology in 2010 from Birla Institute of Technology & Science – Pilani in collaboration with Medical Research Foundation. During his Master's degree internship, he worked on the effect of amino acids mixture on Akt, mTOR, glycogen synthase activity and generation of reactive oxygen species in CHO cells exposed to hyper-glycaemic conditions and published an article. He joined as Junior Scientist in 2010 at Central Research Instrumentation Facility at Vision Research Foundation. Later in 2011, he registered PhD under the supervision of Dr.K.N.Sulochana, Director Dept. of Biochemistry and cell biology. From his doctoral work he published 3 international articles and 2 manuscripts under preparation, filed one patent under Intellectual property of India. During his work he standardized the over expression and purification of protein from *E.coli* in the lab. He acquired the skills in Flow cytometry, HPLC, Mass spectroscopy, fluorescence microscopy, cell culture and spectroscopic analysis. He also involved in the patient care and teaching classes ESO optometry students. He also assisted two PS students project from BITS –Pilani.

BRIEF BIODATA OF SUPERVISOR

Prof. K.N. Sulochana is currently Sr. Professor, R.S. Mehta Jain Department of Biochemistry and Cell Biology, Vision Research Foundation, Chennai. She has been Group leader and Reader in Biochemistry Research Dept, Sankara Nethralaya for nearly 10 yrs, Sr. Research Fellow, National University Singapore, for 2 yrs and as a Sr. Lecturer at Bradford University Singapore campus and Sr. Research Scientist, in Pharma industry for 3 yrs. She did her B.Sc. (Chemistry); M.Sc. (Biochemistry) – Univ. of Madras and Ph.D. (Biochemistry- Enzymology) Sri Venkateswara Univ., India.

Her teaching area includes Basic Biochemistry, Biomolecules, Instrumentation, Clinical Biochemistry and Ocular biochemistry. She has been supervising Ph.D. students registered under BITS-Pilani and Tamil Nadu Dr.MGR Medical University (total students: completed : 2, current students: 5).

Her current interests are Ocular Angiogenesis, Protein- Protein interactions, Molecular mechanisms of metabolic diseases, Drug targets, Design and development of inhibitors of angiogenesis, Pharmacokinetics and Preclinical studies. She has more than 90 Research articles published, 5 reviews, 4 Book Chapters and 5 patents.

She has participated in many National and International conferences. She has received Dr. BC. Roy Award, Silver Jubilee Research Award of Medical Council of India, 1996, Swarnalata Punshi award as "Best Research Worker" Medical Research Foundation, 1997, Women of the Year American Biographical Institute, Inc (2000), The biographical sketch inclusion, Who's Who in the World by Marquis (2001) and Outstanding Woman of the 21st C", American Biographical Institute, NC, USA, 2001.

She's also a life member of professional bodies in Society of Biological Chemistry (I) (Life Member), Association for the promotion DNA fingerprint DNA technology (Life Member), Active participant in Annual Meeting of IERG for the past 7 yrs, Member in ARVO, Member in Association for clinical biochemist Singapore since 2002, Member of the Management development institute of Singapore (MDIS) since Jan-2008.

BRIEF BIODATA OF CO-SUPERVISOR

Dr. P. R. Deepa (Associate Professor, Dept. of Biological Sciences, BITS Pilani) has been involved (since 2005) in teaching, research, and co-ordination at off-campus collaborative programmes of BITS Pilani — Chennai Centre. She is the Course Instructor for students from BITS, Pilani during their internship (Practice School – I and II) at several industries and research organizations in Chennai, Hyderabad and Bangalore. Prof. Deepa serves as Supervisor / Co-Supervisor for PhD students of BITS Pilani.

Prof. Deepa has been collaborating with the Department of Ocular Pathology, Sankara Nethralaya (Chennai) for ongoing research in the evaluation of molecular targets for diagnosis and therapy of retinoblastoma. Her other collaborative research efforts are in the areas of protein biochemical characterization, bioinformatics, bio-mathematical modelling, and bio-chemical engineering. She earned her doctoral degree in 2005 for her research titled "Biochemical Evaluation of a Low-Molecular Weight Heparin (certoparin sodium) in Experimental Atherogenic and Cytotoxic Conditions" (University of Madras).